ROLES OF ETS GENES ER81 AND PEA3
IN THE DEVELOPMENT OF THE
MONOSYNAPTIC STRETCH REFLEX CIRCUIT

by

David Roger Ladle

BS, Brigham Young University, 1995

MS, Brigham Young University, 1997

Submitted to the Graduate Faculty of the

School of Medicine in partial fulfillment

of the requirements for the degree of

Doctor of Philosophy

University of Pittsburgh

2002

UNIVERSITY OF PITTSBURGH

SCHOOL OF MEDICINE

This dissertation was presented

by

David Roger Ladle

It was defended on

January 17, 2002

and approved by

Karl Kandler, PhD, Assistant Professor, Department of Neurobiology

Peter W. Land, PhD, Associate Professor, Department of Neurobiology

Steven Meriney, PhD, Associate Professor, Department of Neuroscience

Committee Chairperson:

Cynthia Lance-Jones, PhD, Associate Professor, Department of Neurobiology

Major Advisor:

Eric Frank, PhD, Professor, Department of Neurobiology

Acknowledgements

Santiago Ramón y Cajal wrote of students "who had the good fortune to receive an education in the laboratory of a distinguished scientist, under the beneficial influence of living rules embodied in a learned personality who is inspired by the noble vocation of science combined with teaching." As a student of Eric Frank, I count myself among the most fortunate of graduate students. Eric's enthusiasm for scientific work has been contagious, inspiring me through disappointment and sometimes repeated failure. While under his direction, I have tried to develop in myself his refined skills of mental discipline and clear articulation in speech and writing. Eric is a natural teacher. His high expectations along with his patience and genuine concern have made my doctoral studies one of the greatest growth experiences of my life.

I thank my loving wife, Melisa, and our three daughters, Rachel, Tiffany, and Elisabeth for their constant support. They brought encouragement and joy to this process. Their love makes me the most fortunate graduate student of all.

I also thank the members of my Dissertation committee, Karl Kandler, Cynthia Lance-Jones, Pete Land, and Steve Meriney, who provided encouragement and honest analysis of my work. Their collective insight greatly increased the quality of this work.

The members of the Frank lab created a spirited, diverse and enjoyable environment in which to work. Particularly, I thank Hsiao-Huei Chen, the "senior post-doc," who has been both a mentor and a great friend.

Table of Contents

List of Figures

Discussion

List of Tables

Analysis of Er81 mutant mice

ROLES OF ETS GENES ER81 AND PEA3
IN THE DEVELOPMENT OF THE
MONOSYNAPTIC STRETCH REFLEX CIRCUIT

David Roger Ladle, PhD

University of Pittsburgh, 2002

The monosynaptic stretch reflex circuit consists of two neural cell types, sensory neurons and α-motoneurons. Ia afferents form synaptic connections with motoneurons projecting to the same or synergistic muscles, but not with motoneurons projecting to unrelated muscles. These synaptic connections form appropriately from the outset suggesting that they may be controlled by expression of specific adhesion molecules in matching sensory and motor neurons. Recently, two ETS-family transcription factors (Er81 and PEA3) were shown to be expressed in subsets of motoneurons and muscle sensory neurons. The expression patterns of these factors suggested that ETS genes might regulate the formation of synaptic connections between Ia afferents and motoneurons. This thesis explores the roles of Er81 and PEA3 in the formation of the stretch reflex circuit inferred from a study of Er81 and PEA3 null-mutant mice.

Analysis of Er81 null-mutant mice revealed that Er81 controls a late step in Ia afferent axon guidance. Ia afferents induce the development of muscle spindles in the periphery and project axons into the spinal cord, but fail to grow axon collaterals into the ventral spinal cord where normally strong monosynaptic connections are formed with motoneurons. Consequently, monosynaptic Ia afferent inputs to motoneurons are greatly reduced in these mice. This severe phenotype precluded determination of whether or not the pattern of remaining Ia afferent inputs was normal.

Intracellular recordings from quadriceps and obturator motoneurons in PEA3 null-mutants, however, revealed that functionally appropriate patterns of Ia afferent input to motoneurons develop normally in the absence of PEA3. PEA3 mutant mice demonstrated a role for PEA3 in the formation of a specific motor pool. Cutaneous maximus muscle motoneurons normally express PEA3. In PEA3 mutants, the majority of these motoneurons fail to migrate and coalesce appropriately into a discrete motor pool. These motoneurons also fail to project axons into the c. maximus muscle. Consequently, the muscle is atrophic.

Thus, Er81 and PEA3 contribute to key developmental stages in the formation of the stretch reflex circuit: the growth of Ia afferents axons toward motoneurons and the formation of appropriate motor pool targets.

1.   Introduction

At birth, the human brain contains approximately 100 billion neurons, and each neuron makes an estimated 10,000 synaptic connections with other neurons (Lagercrantz and Ringstedt, 2001). These myriad connections are not superfluous or random; rather, they are organized into thousands of neural circuits responsible for control of the entire behavioral repertoire of an organism. Circuits damaged by developmental abnormalities or disease can severely limit behavior or lead to death. Thus, the mechanisms by which these circuits are formed and maintained are central questions of current neural science research.

To begin to understand fundamental principles that control the formation of neural circuits, we have studied the development of a simple neural circuit, the monosynaptic stretch reflex (see Figure 1). It consists of only two neural cell types, a sensory neuron, the Ia afferent, and an α-motoneuron. These cells communicate via a glutamatergic synapse. In the periphery, Ia afferents terminate on muscle spindles, specialized mechanorecptors found in skeletal muscle. The Ia afferent coils around the muscle spindle and is activated by changes in the length of the muscle fiber. Ia afferents fire action potentials in response to changes in muscle length, but rapidly adapt and reduce their firing when muscle length reaches a steady state. Thus, the stretch reflex circuit responds to dynamic changes in muscle length.

Synaptic connections between Ia afferents and motoneurons in adult animals are precise. Ia afferents do not make connections with motoneurons that project to unrelated muscles, but rather restrict their inputs to motoneurons that project to the same muscle or
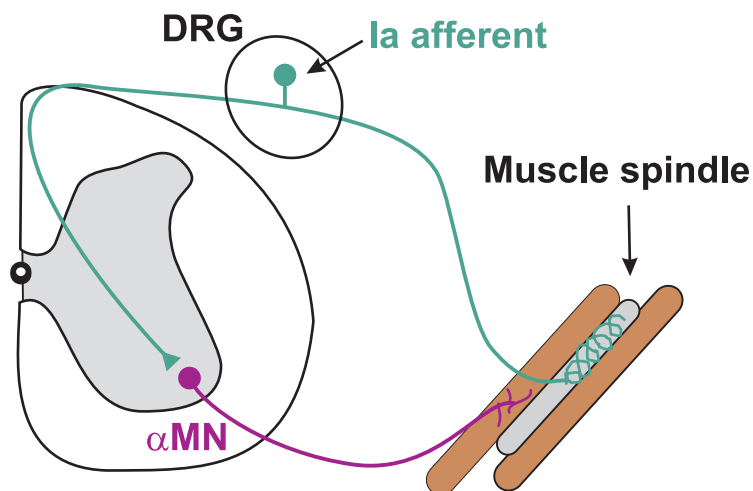
Figure 1. The monosynaptic stretch reflex circuit consists of two neural cell types.
Ia afferents (green) receive sensory input from muscle spindles. Ia afferents project into the dorsal portion of the cord and extend longitudinal axons across several segments rostral and caudal through tracts in the medial dorsal white matter. Ia afferents also make a stereotypic collateral projection into the ventral gray matter. Here monosynaptic connections are formed on the somata and proximal dendrites of α-motoneurons (α-MN, purple). Drawing adapted from Arber et al., 2000.

muscles that have related functions. Both Ia afferents and motoneurons are accessible for study via projections in the dorsal and ventral roots, respectively. Hence, it is possible to test for the presence of synaptic connections during development and to determine if those connections are appropriate. The study of the stretch reflex circuit can, therefore, yield insights into the mechanisms responsible for the formation of appropriate synaptic connections between identified populations of neurons in the central nervous system.

1.   Development of stretch reflex circuit

In general, the major stages in the development of neural circuits are: the determination of neuronal identity; guidance of developing axons to target regions; and the formation of selective synaptic connections (Albright et al., 2000). The cell types that form the stretch reflex circuit, motoneurons and Ia afferents, have been subjects of intense research for many years. Significant progress has been made in understanding how each cell type develops and how it contributes to the formation of the stretch reflex.

A.1   Determination of neuronal identity—motoneurons

Neuronal identity is defined by an expression pattern of molecular markers that distinguish one population of neurons from other populations (Lee and Pfaff, 2001). In the spinal cord, neurons are divided into two major classes: interneurons that project axons intraspinally, and motoneurons that project axons to muscle targets in the periphery. In general, interneurons in the dorsal half of the spinal cord relay sensory information from the periphery to higher centers in the brain. Interneurons located in the ventral portion of the cord form circuits that modulate motor output. In the ventral cord,

motoneurons and interneurons are generated in distinct regions in response to graded levels of sonic hedgehog (Shh), a diffusible factor secreted by the floor plate and notochord (Briscoe and Ericson, 2001; Briscoe et al., 2000). Progenitor cells that give rise to ventral interneurons and motoneurons are divided into two classes: Class I and Class II. Class I progenitors (p0 and p1 cells) express the transcription factor Dbx2 while Class II progenitors (p2, p3, and pMN cells) express Nkx6.1. Expression of Dbx2 is inhibited by Shh, thus Class I progenitors are located in the dorsal portion of the ventral neural tube and give rise to more dorsal interneuron types, V0 and V1 interneurons. In contrast, Nkx6.1 expression is induced by Shh secreted by the floor plate and notochord. Therefore Class II progenitors are found more ventrally than Class I progenitors. Class II progenitors give rise to V2 and V3 interneurons and motoneurons. The complimentary repression and induction of Class I and II genes by Shh creates defined domains of progenitor cells in the ventral neural tube. Motoneurons arise from pMN progenitor cells located in the middle of the Class II band. These progenitor cells express Nkx6.1, but not Irx3 (p2 progenitors) or Nkx2.2 (p3 progenitors). This distinct transcription factor signature is required for generation of motoneurons. Indeed, loss of Nkx6.1 results in a reduction in the number of motoneurons (Sander et al., 2000).

The expression of several transcription factors is required for the formation of motoneuron identity. Islet-1 is expressed by post-mitotic motoneurons and a subset of ventral interneurons. In the absence of Islet-1 protein, motoneurons die shortly after their birth indicating that Islet-1 is an essential factor required for motoneuron survival (Pfaff et al., 1996). HB9, a homeobox transcription factor, is expressed by some late-stage motoneuron progenitor cells and by all post-mitotic motoneurons (Arber et al., 1999).

Motoneurons in mice lacking HB9 are generated in normal numbers, but several elements of motoneuronal identity are perturbed. For example, at limb levels of the spinal cord motoneurons fail to form distinct medial and lateral motor columns (see below) and some motor axon projections are misrouted. Significantly, some motoneurons transiently express Chx10, a marker of V2 interneurons. Thus, HB9 is a critical factor that influences many elements of motoneuronal identity (Arber et al., 1999).

Expression of additional factors by subsets of motoneurons delineates several subdivisions within the motoneuronal class of spinal neurons. As post-mitotic motoneurons migrate laterally away from the midline, they settle into discrete columns of cells. These columns are defined by functional as well as molecular differences. Motoneurons that project to axial muscles form the medial motor column (MMC) (Sharma et al., 1998). This column is present along the rostral-caudal extent of the cord. Motoneurons that innervate limb muscles migrate more laterally and generate the lateral motor column (LMC). This motor column is present only at limb levels of the spinal cord. As a general rule, dorsally derived muscles are innervated by lateral LMC motoneurons (LMC_L) while medial LMC motoneurons (LMC_M) project to ventrally derived muscles. The MMC is also divided into lateral and medial portions. The MMC_L is found only in thoracic segments, however.

The four columnar divisions of motoneurons can be distinguished by combinatorial expression of LIM homeodomain (LIM-HD) proteins (Tsuchida et al., 1994). Following motoneuronal birth, all motoneurons are identified by coexpression of Islet-1 and Islet-2. Individual motor columns are distinguished by expression of additional LIM-HD proteins, Lim-1 and Lim-3. MMC_M motoneurons solely express

Lim-3, and LMC_L motoneurons uniquely express Lim-1. Thus, MMC_M and MMC_L motoneurons are differentiated by expression of Lim-3, and LMC_M and LMC_L motoneurons are distinguished by Lim-1 expression.

Division of motoneurons into four molecularly and functionally distinct columns allows a first approximation of motoneuronal specificity. To date, only a few molecular markers have been shown to label subsets of motoneurons in a particular column. A member of the forkhead class of transcription factors, thymocyte winged helix (TWH), is expressed in subsets of lumbar, but not cervical, motoneurons and a subset of ventral interneurons in mice at birth (Dou et al., 1997). Early in development, however, progenitor cells in the neuroepithelium also express TWH. In mice lacking TWH function, the number of MMC motoneurons is reduced while the number of LMC motoneurons is increased. In addition, the number of ventral interneurons is increased. MMC motoneurons are born before LMC motoneurons or interneurons, thus in the absence of TWH, progenitor cells continue to proliferate and fail to generate appropriate numbers of early-born neurons (Dou et al., 1997). The ETS transcription factors Er81 and PEA3 are also expressed by subsets of motor pools, but not interneurons. In chick, the combinatorial expression of ETS genes and other LIM-HD genes uniquely identifies many limb motor pools (Lin et al., 1998). The possible contribution of these molecules to stretch reflex circuit development will be discussed in detail below.

A.2   Determination of neuronal identity—Ia afferents

DRG sensory neurons are divided into three major categories based on the selective expression of three receptor tyrosine kinase molecules: trkA, trkB, and trkC.

The neurotrophin NT3 activates the trkC receptor, BDNF activates trkB receptors, and NGF activates trkA receptors (Patapoutian and Reichardt, 2001). TrkC is expressed primarily by large-diameter muscle sensory neurons such as Ia and Ib afferents, while trkA is expressed primarily by small-diameter cutaneous afferents (Chen and Frank, 1999).

These classes of sensory neurons are generated from neural progenitor cells that express two related transcription factors, neurogenin 1 and 2 (ngn1 and ngn2) (Anderson, 1999; Gradwohl et al., 1996; Ma et al., 1996). Large-diameter sensory neurons (most trkB+ and trkC+ neurons) are derived from ngn2+ progenitor cells. Small-diameter sensory neurons, the trkA+ population, are generated later by ngn1+ progenitors (Ma et al., 1999). Ngn1+ progenitors also generate a later born population of large-diameter neurons. There is evidence that ngn1 can function in place of ngn2. In mice lacking ngn2, large-diameter sensory neurons are generated in an ngn1-dependent manner, but the generation of these neurons is delayed. It is unclear, however, if ngn2 can completely replace the function of ngn1 (Ma et al., 1999).

TrkC+ afferents require NT3 for survival. Mice deficient in NT3 have no trkC+ sensory neurons and, consequently, no Ia or Ib afferents (Farinas et al., 1994; Farinas et al., 1996). TrkC+ afferents are born relatively early during neurogenesis in the DRG. Before these neurons have extended processes that reach their peripheral targets, Ia afferents are sustained by NT3 that is produced in the mesenchyme surrounding the DRG (Ernfors et al., 1992; Farinas et al., 1996; Patapoutian et al., 1999). Later, as sensory axons reach their target muscles, they are sustained by NT3 produced in muscles (Oakley et al., 1995; Oakley et al., 1997; Wright et al., 1997).

B.1   Axon guidance—motoneurons

A key element in the formation of the stretch reflex is the proper guidance of

motor and sensory axons in the periphery to appropriate muscle targets. As motor axons

exit the spinal cord through the ventral root, some motoneurons grow axons into the

dorsal limb while others grow into the ventral limb (Landmesser, 1978; Tosney and

Landmesser, 1985). This differential growth is controlled by a cell-intrinsic factor

present in motoneurons. LMC_L motoneurons (Lim-1+) project axons into the dorsal

limb, but not into the ventral limb. In the absence of Lim1, LMC_L motor axons no longer

discriminate between dorsal and ventral pathways and send axons into both the dorsal

and ventral limb (Kania et al., 2000).

As motor axons extend in the limb toward muscle targets, the axons interact with

surrounding tissue to find specific targets, but the mechanism of this interaction is

unknown (Jacob et al., 2001). Motoneurons are spontaneously active during axon

extension and may use this activity as a means of testing contacts with peripheral tissues.

Significantly, the bursting patterns of axons destined to project to flexor muscles are

different from those projecting to extensor muscles (Milner and Landmesser, 1999).

Spontaneous activity of motoneurons, although it may modulate interactions, is not

required for correct axon guidance of motoneurons to their correct targets. Neurons in

mice lacking munc18-1, a neuron-specific membrane-trafficking protein, fail to release

synaptic neurotransmitters so all synaptic activity is blocked (Verhage et al., 2000).

Motor axons in these mutants, however, project to appropriate muscle targets and form

neuromuscular junctions. These data suggest that chemical interactions between motor

axons and myotubes, which are not dependant on motoneuronal activity, can direct the

formation of appropriate motoneuronal connections.

There is some evidence that ephrin-Eph receptor signaling may be involved in motor axon guidance in the periphery as well as in positionally selective innervation of target muscles (Helmbacher et al., 2000; Kilpatrick et al., 1996; Koblar et al., 2000; Wang et al., 1999; Wang and Anderson, 1997). The interactions of ephrin ligands with Eph receptor kinases have been most intensely studied in the developing retinal-tectum system (O'Leary and Wilkinson, 1999). Members of the ephrin-A family of molecules are GPI-linked extracellular molecules expressed in an increasing gradient along the anterior-posterior axis of the optic tectum in chick. EphA receptor kinases are expressed on axons of retinal ganglion cells (RGC) that project to the tectum. The increasing gradient of ephrin expression along the rostral-caudal axis of the tectum is repulsive to axon growth. Thus, axons that express relatively little EphA receptor will be able to grow more posteriorly in the tectum than axons that express high levels of EphA receptor. RGC axons originating from the temporal portion of the retina do, indeed, express higher levels of EphA receptors than axons originating from the nasal half of the retina. Thus temporal axons project to the more anterior portion of the tectum while nasal axons project more posteriorly. In this way, a map of the visual world is topographically mapped onto a target structure in the brain, exhibiting one way in which ephrin-Eph signaling is involved in axonal guidance.

After motor axons arrive at an appropriate muscle they begin to initiate contacts with myotubes. In some muscles, these contacts are made with an approximate topographic distribution: motoneurons from rostral regions of a motor pool innervate rostral portions of the muscle target. This topographic arrangement appears to be

controlled by ephrin signaling (Feng et al., 2000). All five of the Ephrin-A genes are expressed in developing muscles and three EphA receptor kinases (EphA3-5) are expressed by subsets of motoneurons (Feng et al., 2000). The rostral-caudal distribution of motoneuron inputs to gluteus muscle is controlled by graded expression of ephrin-A5 by muscle fibers. In normal mice, motoneurons from the rostral portions of the gluteus motor pool selectively innervate rostral sections of gluteus muscle and more caudal motoneurons innervate caudal sections (Brown and Booth, 1983). Overexpression of ephrin-A5 in mice causes a loss of this rostral-caudal innervation bias; motoneurons now innervate the muscle more uniformly (Feng et al., 2000). Mice lacking both ephrin-A2 and eprhin-A5 demonstrate a loss in topographical bias of motor innervation of the diaphragm (Feng et al., 2000). The both gain-of-function and loss-of-function experiments demonstrate that ephrin signaling controls selective innervation of muscles by motoneurons.

B.2   Axon guidance—Ia afferents

Appropriate guidance of muscle sensory axons in the periphery depends on motor axons. Removal of motoneurons before axons grow into the limb results in misrouting of muscle sensory axons. These axons fail to innervate muscle and instead project in cutaneous nerves (Landmesser and Honig, 1986). Recent studies have shown that muscle sensory and motor axons fasciculate with each other as they course toward muscle targets, suggesting that sensory axons may simply follow motor axons to their targets (Honig et al., 1998).

Muscle sensory afferents are capable, however, of some independent projection.

Initially, unfasciculated muscle sensory axons intermingle with both cutaneous and motor axons in the spinal nerve. Muscle sensory axons do not fasciculate with cutaneous axons, however, indicating that these axons discriminate between possible partners. Moreover, some muscle sensory axons travel independently over significant distances in muscle nerves before becoming fasciculated with motor axons (Honig et al., 1998).

This finding raises the question of whether muscle sensory axons are predetermined to innervate a particular muscle target as motoneurons are. This is difficult to test experimentally because sensory neurons are not found in stereotyped locations in the DRG as motoneurons are found in discrete locations in the spinal cord. Sensory neurons, even if misrouted to novel muscles, form synaptic connections with motoneurons that project to the same muscle (Wenner and Frank, 1995). Thus, the current evidence implies that sensory neurons are dependant on signals from the periphery to form selective synapses with motoneurons.

Ia afferents contacting primary myotubes initiates the formation of muscle spindles by stimulating the differentiation of intrafusal muscle fibers (at E15 in mouse; Kozeka and Ontell, 1981). Motor innervation of these fibers by γ-motoneurons occurs later and muscle spindles appear morphologically mature by P0. Muscle spindles become sensitive to stretch before birth (Kudo and Yamada, 1985). The response of the Ia afferents to stretch in the earliest developing spindles is tonic and does not adapt like the response of mature spindles. Adaptation is observed prenatally, however, before full maturation of the spindle (Patak et al., 1992).

Sensory input is critical for maintenance of muscle spindles. Transection of motor and sensory axons in newborn rats results in the loss of all spindles in the

denervated area within 5-10 days (Zelena, 1994). This degeneration begins with the withdrawal of axons from the spindles followed by gradual dedifferentiation of intrafusal muscle fibers (Kucera et al., 1993).

B.3   Axon guidance—central projections of Ia afferents

After muscle contacts are established, Ia sensory neurons project axon collaterals ventrally in the spinal cord to form synaptic connections with motoneurons. TrkA+ sensory neurons are sensitive to repulsive cues from the ventral cord and restrict axon growth to the dorsal portion of the cord. Ia afferents are insensitive to this signal, however. Could Ia axons be selectively sensitive to an attractant molecule produced by the ventral cord? Currently, the evidence does not suggest such a factor. To the contrary, the spinal cord appears to act as a permissive environment for Ia axon growth. Replacement of the ventral spinal cord by a duplicate dorsal cord has no affect on Ia afferent growth; axons continue to grow normally in the duplicated region. These results suggest that in normal spinal cord the growth of Ia afferents in the dorsal region is regulated by local cues instead of an attractant factor from the ventral cord (Sharma and Frank, 1998).

The termination of axon growth and resulting elaboration of synaptic arbors appears to be regulated by a local cue in the ventral horn, possibly even NT3 secreted by motoneurons. Ectopic expression of NT3 in the spinal cord induces muscle sensory afferent termination and aborization in locations other than their normal targets, but close to regions of high NT3 expression (Ringstedt et al., 1997). *In vitro* experiments demonstrate that NT3 promotes terminal branching of axons of DRG neurons (Lentz et

al., 1999). Against this idea, however, NT3 null mutant mice crossed with myo-NT3 mice that overexpress NT3 in muscle have normal projections and aborizations of Ia afferents (Wright et al., 1997). Thus, in the absence of NT3 produced by the CNS, Ia afferents are able to recognize motoneuron partners and generate synaptic arbors. A possible explanation for this result is that motoneurons, which are trkC+, may retrogradely transport NT3 from the muscle and release it into the spinal cord causing Ia afferents to arborize (Chen and Frank, 1999). Alternatively, however, factors other than NT3 may promote arborization of Ia afferents in the spinal cord.

C.   Formation of specific Ia afferent-motoneuron connections

A hallmark of the stretch reflex circuit is functional specificity (Frank and Mendelson, 1990). Synaptic connections are strongest between Ia afferents and motoneurons that project to the same muscle (homonymous connections). Synergistic connections between Ia afferents and motoneurons that project to related muscles are somewhat less strong. In contrast, Ia afferents make very weak connections with motoneurons that project to antagonistic or functionally unrelated muscles.

Ia afferent inputs to quadriceps and obturator motoneurons provide an excellent example of the specificity of the stretch reflex. The quadriceps muscle group consists of four synergistic muscles that act to extend the knee. Ia afferents from all four muscles make strong homonymous inputs, and make relatively strong synergistic inputs to other quadriceps motoneurons. Notably, although all four muscles act to move the knee through the same tendon, selective sensory input patterns to these motoneurons exist. That is, homonymous connections are stronger than synergistic ones. Similarly, Ia

afferents projecting to obturator group muscles make strong projections to obturator motoneurons. Even though motoneurons that project to both quadriceps and obturator group muscles are located in the same spinal segments and have overlapping dendritic fields, there are no significant synaptic inputs from obturator Ia afferents to quadriceps motoneurons and vice versa. Thus, Ia afferents are able to distinguish between positionally similar motoneuron targets with great accuracy.

How is this specificity achieved? Coordinated activity between Ia afferents and motoneurons that project to the same muscle may strengthen functionally appropriate connections, while uncoordinated activity between synaptic pairs projecting to different muscles may weaken functionally inappropriate connections. Alternatively, Ia afferent connections with motoneurons may be formed correctly from the beginning, most likely through a chemically mediated process. The chemical specification hypothesis was first advanced by Sperry to explain the results of his experiments on axon guidance in the optic tectum (Sperry, 1963). Identification of ephrin-Eph signaling interactions guiding axons in the tectum has strengthened his argument that at least the initial stages of synaptic development are directed by chemical signals in many systems (Cheng et al., 1995; Frisen et al., 1998; Monschau et al., 1997).

Current experimental evidence supports the hypothesis that sensory-motor connections in the stretch reflex circuit are also formed in a non activity-dependent manner. Elimination of coordinated activity between functionally related sensory and motoneurons did not disrupt the specific pattern of sensory connectivity (Mendelson and Frank, 1991). Chick embryos were paralyzed by daily injections of curare, eliminating movements that could coordinately activate the stretch reflex circuit. Intracellular

recordings from identified motoneurons demonstrated that the specific pattern of synaptic input from Ia afferents was unchanged in curare-treated embryos. Additionally, intracellular recordings from mouse embryos showed that from the earliest times it was possible to make recordings and during a time that many Ia-motoneuron contacts are being made (E17), Ia afferent connections to motoneurons were specific (Mears and Frank, 1997).

These experiments suggest that Ia afferents and motoneurons need not be synchronously active for appropriate connections to form. They do not rule out, however, the possibility that sensory and motoneurons must be active, even if not temporally coordinated, to develop synaptic connections (Frank, 1987). Paralysis of chick embryos with curare does not eliminate spontaneous motoneuron firing, only contraction of muscle in response to motoneuron activity. Presumably, sensory afferents are also spontaneously active. Experiments in the visual system have shown that axon guidance and initial synaptic connections require presynaptic neurons to be electrically active (Catalano and Shatz, 1998). Blockade of action potentials in lateral geniculate nucleus axons by administration of TTX caused these axons to fail to project appropriately to layers of visual cortex. Axons that reached the cortex were not topographically organized as in normal animals. Thus, developing neurons may require general activity to form appropriate synaptic connections.

The peripheral targets of sensory neurons are important in the formation of selective synaptic connections. The major limb muscle groups in chick are derived from dorsal and ventral muscle masses. Replacement of ventral muscles by duplicate dorsal muscles before sensory and motor axons reached the limb made it possible to determine

the role of muscle targets in generating synaptic specificity. Motor and sensory axons entering the duplicated dorsal muscles passed through the ventral proximal pathway and normally would have innervated ventral muscles. Recordings from identified motoneurons projecting to native dorsal muscles showed that Ia afferents supplying duplicate dorsal muscles made monosynaptic connections with the appropriate native dorsal motoneurons (Wenner and Frank, 1995). Importantly, these Ia afferents would have normally innervated ventral muscles. Thus, Ia afferent connections with motoneurons are directed by signals they receive from target muscles in the periphery.

2.   ETS genes identify motor pools and specific sensory neurons

The experiments described above demonstrate that patterned neuronal activity is not required for development of specific synaptic connections in the stretch reflex circuit. In addition, the specificity of connections is directed by interactions with target muscles. These facts support the chemical specification hypothesis advanced by Sperry (Sperry, 1963). Unlike the tectal system, however, the molecules that direct connections in the stretch reflex remain unknown. Recent studies in chick have shown that Er81 and PEA3, members of the ETS transcription factor family, are expressed in subsets of sensory and motoneurons that project to the same muscles (Lin et al., 1998). For example, sensory and motoneurons projecting to adductor muscles both express only Er81, while neurons projecting to sartorius and iliotrochanterici muscles express only PEA3.

ETS expression in sensory and motoneurons appears to be dependent on contact with peripheral targets. Er81 and PEA3 expression is first detected in motoneurons and sensory neurons about the time that axons from these cells reach their targets in the limb.

Limb ablation in chick embryos at stages before or around the time when axons reach the

limb results in loss of ETS expression in motoneurons and significant reduction in ETS

expression in sensory neurons. Ablation of limbs at a later stage, however, does not

disrupt the ETS expression patterns, suggesting that patterns of expression are induced

and fixed soon after axon arrival at the target. A possible mechanism for this induction is

discussed below.

The expression pattern of ETS genes as well as the induction of these factors by

interactions with the periphery makes ETS genes attractive candidates for molecules that

regulate formation of the stretch reflex circuit. The aim of this thesis was to explore

potential roles of these ETS factors in the development of the stretch reflex circuit.

Before considering these experiments, however, it is useful to review the role of ETS

factors in other tissues to understand general principles of ETS factor function,

regulations and downstream targets.

2.1 Roles of ETS genes in other tissues

ETS transcription factors are named because they share a common DNA-binding

sequence, the ETS domain (Karim et al., 1990). Structural analysis of the ETS domain

suggests that it is a variant of the winged helix-turn-helix motif (Liang et al., 1994). The

founding member of the family, Ets-1, was identified as an oncogene contained in the

avian erythroblastosis virus, E26 (E twenty-six = Ets) (Leprince et al., 1983; Nunn et al.,

1983). Approximately 30 family members have been identified (Sharrocks, 2001). ETS

genes are also grouped into 10 sub-families based on sequence similarities observed in

the ETS domain as well as other conserved domains. The PEA3 sub-family includes

PEA3 (polyomavirus enhancer activator 3; Xin et al., 1992), Er81 (ETS-related 81; Brown and McKnight, 1992), and ERM (ETS related molecule; Monte et al., 1994).

ETS transcription factors primarily function as transcriptional activators, but particular family members have been shown to repress transcription as well (Mavrothalassitis and Ghysdael, 2000). ETS factors can bind DNA alone, but interactions with numerous other transcription and DNA-binding complex factors have been demonstrated and these interactions enhance binding and transcriptional activation by ETS proteins (Sharrocks, 2001). The ETS domain is critical for ETS protein interaction with DNA, but is also important in protein-protein interactions (Li et al., 2000).

ETS proteins are targets of important intracellular signaling pathways. Activation of MAPKs by growth factors or cytokines in turn activates downstream kinases such as ERK, JNK, and p38 (Whitmarsh et al., 1995). These kinases have been shown to phosphorylate various ETS proteins (Gille et al., 1992). Phosphorylation can enhance DNA binding and transcriptional activation of ETS proteins (Gille et al., 1995).

PEA3 and ERM expression is dependent on FGF8 signaling in zebra fish (Raible and Brand, 2001; Roehl and Nusslein-Volhard, 2001). In embryos lacking FGF8, domains of PEA3 and ERM expression are reduced. Conversely, ectopic expression of FGF8 induces expression of both PEA3 and ERM in novel locations. Notably, FGF8 (along with FGF4, FGF10, and Shh) play crucial roles in the development of the limb bud (Crossley et al., 1996; Lewandoski et al., 2000; Martin, 1998). Consequently, expression of Er81 and PEA3 in sensory and motoneurons is likely induced by FGF signaling present in the developing limb. This may explain why limb ablation at critical

times in chick dramatically reduces ETS gene expression in sensory and motoneurons

(Lin et al., 1998).

Approximately 200 identified genes contain ETS binding sequences in their

promoters and are putative targets of ETS gene activation (Sementchenko and Watson,

2000). The large number of targets underscores the importance of ETS factors in

developing and mature tissues. Of particular interest, ETS genes have been shown to

activate transcription of at least one cadherin gene (E-cadherin) (Gory et al., 1998). The

cadherins are a family of cell surface molecules concentrated at synaptic junctions in the

CNS (Shapiro and Colman, 1999). ETS factors may regulate the expression of particular

cadherins that mediate the formation of synaptic connections in the stretch reflex circuit.

The role of cadherins in the development of the stretch reflex circuit will be explored

more fully in the Discussion.

Loss-of-function experiments have shown that ETS family members are critical

for development of specific cell types, particularly during hematopoiesis. Knock-out

mice of Ets-1 and PU.1 (a Spi sub-family ETS gene) fail to develop T-cells and

megakaryocytes, respectively (Bories et al., 1995; Muthusamy et al., 1995 and

McKercher et al., 1996; Scott et al., 1994). This suggests that ETS genes play a critical

role in the specification of cellular identity. Within nervous system development, the

identification of the ETS-related gene, Pet-1, is of particular interest (Hendricks et al.,

1999). The expression of this protein is restricted to the serotonergic subpopulation of

CNS neurons. Additionally, genes necessary for the serotonergic phenotype (5-HT1a

receptor, serotonin transporter, and tryptophan hydroxylase) are directly regulated by

Pet-1 protein. Although loss-of-function experiments have not directly tested the role of

Pet-1 protein, these experiments suggest that ETS proteins may regulate neuronal phenotype.

2.2   ETS gene expression in chick

Many motor pools can be identified by expression of ETS genes (Lin et al., 1998). For example, motoneurons projecting to the adductor muscle express Er81, but not PEA3. Conversely, iliotibialis motoneurons express only PEA3 and not Er81. Many functionally distinct motor pools that are located at the same segmental level express the same ETS gene, so ETS gene expression alone does not uniquely identify all motor pools. Combinatorial expression of ETS genes in addition to that of other transcription factors expressed in subsets of motoneurons greatly increases the number of motoneuron pools that could be uniquely identified. Accordingly, adductor (**A**) and external femorotibialis (**EF**) motoneurons, both of which express Er81, can be distinguished by coexpression of Lim1 (**EF**) or Isl1 (**A**).

Expression of Er81 and PEA3 also defines different subsets of sensory neurons located in the DRG (Lin et al., 1998). PEA3 expression is detected in chick beginning at stage 26-27, while Er81 expression is not detected until stage 29. At this stage there is considerable overlap in expression of Er81 and PEA3 with ~70% of ETS+ sensory neurons expressing both genes. This expression segregates later in development so that by stage 32 only 10% of ETS+ cells express both ETS genes. Almost all trkC+ neurons (marker for muscle sensory afferents) are ETS+, but no trkA+ neurons (marker for cutaneous afferents) express either ETS gene. Strikingly, the ETS phenotype of sensory neurons often matches the ETS phenotype of the corresponding motor pool.

2.3   ETS gene expression in mice

In a pattern similar to that found in chick, Er81 and PEA3 in mice are expressed

in subsets of motoneurons at limb levels (see Figure 2; Arber et al., 2000). As in chick,

some motor pools express Er81, some express PEA3, and others express neither ETS

gene. No motoneurons express both ETS genes. Interestingly, different motor pools that

are found at the same rostral-caudal level and even the same region of the LMC can

express different ETS genes. For example, Er81 is expressed by all quadriceps

motoneurons (located in the LMC_L of spinal segments L1-L2), except those that project

to the rectus femoris head; these express PEA3. Er81 is also expressed in the adductor

muscle group of motoneurons located in the LMC_M of these same spinal segments. ETS

genes additionally label several motor pools located in more caudal segments. Er81 is

not expressed in the brachial level of the cord, but PEA3 is expressed in cutaneous

maximus motoneurons (see Results). Thus, as in the chick, ETS genes label individual

motor pools.

PEA3 and Er81 are also expressed in a subset of sensory neurons in murine DRG

(see Figure 3; Arber et al., 2000). PEA3 expression is first detected at E12.5 followed by

Er81 expression at E13.0. As in the chick, a majority of ETS-expressing sensory neurons

coexpress PEA3 and Er81 early in development (~90% at E13.5). Throughout

development there is a high degree of coincidence between Er81 expression and the

muscle sensory afferent markers trkC and parvalbumin (PV). The calcium binding

protein PV has been shown to label both Ia and Ib afferents robustly in the periphery as

well as the somata of these afferents in the DRG (Celio, 1990; Copray et al., 1994). Er81
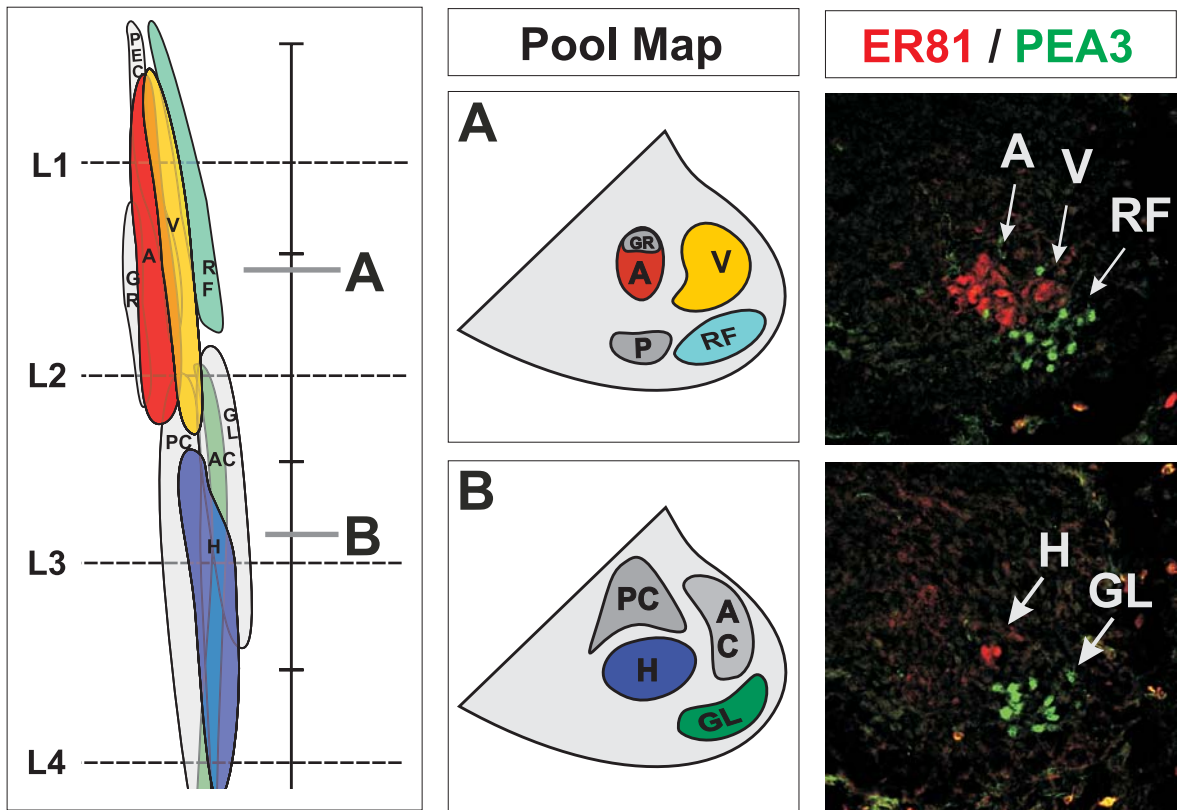
Figure 2. Er81 and PEA3 are expressed by subsets of lumbar motoneurons in mouse embryos. *Left panel*: Schematic diagram of motor pools in lumbar segments L1-L4 seen in horizontal section (modified from McHanwell and Biscoe, 1981). *Center panels*: Motor pool schematic in transverse section. **A** and **B** indicate sections at corresponding levels to those in left panel. A: adductor; GR: gracilis; V: vasti; RF: rectus femoris; P: pectineus; PC: posterior cruz; AC: anterior cruz; H: hamstring; GL: gluteal. *Right panels*: Double label immunohistochemistry for Er81 (red) and PEA3 (green). A, V and H motoneurons express Er81, and RF and GL motoneurons express PEA3. Some motoneurons (P, PC, AC) do not express either ETS gene. Figure adapted from Arber et al., 2000.
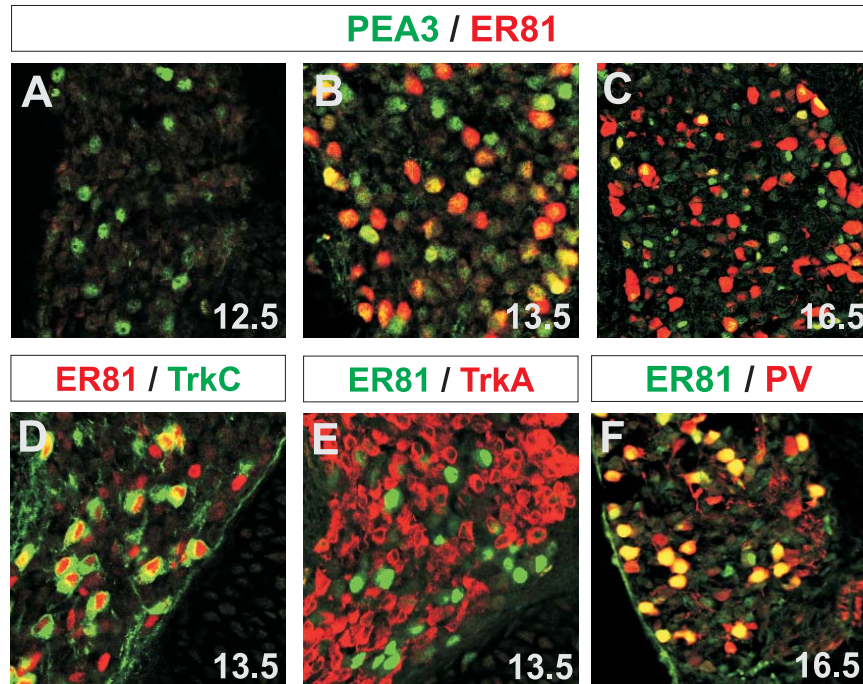
Figure 3. Er81 and PEA3 are expressed in developing DRG neurons in mouse embryos. (**A-C**) Double label immunohistochemistry for Er81 (red) and PEA3 (green) demonstrates time course of ETS expression in DRG. (**A**) PEA3 is first expressed in DRG cells at E12.5. (**B**) By E13.5, Er81 and PEA3 are coexpressed in ~60% of ETS+ neurons. (**C**) By E16.5, Er81 is expressed in almost all ETS+ cells while PEA3 expression is reduced. The incidence of coexpression of Er81 and PEA3 has decreased to ~15%. (**D-F**) Er81 is expressed in trkC+, but not trkA+ sensory neurons. (**D**) Double label immunohistochemistry for Er81 (red) and trkC (green) in E13.5 DRG. Er81 is expressed in nearly all trkC+ neurons. In addition, Er81 also appears to be expressed by a population of trkC- cells (~30% of Er81+ cells). (**E**) Double label immunohistochemistry for Er81 (green) and cutaneous afferent marker, trkA (red) in E13.5 DRG. Er81 is not expressed in trkA+ neurons. (**F**) Double label immunohistochemistry for Er81 (green) and muscle sensory afferent marker, parvalbumin (PV, red) in E16.5 DRG. Nearly all PV+ neurons (>95%) express Er81. Figure adapted from Arber et al., 2000.

is not found in cells expressing the cutaneous sensory neuron marker, trkA. In contrast to the pattern in chick, Er81 is expressed in nearly all PV+ neurons until at least P10. On the other hand, PEA3 expression in sensory afferents declines during development; by E15.5 only 10% of PV+ neurons also express PEA3.

3.   Conclusions

Er81 and PEA3 are the first molecules identified that label functionally connected sensory and motoneurons. The temporal and spatial expression pattern of Er81 and PEA3 suggests that these factors, or downstream genes they regulate, might control the formation of specific connections in the development of the stretch reflex circuit. In addition, ETS gene expression is regulated by signals in the limb, consistent with previous results that implicate muscle targets as controlling the specificity of synaptic connections (Wenner and Frank, 1995). If Er81 and PEA3 expression in sensory and motoneurons provide signals for specific synapse formation, perturbations in expression of these genes would be expected to disrupt the pattern of these connections. To test this hypothesis, null allele mutant mice were generated for both Er81 and PEA3. Analysis of these mice is presented in the following sections.

2. Materials and Methods

1. PCR determination of mouse genotype

2 mm tail samples were collected from 2-3 day-old pups. Tail samples were digested in Proteninase K enzyme cocktail overnight at 57ºC. Digested samples were dilulted 1:500 and processed for PCR. Reactions were run with 6.0 pmol of primers appropriate for specific strains. Primer sequences for Er81 and PEA3 strains are as follows: Er81 endogenous primers: 5'-ATTTCATTGCCTGGACTGGACGAG, 3'-TCACTCACAGAATGTTGTCTCTCC; Er81 tau-insert primers: 5'-CATGGCTGAGCCCCGCCAGGAGTTCG, 3'-CTGCGGTCCCCGGATTTCCCAG; PEA3 endogenous primers: 5'-GGAATCTTGGGCCTTGAGAACAGC, 3'-GTGTGATGTACATATGCCCTAACC; PEA3 NLS-lacZ insert primers: 5'-GAAGACCCCCGCATGGCTCGCGATG, 3'-GATCTTCCAGATAACTGCCGTCACTCC. Products of PCR were resolved using gel electrophoresis (1.5% agarose in TAE).

2. Isolated spinal cord preparation

The animals used in these experiments ranged in age from P4 to P10. Animals are anesthetized on ice for 1-2 minutes and placed on a dissecting dish cooled to 4°C by a Peltier device. Once the abdominal skin is removed and the chest cavity opened, the animal is perfused with 5ml of ice-cold aerated Ringer solution. Following perfusion, the animal is decapitated and eviscerated.

The same concentration of Ringer's solution is used for perfusion, dissection and recording. The solution contains: NaCl (127 mM), KCl (1.9 mM), KH_2PO_4 (1.2 mM),

$CaCl_2$ (2 mM), $MgSO_4$ (1 mM), $NaHCO_3$ (26 mM), supplemented with 3.7 g/l (20.5 mM) D-glucose.

Working from the dorsal surface, the skin is removed as well as limbs whose muscle nerves will not be isolated in a particular experiment. For lumbar experiments the vertebral column is transected at T5 and all rostral tissue is discarded. For brachial experiments tissue caudal to L2 is discarded.

The isolated vertebral column and attached limb(s) are then transferred to a larger dissecting chamber filled with 100 ml Ringer solution, recirculated at 12 ml/min. The reservoir of Ringer is kept ice-cold and is saturated with 95% O_2 : 5% CO_2 via a bubbler. The temperature in the dissecting chamber is 15 °C, which appears to be optimal for the isolation of the spinal cord.

The dorsal surface of the spinal cord is exposed by removing the axial muscles over the vertebral column as well as the dorsal laminae of each vertebra. The dura mater is then removed from the dorsal surface along the length of the cord. Next, unneeded dorsal and ventral roots are cut proximal to the DRG. This allows the cord to float above the open vertebral canal promoting rapid, continuous fluid flow around the experimental region of the cord.

The preparation is now stable in the bath for up to two hours, thus allowing sufficient time to complete careful dissection of other muscle nerves (see Figure 4). After all muscle nerves have been dissected, the final preparation consisting of the muscle nerves, the DRG and the spinal cord is isolated by cutting through the body of each of the remaining vertebrae (see Figure 5).
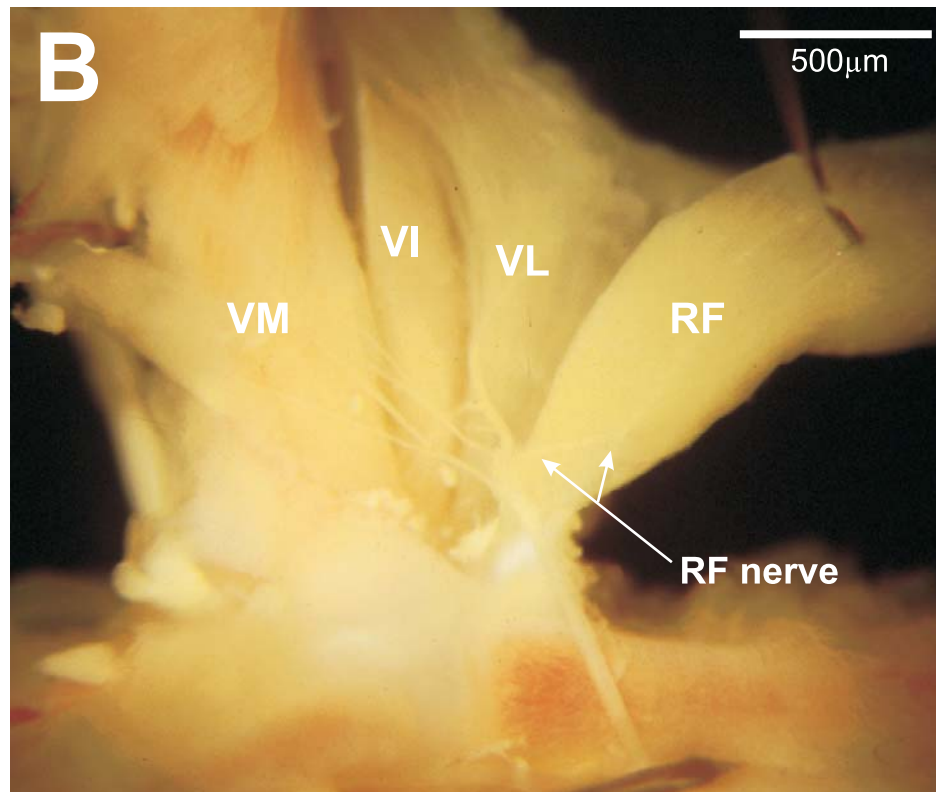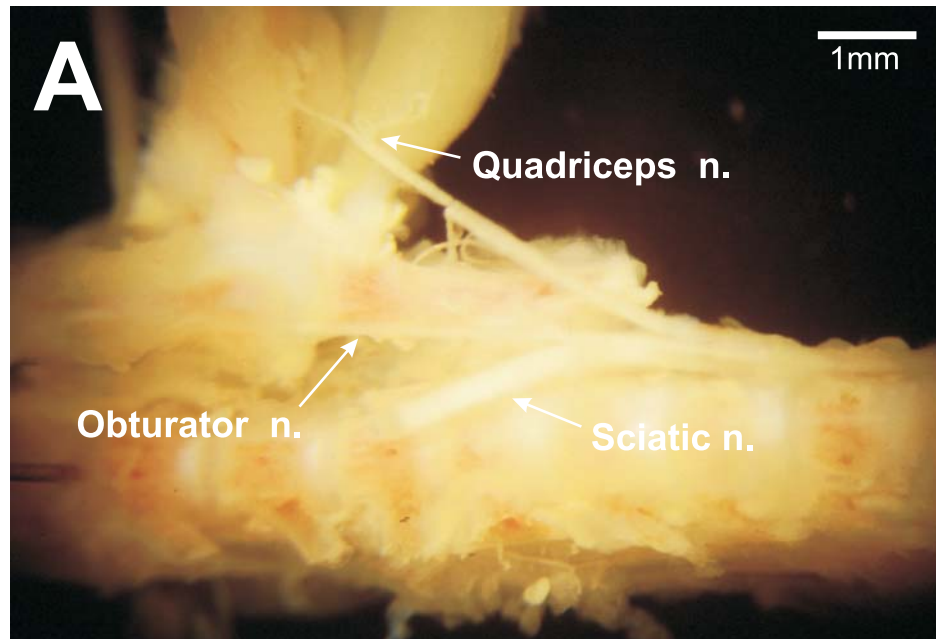
Figure 4. Dissection of Quadriceps and Obturator muscle nerves. (A)
Photograph of deep ventral surface of pelvic region in P10 mouse. Labels indicate sciatic
nerve (cut), common obturator nerve, and quadriceps nerve (the terminal branches of the
posterior division of the femoral nerve). **(B)** Photograph of quadriceps muscle group and
supplying nerve branches. Labels indicate the four muscle heads of the quadriceps
group: vastus medialis (VM), vastus intermedius (VI), vastus lateralis (VL), and rectus
femoris (RF). The branches of the quadriceps nerve that project to RF are also indicated.
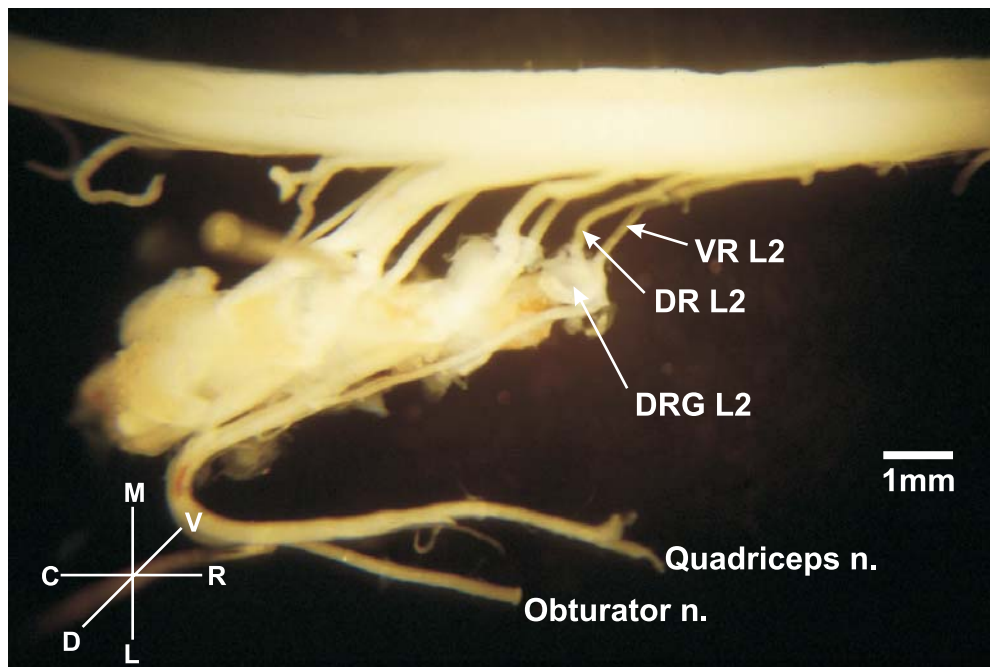
Figure 5. Isolated spinal cord preparation. Photograph of typical dissection of spinal cord and muscle nerves for ventral root or intracellular recordings. Muscle nerves, such as quadriceps and obturator, are drawn into separate suction electrodes for stimulation. For ventral root recordings, ventral roots are transected proximal to DRG and proximal cut end drawn into suction electrode. For intracellular experiments, microelectrodes are advanced by a micromanipulator through the cut medial surface of the cord.

The preparation is then transferred from the dissecting chamber to a recording chamber filled with recirculating Ringer solution at 21°C. The preparation is allowed to equilibrate at this temperature for approximately 10 minutes. The bath temperature is then slowly elevated using a Warner Instruments TC-324 temperature controller and the preparation is left undisturbed for 1.5 hours prior to recording to stabilize at the recording temperature (see below).

3. Extracellular recordings from dorsal and ventral roots

Intracellular recordings from motoneurons are a standard technique used to determine the responses of motoneurons to stimulation of sensory afferents. A drawback of this technique, however, is the limited amount of data that can be collected from a given animal. On the other hand, a quick overall view of sensory-motor connections can be made with extracellular ventral root recordings. This technique measures the compound responses of all motoneurons exiting from a particular ventral root. Although information about responses from individual motoneurons cannot be obtained with this technique, its advantages made it desirable in screening for possible defects in ETS mutant mice (see Figure 6).

Extracellular recordings are made at 25°C in a chamber filled with recirculating, oxygenated Ringer's solution (3 ml chamber volume; 9 ml/min flow rate). Extracellular potentials are recorded differentially between the inside of the suction electrode placed on the dorsal or ventral root and a second electrode placed nearby. In the case of ventral root recordings, the ventral root is drawn into a suction electrode and a tight seal is formed between the suction electrode and the surface of the spinal cord. For dorsal root
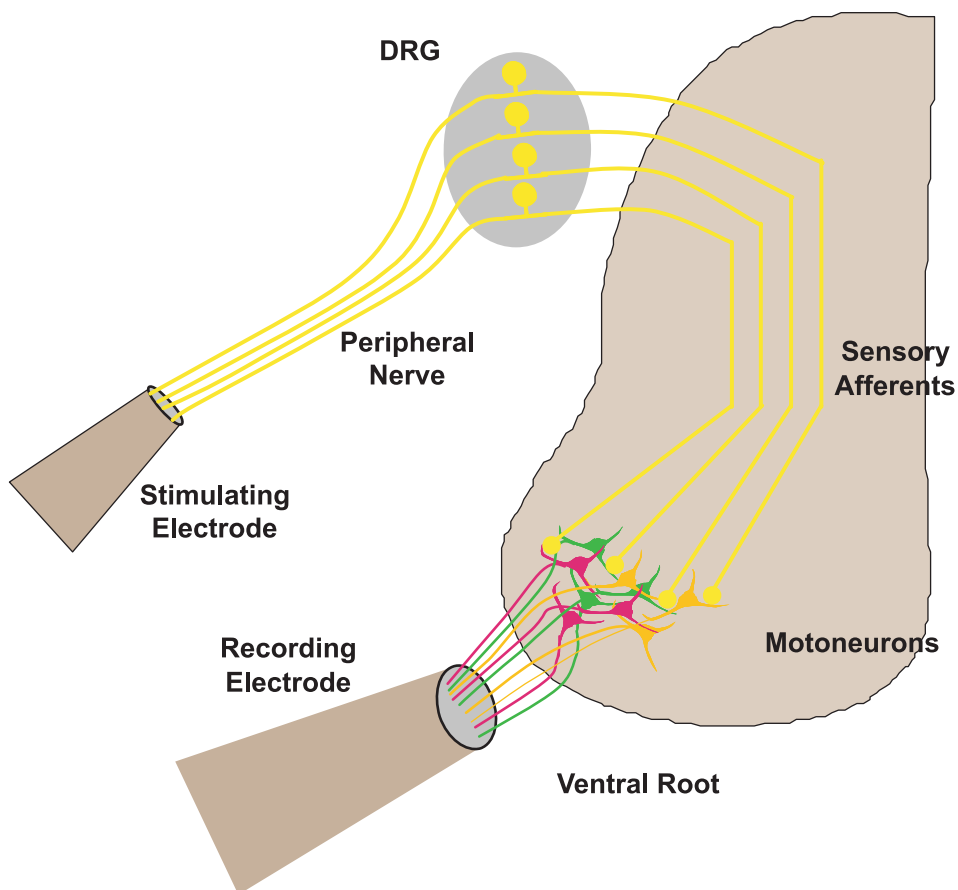
Figure 6. Extracellular ventral root recordings monitor response of motoneurons to sensory stimuli. The ventral root recording technique records compound responses (both action potentials and synaptic potentials) from all motor axons (indicated by various colors) contained in a ventral root. Sensory afferents in a separate suction electrode are activated via an electric stimulus. This technique does not provide information about which motoneurons are contributing to the signal, but provides a measure of the average input to all motoneurons from the sensory afferents that are stimulated.

recordings the seal is formed against the surface of the DRG.

Each muscle nerve is drawn into a separate suction electrode and stimulated electrically (0.1 ms at 4.0-9.0 V) via a Grass S8800 stimulator and a Grass Stimulus Isolation Unit. This stimulation evokes a maximal ventral root response without significant spread of the stimulus to other nerves.

The recorded potential is amplified with a Grass P15C A.C. preamplifier (0.1 Hz Low- and 2kHz High-Pass Filter) to an Axon Instruments PCI-MIO-16E A/D interface board. Traces are stored on an IBM-PC using custom software. Traces are also visualized on an oscilloscope. Recorded traces are averages of 8 to 20 individual stimuli applied at 0.5-1.0 Hz.

3.1.   Theory of extracellular ventral root recordings

Ventral root recordings measure compound action potentials as well as compound subthreshold synaptic potentials in much the same way that intracellular recordings measure the membrane potential of single neurons. This is made possible by the fact that action potentials (APs) and excitatory post-synaptic potentials (EPSPs) generated in the somata of motoneurons are propagated along the axons, albeit with attenuation of subthreshold signals. Because the entire axon of the sensory or motoneuron is located in the recording pipette, the changes in membrane potential of the axon can be amplified and recorded. This technique is analogous to placing a microelectrode in the soma of each neuron and then summing the recorded potentials together in the recording electrode.

For example, a subthreshold membrane depolarization originating in the soma of a motoneuron is propagated passively down the axon as a small positive current traveling longitudinally down the axon. As this positive current enters the suction electrode, the interior of the electrode becomes more positive than the bath outside the electrode (ground); this is reflected by a positive potential that is recorded by the wire in the pipette. After the current passes, this positive potential then decays to zero as longitudinal currents discharge the membrane.

Recordings of APs are made in the same way as synaptic potentials, but the recorded waveform is more complicated due to the positive and negative currents that accompany the action potential. As the AP approaches the recording electrode a longitudinal positive current precedes it, the same as with a propagating synaptic potential. As the leading phase of the AP enters the electrode, however, the positive potential is reversed due to the strong positive *inward* current generated by Na^+ ions entering the axon that makes the interior of the electrode negative with respect to ground. As the falling phase of the AP enters the electrode (positive *outward* current generated by K^+ ions leaving the axon), the interior again becomes positive with respect to ground and then decays back to zero, as with EPSPs.

3.2. Quantification of monosynaptic amplitudes in ventral root recordings

The amplitude of the monosynaptic component of each ventral root recording is determined by comparison with an age-matched monosynaptic model trace (see Figure 7). This model trace is generated by reducing the stimulus voltage to the level at which a minimum EPSP is evoked in the ventral root record. This stimulus activates only the
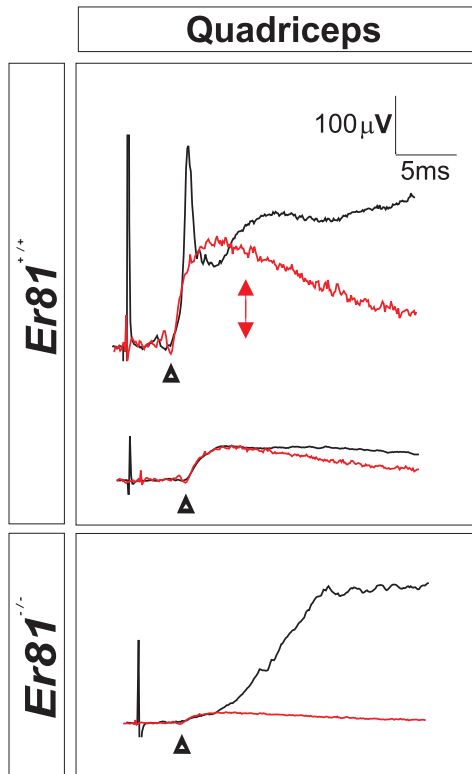
Figure 7. Monosynaptic component of recorded traces are quantified using model traces. Panels show L3 ventral root potentials evoked by stimulation of quadriceps muscle in Er81 normal (*top panel*) and Er81 mutant (*bottom panel*) mice. Black traces are responses to full-strength stimulation. All red traces are scaled versions of a single minimal stimulation response from an age-matched normal animal. Minimal stimulation activates only Group I afferents and evokes only monosynaptic potentials in motoneurons via Ia afferent inputs. The model trace is scaled up or down in the vertical dimension (indicated by arrows) under software control to match the peak of the early component of the full-strength ventral root potential. If an action potential is contained within the monosynaptic component, the model trace is scaled such that the rising phase of the experimental and model traces are superimposed. The point at which the two slopes diverge is considered to be the beginning of the action potential. The monosynaptic amplitude is then taken as the peak of the monosynaptic model. Black arrowheads indicate the beginning of the synaptic potential.

largest diameter fibers—the group I afferents. Within this group only Ia afferents make monosynaptic connections with motoneurons. Additionally, minimal stimulation is unlikely to activate interneurons; therefore the recorded potential represents only monosynaptic input. This minimal EPSP has a steep rising phase, followed by a smooth exponential decay with no shoulders. The absence of shoulder potentials confirms that there is little, if any, contamination from polysynaptic inputs to motoneurons. The time interval between stimulus and the onset of the minimal EPSP decreases with age, thus it is critical to use a model trace from an age-matched animal.

The monosynaptic amplitudes of recorded traces are determined offline. Different models are used for each muscle nerve as well as for each ventral root recorded from, in order to match peripheral conduction time and types of input between the experimental and model traces as closely as possible. The model trace is scaled up or down in the vertical dimension (in μV) under software control to match the peak of the early component of the recorded ventral root potential (see Figure 7). If the response being measured includes an action potential within the monosynaptic component (see Figure 7, top panel), the model trace is scaled such that the rising phases of the experimental and model trace are equal. The point at which the two slopes diverge is considered to be the beginning of the action potential. The monosynaptic amplitude is then taken as the peak of the monosynaptic model. Student's t-test is used to evaluate statistical significance ($p < 0.05$).

4.   Intracellular recordings from identified motoneurons

Muscle nerves innervating vasti (vastus medialis, vastus intermedius, and vastus lateralis), rectus femoris, and adductor muscles were dissected and stimulated separately. Unlike in extracellular experiments, the spinal cord was hemisected to maximize oxygen availability for motoneurons. This was accomplished by first separating the dorsal half of the spinal cord along the midline with fine scissors. Then the ventral half of the cord is also separated along the midline (see Figure 8 and Mears and Frank, 1997). Recordings were made at 30º C in a custom perfusion chamber designed to accommodate high flow rates (chamber volume 2.5 ml; flow rate 35 ml/min).

Electrodes are constructed of 1.2 mm thin-wall glass micropipettes with filaments from World Precision Instruments pulled on a Model P-80/PC Flaming/Brown micropipette puller. Electrodes are filled by capillary action with 2M potassium methylsulfate and beveled on a Sutter Instrument BV-10 KT Brown Type micropipette beveler to a resistance of 90-180 MΩ (Brown and Flaming, 1986). In some experiments, 200 mM QX-314 was added to reduce the amplitude of antidromic action potentials (Alamone Labs, Jerusalem, Israel; Llinas and Yarom, 1981).

A Sutter Instrument MP-285 motorized micromanipulator was to position the microelectrode, which was introduced through the cut medial surface of the spinal cord. Recorded signals were amplified using an Axon Instruments Axoprobe-1A multipurpose microelectrode amplifier, digitized (10 pts/ms) via a National Instruments A/D interface board, and stored on an IBM-PC using custom software. Stored traces are the average response of 8-20 individual stimuli applied at 0.5-1.0 Hz.
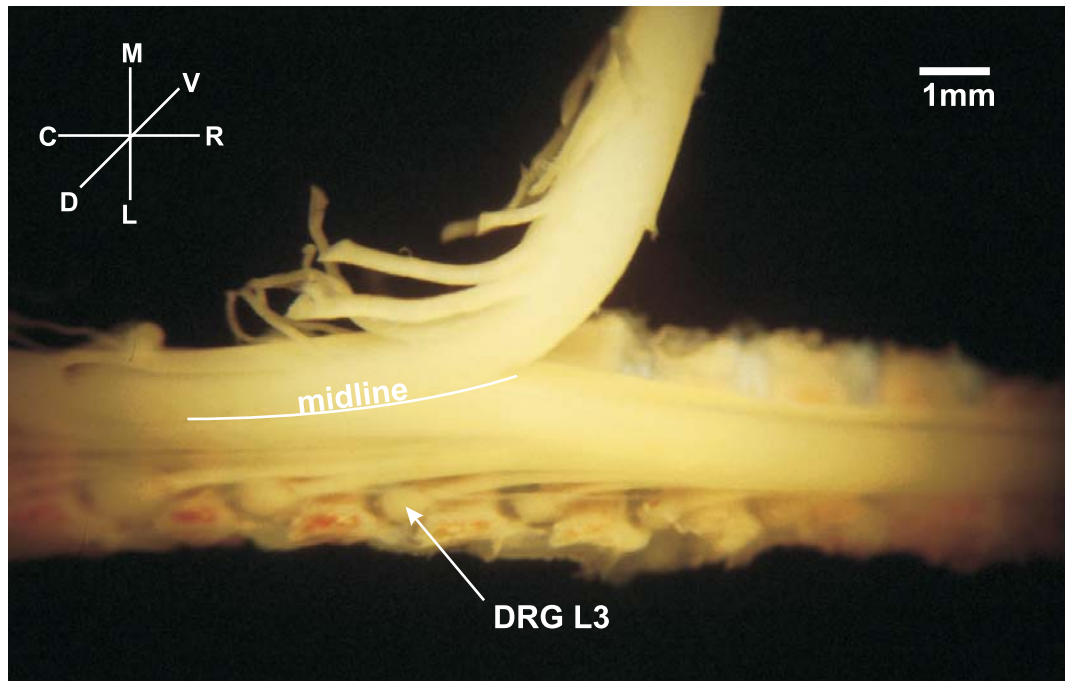
Figure 8. Example of hemisected spinal cord preparation. Photograph from dorsal surface of lumbar region of P10 spinal cord. Dorsal and ventral roots on one side of the cord have been cut. Intact dorsal roots and DRG can be seen between vertebrae. Spinal cord is separated along the midline, beginning at the rostral end of the cord.

Each muscle nerve was placed into a separate suction electrode and stimulated via a Grass S88 stimulator (3.0-5.5V amplitude; 0.1ms duration). Motoneurons were identified by antidromic activation via one of the muscle nerves. The antidromic potential recorded at the soma is the result of a back-propagating action potential initiated at the distal end of the motoneuron axon.

4.1.   Analysis of intracellular records

Monosynaptic models were obtained from each animal for each homonymous projection (i.e. RF sensory afferents to RF motoneurons). This model was then used to quantify the monosynaptic component of full-strength stimuli applied to muscle nerves in both normal and PEA3 mutant mice as described above (see also Figure 25). Student's t-test was used to determine statistical significance ($p<0.05$).

5.   Selective stimulation of muscle sensory afferents

Ia afferents have high sensitivity to changes in muscle length and are strongly activated by brief, small amplitude passive stretches of the muscle. Conversely, Ib afferents are selectively stimulated through low amplitude stimulation of the ventral root that activates α- but not γ-motoneuron axons. This stimulus generates sufficient muscle tension to excite Ib afferents. Muscle spindles are thereby unloaded, effectively silencing Ia afferents.

In these experiments, Ia and Ib afferents innervating the rectus femoris muscle of the quadriceps group were stimulated. The surrounding denervated muscles were dissected away, leaving only the innervated rectus femoris attached to both the pelvic

bone and the patellar tendon. In the recording chamber, pins through the patella and through the pelvic bone immobilize the muscle. The muscle is pinned at a length of 0.8X to 1.2X resting length.

5.1. Selective stimulation of Ia afferents

Small amplitude stretches are delivered to the muscle by slightly deflecting the pin through the patella with a stiff broom straw connected to a piezoelectric device driven by a Grass S8800 stimulator. A standard stimulus of 150 V for 1.0 ms results in a deflection of the broom straw of approximately 100 μm, although the actual deflection of the muscle is less.

5.2. Selective stimulation of Ib afferents

α-Motoneuron axons are activated via a stimulating suction electrode placed on the distal cut end of a ventral root. The stimulus strength is adjusted to determine the minimum stimulus required for robust muscle contraction when observed by eye, usually between 3.0-4.0V (duration=0.1 ms). Because γ-motoneuron axons that innervate muscle spindles are substantially smaller and thus have a substantially higher threshold than α-motoneuron axons, this low stimulus is unlikely to activate significant numbers of γ-motoneuron axons.

6. Motoneuron dendrite labeling with HRP

Lumbar segment L3 ventral roots were labeled with HRP to visualize motoneuron cell bodies and dendrites. Lumbar spinal cords were dissected as described above.

Ventral and dorsal roots were transected proximal to the DRG. The L3 ventral root was drawn into a tight-fitting glass capillary. The Ringer's solution inside the capillary was removed and replaced with a saturating solution of HRP and 50 mg/ml lysolecithin in water. The HRP solution was allowed to incubate for 45 minutes and then removed. The spinal cord preparation was incubated overnight at 25ºC. The preparation was fixed with 4% paraformaldehyde and embedded in gelatin-albumin. Transverse sections (50 μm) were made on a freezing microtome and reacted for HRP product. Images were acquired using IPLab software with a Princeton Instruments MicroMax cooled CCD camera and stored on a Macintosh G4 computer.

7.   Fluorescent labeling of sensory and motoneurons

Sensory and motoneurons projecting in different muscle nerves were labeled with 3000 MW tetramethylrhodamine- or fluorescein-dextran (Molecular Probes, Eugene, OR). The brachial region of the spinal cord was isolated as described above and the pectoralis minor-cutaneous maximus and biceps nerves were dissected. The dorsal and ventral roots supplying the brachial plexus were left intact. Each nerve was drawn into separate tight-fitting glass capillaries. The Ringer's solution in the capillary was then removed and exchanged with dextran dye solution. The dextran dye solution contained 100 mg/ml of 3000 MW fluorescent-conjugate dextran and 1% lysolecithin dissolved in water. The dye was left in the capillaries overnight to maximize retrograde transport (Reiner et al., 2000). The spinal cord and muscle nerve preparation was incubated overnight (15-17 hours) at 30º C in a recirculating (35 ml/min) oxygenated bath. Spinal cords were fixed for 1-2 hours in 4% paraformaldehyde, then equilibrated in 30% sucrose

solution for cryoprotection. Muscle nerves were removed and the spinal cord and DRG were trimmed to include only C4-T1 segments. Tissue was embedded in mixture containing OCT embedding medium and 30% sucrose (50:50 v:v). Transverse sections (20 μm thick) were cut with a cryostat. Slides were protected with Gel-Mount aqueous mounting medium and a glass coverslip. Fluorescent cells were visualized using a UV light source with appropriate filters on a Nikon light microscope. Images were acquired using a Princeton Instruments MicroMax cooled CCD camera with IPLab imaging software and stored on a Macintosh G4 computer.

7.1.   Analysis of fluorescently labeled motor and sensory neurons

Numbers of labeled motoneurons were determined by analyzing serial sections through the C4-T1 spinal segments. The rostral boundary of each spinal segment was judged to be the section in which dorsal root fibers could first be seen entering the dorsal horn. Spinal segments averaged 600 μm in length (approximately 30 20 μm sections). Nuclei of labeled cells were brighter than the surrounding cytoplasm and motoneurons in each section were counted if a complete nucleus was observed. Labeled sensory neurons in each section containing DRG tissue were counted if the cell profile was larger than 15 μm.

Pool maps of labeled MAT motoneurons were constructed for C7 and C8 segments. Beginning at the rostral end of each segment, bright-field and fluorescent images were captured of every third section (10 sections total for a 600 μm segment). Bright-field images of each of the 10 sections were aligned using Adobe Photoshop such that the midline and lateral gray-white border in individual sections were in register. The

fluorescent images corresponding to the 10 bright-field images were displayed as overlays on one of the bright-field images from the center of the segment. Pool maps, therefore, show approximately one-third of the total number of labeled cells observed in a given segment.

8.   Determination of total motoneuron number

Sections from dextran-labeled preparations were counterstained with thionin to determine the total number of motoneurons per spinal segment. Motoneuron counts were restricted to the LMC and individual motoneuron profiles were counted only if they had a "large soma, a clear nucleus with intact nuclear membrane, and at least one large clump of nucleolar material" (Clarke and Oppenheim, 1995). Oppenheim reports that analysis of serial sections considerably thinner than those used in this study (8-12 um) motoneurons displayed all three characteristics in less than 2% of adjacent sections (Clarke and Oppenheim, 1995). Use of these exacting criteria in counts of the thicker sections (20 um) used in this study is, therefore likely to yield accurate results without employing standard correction calculations. Counts were made of every third section throughout a spinal segment. The total number of motoneurons per segment was then calculated as 3 times the number of counted profiles.

Regions of interest were delineated to determine the number of motoneurons in different compartments of the LMC. In both PEA3 mutant and normal animals, motoneurons in the LMC were found in two clusters separated by a region of gray matter relatively devoid of motoneurons (see Figure 18). Motoneurons located in the more dorsally located clustered were scored as being located in the dorsal compartment.

Motoneurons located outside the dorsal cluster were counted in the ventral compartment. The number motoneurons residing in each compartment were counted in every third section throughout a spinal segment. The total number of motoneurons located in each compartment was then calculated as 3 times the number of counted profiles in each compartment. A similar method was employed in determining the number of labeled MAT motoneurons located in each LMC compartment. To aid in this analysis, a line bounding the dorsal cluster was drawn on bright-field images of each section in a segment using PhotoShop. Labeled cells observed in the corresponding fluorescent images of each section were then scored as being either in the dorsal or ventral compartment, based on their location. Again, every third section throughout a segment was counted. The total number of labeled cells was then calculated as 3 times the number of cells counted in each compartment.

3.   Analysis of Er81 null-mutant mice

1.   Er81 mutant mice are ataxic.

A clear motor coordination defect is observed in Er81 mutant mice as early as P4. Movement of the four limbs together is often uncoordinated making the resulting movements spastic. Although mutants are born at the normal Mendelian frequency, they are smaller than littermates. Mutant animals die within 3-4 weeks after birth. Heterozygous pups develop normally and both anatomical and physiological analyses have revealed no defects. Therefore, wild type and heterozygous animals will be referred to as normal animals.

2.   A subset of muscle sensory afferents is affected in Er81 mutants.

Because Er81 is expressed in nearly all trkC+ neurons (see Introduction), we first investigated the responses of muscle sensory neurons in Er81 mutants. Electrically evoked action potentials in sensory axons were recorded with extracellular suction electrodes in the dorsal root. At P8-9, the average amplitude of the compound action potential recorded following quadriceps muscle nerve stimulation in Er81 mutants was not statistically different from that observed in normal animals (216µV versus 260µV; n=4 and n=6, respectively; see Figure 9). The similarity in amplitude suggests that sensory axons are present in normal numbers and survive postnatally. This corroborates anatomical evidence provided by Silvia Arber that sensory neurons in general are born in normal numbers and survive postnatally. More specifically, sensory neurons that would
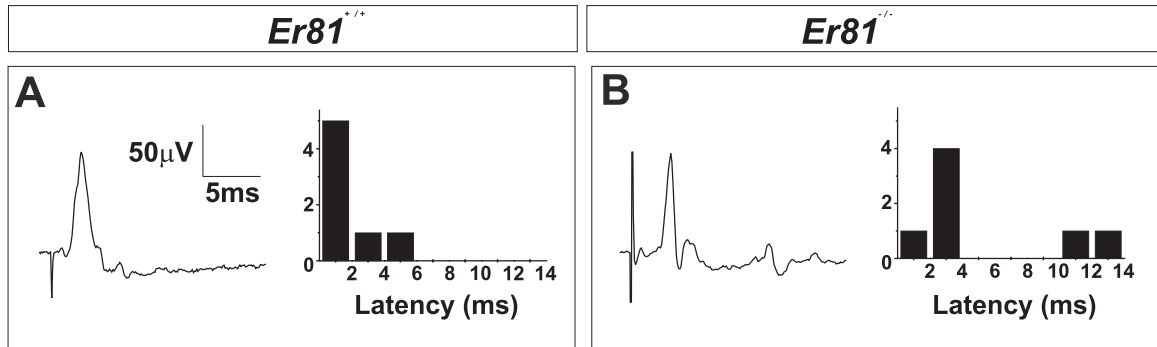
Figure 9. Electrical stimulation of quadriceps sensory afferents recorded at dorsal root L3. At P8-9 the average amplitude of Group I afferent compound action potentials in normal mice (**A**) was not different from response in Er81 mutant mice (**B**) [normal 260μV (n=6) and mutant 216μV (n=4)]. The latency of Group I response in dorsal roots was longer in mutants than in normal animals as shown by the histograms in **A** and **B**. Note also the existence of more slowly conducting afferents in **B**.

have expressed Er81 (visualized with a 5' probe for the truncated Er81transcript) are generated and survive postnatally as well in Er81 mutants (Arber et al., 2000).

Although the numbers of muscle sensory axons were unchanged in mutant mice, two elements of the dorsal root response indicated that sensory axons were not completely normal. First, the conduction time of Group I afferents (latency to first peak in the response) was significantly longer in Er81 mutants by 1.5ms. In addition, very long latency responses were often observed in traces from mutant animals. These peaks had latencies of 10-14 ms and represent axons with very low conduction velocities. Such fibers were not observed in normal animals. The slower conduction velocity suggests that many Group I sensory axons may be of smaller caliber, perhaps because they are atrophic.

To further examine the change in Group I responses we recorded in the dorsal root the responses to selective stimulation of the two major classes of Group I afferents: Ia and Ib afferents. Ib afferents terminate on Golgi tendon organs (GTO), specialized mechanoreceptors located at the myotendinous junction (MTJ) of almost all muscles. In response to muscle contraction, the GTO is stretched resulting in deformation of the Ib axon terminal and, consequently, in the generation of a burst of action potentials. Unlike Ia afferents that project strongly to motoneurons, Ib afferents project only to spinal interneurons (Jami, 1992). Ib afferents make major projections to lamina VII where they form synapses with Ib interneurons. Ib interneurons, which can be either excitatory or inhibitory, project to motoneurons up to several segments away.

Selective activation of Group Ib afferents revealed no defects in Er81 mutants (see Figure 10). Ib, but not Ia, afferents are activated by muscle contraction following
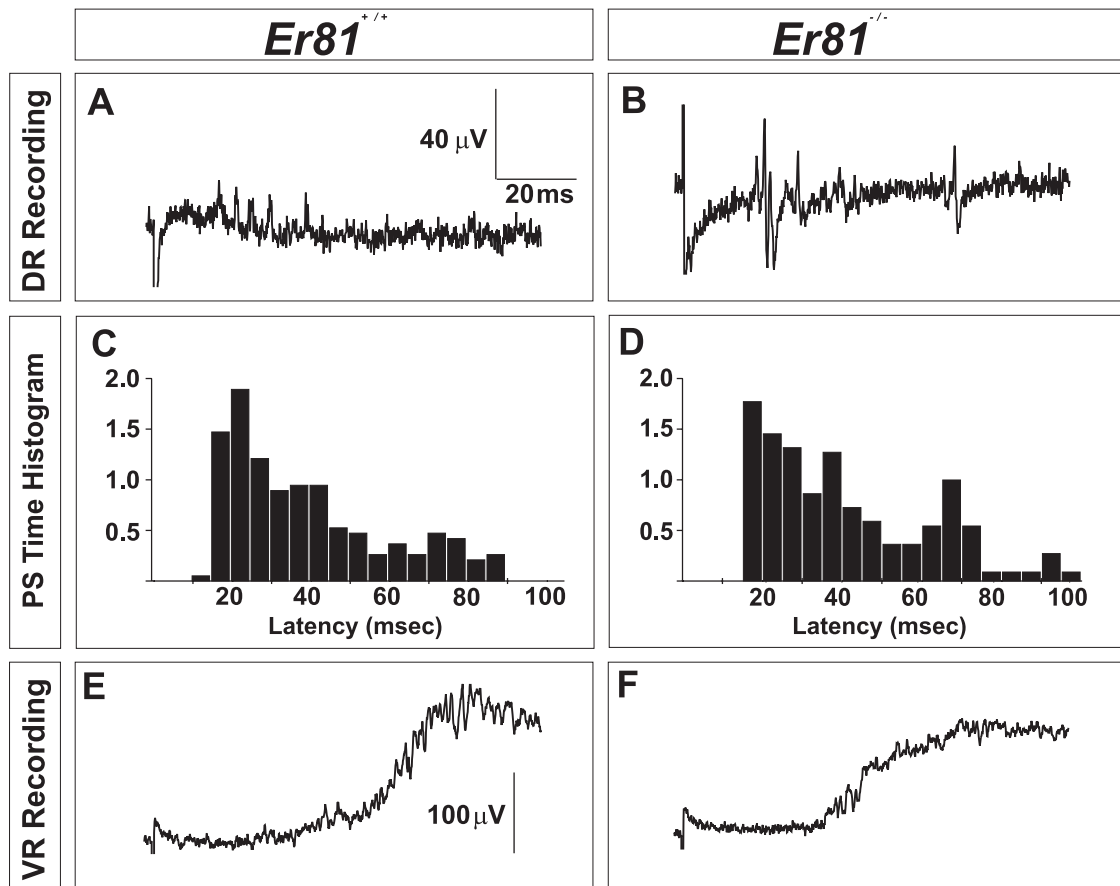
Figure 10. Ib afferent responses recorded at dorsal and ventral roots appear normal in Er81 mutants. (**A, B**) Selective stimulation of Ib axons innervating the RF head of the quadriceps muscle recorded in the L3 dorsal root. A single stimulus elicits a burst of several action potentials in both Er81 normal (Er81^{+/+}) and mutant (Er81^{-/-}) mice (7.6 1.5 in 7 mutant mice and 8.2 + 1.6 in 7 normal mice). (**C, D**) Post stimulus time histograms (~20 trials, shown as spikes / bin) show that latency and distribution of action potentials are similar in both normal and mutant mice. (**E, F**) Ib afferent stimulation evokes a similar delayed synaptic response in motoneurons, recorded at ventral root L3, in normal and mutant mice. The slow rising phase of this potential is the result of asynchronous inputs from interneurons. Calibrations in **A** and **E** also apply to **B** and **F**.

stimulation of motor axons in the ventral root (see Materials and Methods). In response to this stimulation, Ib afferents in normal animals fire a volley of 7-8 spikes beginning about 15 ms after the stimulus (see Figure 10A). Ib responses from Er81 mutants recorded in the dorsal root yielded similar results to those observed in normal animals (see Figure 10B). Thus, although Er81 is expressed in the great majority of trkC+ afferents, which include Ib afferents, this class of sensory neuron is not obviously affected by loss of Er81.

In contrast, Ia afferents in Er81 mutant animals did not respond well to adequate stimuli. Ia afferents in normal animals fire an action potential reliably in response to small stretches of the tendon at frequencies up to 20Hz; afferents in older animals can respond to frequencies of 100-200Hz (see Figure 11). Stretches of the whole muscle evoke responses from several muscle spindles and, consequently, several Ia afferents. The same stimulation paradigm in mutant animals reveals that few afferents can respond reliably at >10Hz. In fact, some mutants failed to respond to small stretches at any frequency. Additionally, the average amplitude of the Ia afferent response was reduced in mutant animals, indicating the number of Ia afferents recruited by the selective stimulus was reduced. Thus, it appears that Ia sensory afferents are selectively affected by Er81 mutation. These results could be a result of defects in the maturation of muscle spindles or by a direct effect of the Er81 mutation on Ia afferents. These possibilities are explored in the Discussion.

3.   Monosynaptic inputs to motoneurons are reduced in Er81 mutant mice.

Because Ia afferents appeared to be selectively affected by the Er81 mutation, we
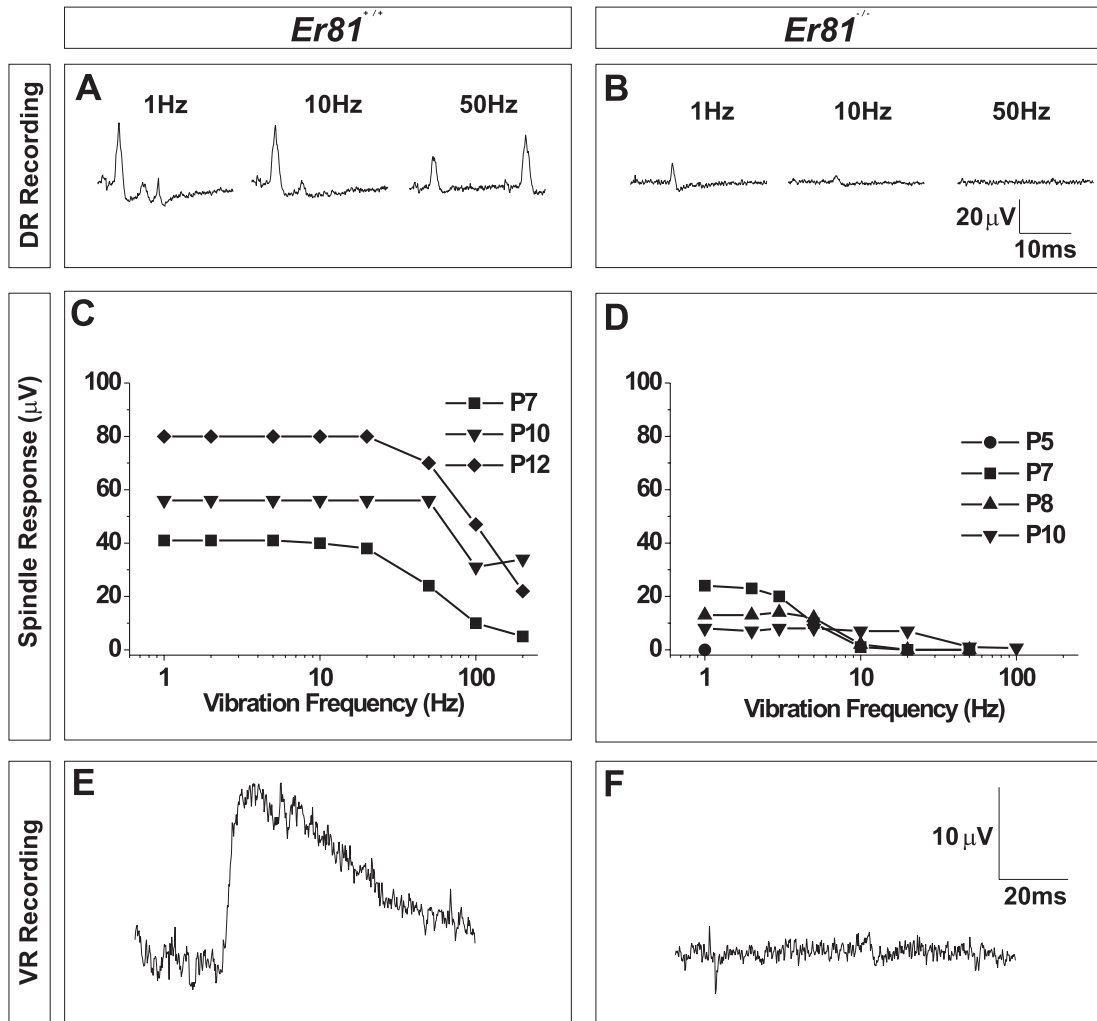
Figure 11. Responses of muscle spindle (Ia) afferents are reduced in Er81 mutants.

(**A-D**) Selective stimulation of Ia afferents in rectus femoris recorded at dorsal root L3.

(**A, B**) Averaged traces show Ia afferent action potentials from Er81 normal and mutant

mice elicited at different stimulus frequencies. Average amplitude in Er81 mutants is

decreased at all frequencies, suggesting that fewer spindles are responding to each

stimulus. Single Ia afferent action potentials measure ~11μ**V** in both Er81 normal and

mutant mice (normal: 11.3 $\pm$ 0.6μ**V**; ER81 mutant: 11.9 $\pm$ 0.7μ**V**). (**C, D**) Average

response amplitudes at different frequencies from normal and mutant animals of various

ages. Spindle afferents in normal animals respond maximally to stimuli up to 20Hz, and

many respond strongly to stimuli at higher frequencies. Spindle afferents in mutants,

however, do not respond well to stimuli above 10Hz and, in some animals, no response is

detected. (**E, F**) Selective stimulation of Ia afferents in normal mice (P7) evokes a

monosynaptic response in motoneurons (ventral root recordings at L3). No synaptic

potentials were recorded from ventral root L3 by selective stimulation of Ia afferents in

Er81 mutant mice (P6). Calibrations in **B** and **F** apply to **A** and **E**, respectively.

focused on the central synaptic connections of these afferents with motoneurons. Stimulation of whole dorsal roots in normal animals evokes a large, complex EPSP in motoneurons recorded at the ventral root. Inputs from Ia afferents, which form the only monosynaptic sensory inputs to motoneurons, evoke synchronous action potentials in large numbers of motoneurons (see Figure 12). In Er81 mutant mice, however, the monosynaptic component of the motoneuron response is significantly reduced. In fact, the input is sufficiently weak that no action potentials are generated in response to this stimulus. The reduction in the monosynaptic component of the ventral root potential was consistently observed at lumbar levels L1-L6.

On the other hand, sensory inputs transmitted via interneurons are qualitatively normal in Er81 mutants. Stimulation of the saphenous nerve, which projects to the skin and contains no muscle sensory afferents, evoked only polysynaptic potentials in motoneurons from both Er81 normal and mutant animals. The potentials recorded from Er81 mutants had similar amplitudes and time courses as those in normal animals. Activation of interneuronal networks by Ib afferents also appears to be normal in Er81 mutants. Selective stimulation of Ib afferents in normal animals elicits an EPSP in motoneurons with a latency of ~25 ms (see Figure 10). This long latency is the combination of extraspinal and intraspinal components. The time required for muscle contraction, Ib afferent activation and peripheral conduction of action potentials represents the extraspinal delay. Dorsal root recordings suggest that this delay is approximately 15ms. The intraspinal delay is the result of time required for Ib interneuron activation and the subsequent activation of target motoneurons. Ventral root potentials evoked by Ib afferent stimulation had similar latencies in both Er81 normal and
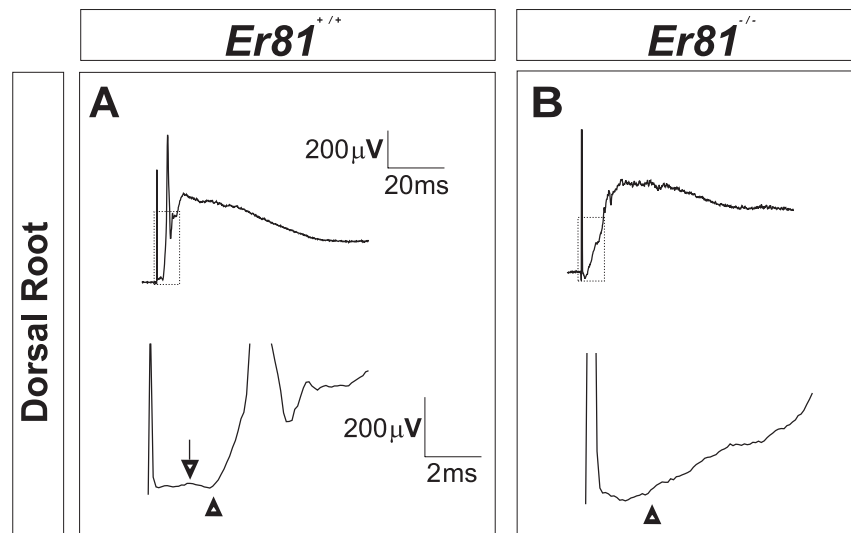
Figure 12. Short-latency sensory inputs fail to elicit motoneuron action potentials in Er81 mutant mice. (**A, B**) Stimulation of sensory fibers in the L3 dorsal root elicits a large ventral root potential in both Er81 normal (Er81$^{+/+}$) and mutant (Er81$^{-/-}$) mice. Responses are redrawn on expanded time scale in lower trace. Er81 mutant mice have greatly reduced responses at short latencies, which corresponds to that of monosynaptic connections (beginning of monosynaptic response indicated by solid arrowhead). In Er81 normal mice (**A**), the monosynaptic component is suprathreshold in many motoneurons, resulting in a compound action potential on the rising phase of the synaptic response, while in Er81 mutant mice (**B**), the early components are never sufficient to elicit action potentials.

mutant animals. These experiments show that Ib afferents are activated normally in the periphery, have normal conduction properties, and make functional connections with spinal neurons in Er81 mutant mice (see Figure 10).

Reduced monosynaptic sensory-motor connections are also observed following stimulation of individual muscle nerves. Motoneuronal responses were recorded following stimulation of nerves supplying individual hindlimb muscles. There was a significant reduction in the monosynaptic component of the ventral root EPSPs in all muscle nerves tested (see Figure 13 and Table 1). This effect was independent of the ETS phenotype of the target motoneurons. For example, responses to both obturator and gluteus nerve stimulation were approximately 3% of normal, despite the fact that obturator motoneurons express Er81 and gluteus motoneurons express PEA3. Interestingly, significant residual ventral root responses, approximately 25% of normal amplitude, were evoked following stimulation of muscle nerves that supply the distal hindlimb (peroneal and tibial nerves; see Table 1). Consistent with the delayed peripheral conduction time observed in the dorsal root, residual monosynaptic connections in Er81 mutants were delayed 1-2ms.

Selective activation of Ia afferents supplying the RF muscle in normal animals evokes a monophasic EPSP with a latency corresponding to that of monosynaptic connections with motoneurons (see Figure 11E). In all mutant animals, however, selective stimulation of quadriceps Ia afferents evoked no measurable ventral root potential (see Figure 11F). The results of electrical and selective Ia afferent stimulation experiments thus show that monosynaptic inputs to motoneurons in Er81 mutants are reduced due to a selective defect in Ia afferents.
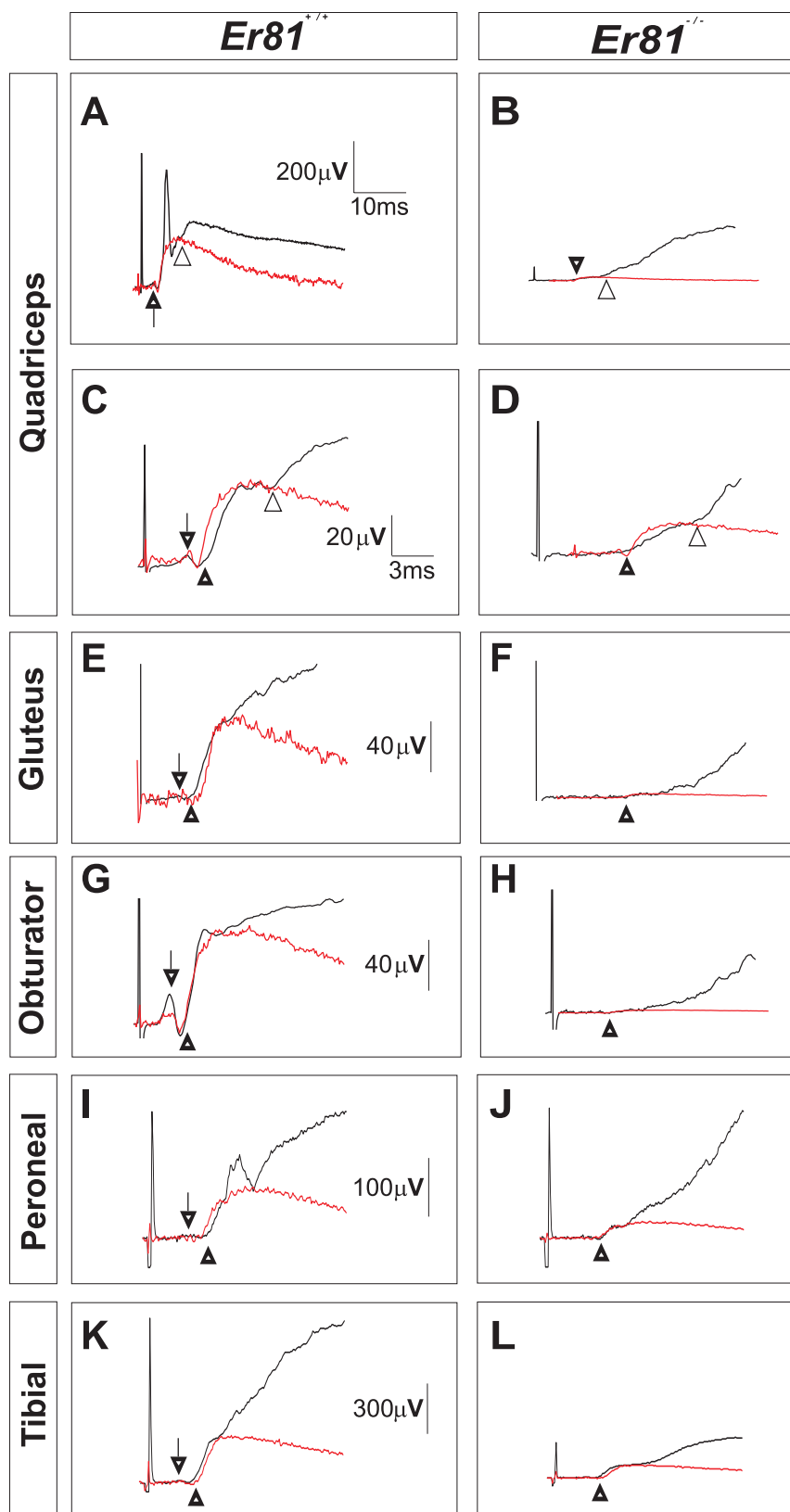
Figure 13. Monosynaptic inputs to motoneurons are reduced in Er81 mutant mice.

(**A-D**) Stimulation of low threshold (Ia and Ib) sensory fibers in quadriceps nerve evokes synaptic responses in L3 motoneurons. Model traces (red) are from age-matched normal animals and are scaled to illustrate the monosynaptic component of each trace. In most normal mice (**A**), the monosynaptic response is suprathreshold and generates large numbers of action potentials. Open arrowheads in **A-D** indicate the beginning of the polysynaptic component of each trace. Although polysynaptic responses are present in Er81 mutant mice (**B, D**), the monosynaptic component is substantially reduced. (**E, F**) Stimulation of gluteus muscle sensory afferents elicits synaptic responses from L5 motoneurons. The monosynaptic components of the response are nearly absent in Er81 mutant mice, although later components remain. (**G, H**) Obturator muscle sensory afferents evoke synaptic responses from L3 motoneurons. Again, monosynaptic components are significantly reduced in Er81 mutant mice. Stimulation of peroneal (**I**, **J**) and tibial (**K**, **L**) muscle sensory afferents evokes approximately 25% of normal monosynaptic response in L5 motoneurons from Er81 mutant animals.   Finally, a small terminal potential (solid arrow in **A**, **C**, **E**, **G**, **I**, and **K**) precedes the synaptic response in normal mice, but is absent in mutant mice. This terminal potential is resistant to repetitive stimulation (up to 50Hz). Black arrowheads indicate the beginning of synaptic potential. Calibrations shown for Er81 normal panels apply to corresponding Er81 mutant panels. Panels **C-L** are shown at same time scale.

Table 1. Monosynaptic amplitudes evoked via stimulation of muscle nerves are reduced in Er81 mutant mice.

Peripheral Nerve	Er81$^{+/+}$	Er81$^{-/-}$	% of Normal
Quadriceps	179.6 $\pm$ 24.6 (16)	15.4 $\pm$ 3.2 (12)	8.6
Obturator	182.3 $\pm$ 20.9 (9)	4.4 $\pm$ 0.8 (8)	2.4
Gluteus	65.1 $\pm$ 14.8 (4)	1.7 $\pm$ 0.2 (4)	2.6
MBS	141.0 $\pm$ 25.5 (7)	10.2 $\pm$ 3.5 (6)	7.2
Peroneal	117.6 $\pm$ 26.3 (7)	25.7 $\pm$ 3.9 (7)	21.9
Tibial	229.4 $\pm$ 36.5 (7)	61.8 $\pm$ 12.6 (7)	26.9

Monosynaptic amplitude in μ**V** $\pm$ SEM. ( ) = n for each sample. All muscle nerve comparisons are significant ($p < 0.05$, Student's t-test). Ventral root recordings were made from either L3 (quadriceps and obturator) or L5 (gluteus, MBS [muscle branch of sciatic nerve], peroneal and tibial).

4.   Defects in Ia afferents are responsible for the reduction in sensory-motor

connections.

We next investigated the possible mechanisms for the reduction in monosynaptic

input to motoneurons. One possibility is that Ia axon collaterals project normally within

the spinal cord, but synaptic transmission to motoneurons is impaired. Alternatively, Ia

axon collaterals might fail to project to the appropriate region of the spinal cord. Ventral

root recordings provided indirect evidence that Ia afferents did not project into the ventral

horn. Electrical stimulation of muscle nerves results in synchronous activation of many

sensory afferents. The close proximity of Ia afferent collaterals to motoneurons in

normal mice can, with this stimulation paradigm, lead to passive depolarization of

motoneuronal dendrites before synaptic transmission occurs (Munson and Sypert, 1979a;

Munson and Sypert, 1979b; Watt et al., 1976). The amplitude of this terminal potential

depends on the number of Ia afferents activated by a stimulus; activation of muscle

nerves containing many spindles will generate a larger terminal potential than stimulation

of a muscle nerve containing fewer spindles. Terminal potentials of various amplitudes

can be seen in all traces from normal animals following muscle nerve stimulation (see

Figure 13). In contrast, terminal potentials were never observed in traces from Er81

mutant animals, even following stimulation of tibial and peroneal nerves, which evoked

approximately 25% of the normal monosynaptic response (see Figure 13).   This

suggested that Ia afferents do not terminate in close proximity to motoneuronal dendrites

in these animals.

The reduction in monosynaptic connections could be explained by a failure of

motoneuron dendrites to elaborate properly. To determine if this was the case, we

backfilled motoneurons in a region of the lumbar cord where approximately 50% of motoneurons express Er81. Motoneuron dendrites in Er81 mutants extend dorsally, approximately to the level of the central canal, as in normal mice (see Figure 14). Therefore, they overlap with the normal projections of Ia afferents. This suggested a potential deficit in the Ia projection itself.

In preliminary experiments, we injected HRP into the quadriceps muscle nerve and observed the central projection of sensory neurons in Er81 mutant mice. These experiments showed that Ia afferent collaterals in postnatal mice do not make their stereotypic axonal projections into the ventral spinal cord where they can make strong synaptic connections. These results were extended by Silvia Arber and will be further elaborated in the Discussion.

The synaptic contacts that are still made between Ia afferents and motoneurons supplying distal leg muscles in Er81 mutants are likely to be made on distal dendrites of motoneurons (Kuno and Llinas, 1970). Evidence for this is observed in ventral root recordings. Analysis of rising phases of monosynaptic responses in Er81 mutants demonstrate that, in addition to the increased latency in response described above, the rise time to the peak of the monosynaptic response is significantly increased by about 50% (1.2 ms vs 2.3 ms, $p < 0.00001$).

5. Conclusions

In conclusion, it appears that the primary cause of the loss of sensory-motor connections in Er81 mutants is a defect in the Ia sensory afferent. In mutant animals these afferents fail to respond robustly to selective stimuli and they provide greatly
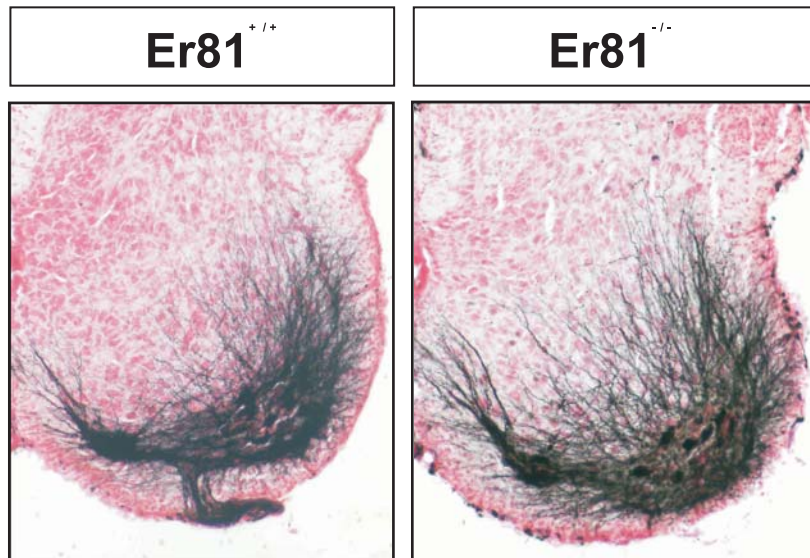
Figure 14. Motoneuron dendrites appear normal in Er81 mutants. HRP labeling of L3 ventral roots in Er81+/+ (P4) and Er81-/- (P6) animals shows that motoneuron dendrites extend both medially and dorsally from the ventral horn. The elaboration of dendrites does not appear to be reduced in Er81 mutants, suggesting that motoneurons are capable of receiving synaptic inputs from muscle sensory afferents and interneurons.

reduced inputs to motoneurons. The reduced inputs are likely to be a consequence of the

failure of Ia afferents to project ventrally in the spinal cord to the region of the

motoneurons. The failure of Ia afferents to respond to muscle stretch may be a direct

result of a defect in the afferents themselves, or to a defect in the development of muscle

spindles. These possibilities will be explored in the Discussion.

4.   Analysis of PEA3 null-mutant mice

1.   Numbers of motoneurons expressing PEA3 are reduced in the brachial spinal cord in PEA3 mutants.

The ETS genes PEA3 and Er81 are expressed by non-overlapping subsets of motoneurons at limb levels in the spinal cord (Arber et al., 2000; Lin et al., 1998). In the lumbar region many subsets express Er81, but in the brachial cord very few motoneurons express Er81. Significant numbers of ventral LMC motoneurons in the brachial cord do express PEA3, however (see Figure 15). Published reports suggested that the PEA3+ population overlapped the distribution of the cutaneous maximus (c. maximus) motor pool (Baulac and Meininger, 1981; Haase and Hrycyshyn, 1985; Holstege et al., 1987; Krogh and Towns, 1984). Accordingly, we investigated the status of this muscle in postnatal PEA3 mutants. The median anterior thoracic (MAT) nerve separates in the axillary region into 5-6 major branches that project to c. maximus as well as 2-3 smaller branches that supply pectoralis minor (Greene, 1935). In PEA3 mutants, fewer branches (1-3) supply the c. maximus muscle and the remaining branches are smaller in diameter. Consistent with this observation, the muscle is atrophic. On the other hand, branches that innervate pectoralis minor, as well as the muscle itself, are normal in PEA3 mutants.

Because of the reduced number and diameter of c. maximus nerve branches in PEA3 mutants, it was difficult to separate this nerve from the pectoralis minor nerve. Pectoralis minor motoneurons are located in a discrete pool dorsal to that of c. maximus motoneurons (Baulac and Meininger, 1981). Also, the pectoralis minor pool contains relatively few motoneurons when compared to c. maximus. Consequently, we
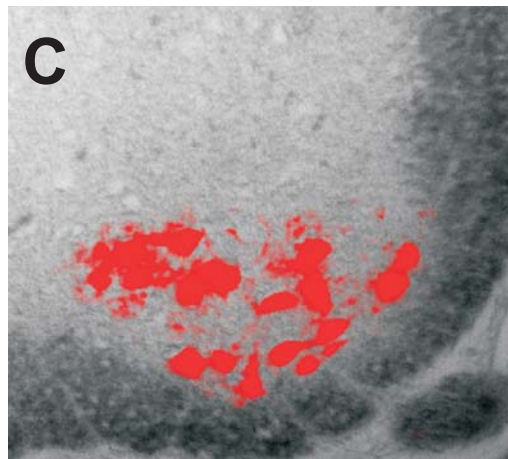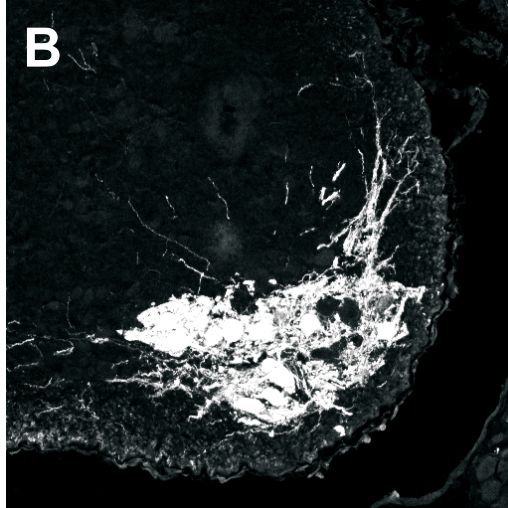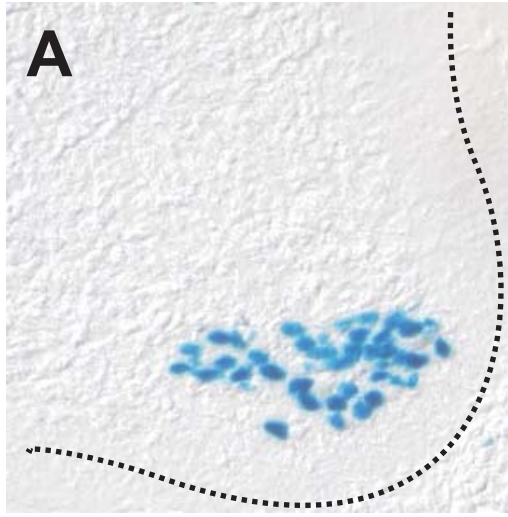
Figure 15. Cutaneous maximus muscle motoneurons express PEA3. (**A**) LacZ staining of PEA3$^{\text{PEA3/nls-LacZ}}$ embryo at E13.5. PEA3 is expressed in a population of ventral motoneurons of the LMC in C7 and C8. Photograph courtesy of Silvia Arber. (**B**) Motoneurons labeled by retrograde fill of c. maximus nerve in P4 normal animal. Note similar position of c. maximus motor pool with region of PEA3 expression. (**C**) C8 motoneurons labeled by retrograde fill of MAT nerve in P7 normal animal. Note correspondence of pool locations with that in **B**.

retrogradely labeled the common c. maximus and pectoralis minor nerve (MAT) to determine changes in the number of motoneurons projecting in this nerve in PEA3 mutants. Significantly, the total number of labeled motoneurons in PEA3 mutants is reduced four-fold compared with normal animals (see Figure 16). Motoneurons located in the region corresponding to the c. maximus pool were dramatically reduced by more than 10-fold (see Figures 17 and 18). The number of labeled motoneurons located dorsal to the c. maximus population in the region of the pectoralis minor pool was unchanged, however (see Figures 17 and 18).

Although the number of labeled motoneurons is dramatically reduced in PEA3 mutants, the distribution of cells along the rostral-caudal axis was not changed (see Figure 19). In both normal and mutant animals, most labeled motoneurons are located in caudal C7 through caudal C8, with small numbers (about 15% of total) in rostral C7 and rostral T1. The rostral-caudal boundaries of the MAT motor pool remain unchanged in PEA3 mutants in all spinal segments. These data suggest that the mechanisms for generating the rostral-caudal distribution of these motoneurons are not affected in PEA3 mutants.

In PEA3 mutant mice, cells that would normally express PEA3 (visualized by expression of lacZ) are found in more dorsal locations at an embryonic stage by which these cells should have settled in their normal ventral location (Silvia Arber, personal communication). The long-term fate of these cells is not known. One possibility is that these neurons fail to extend axons into the periphery and eventually die. Another possibility is that they may respond to their dorsal environment and adopt the fate of more dorsal motoneurons.
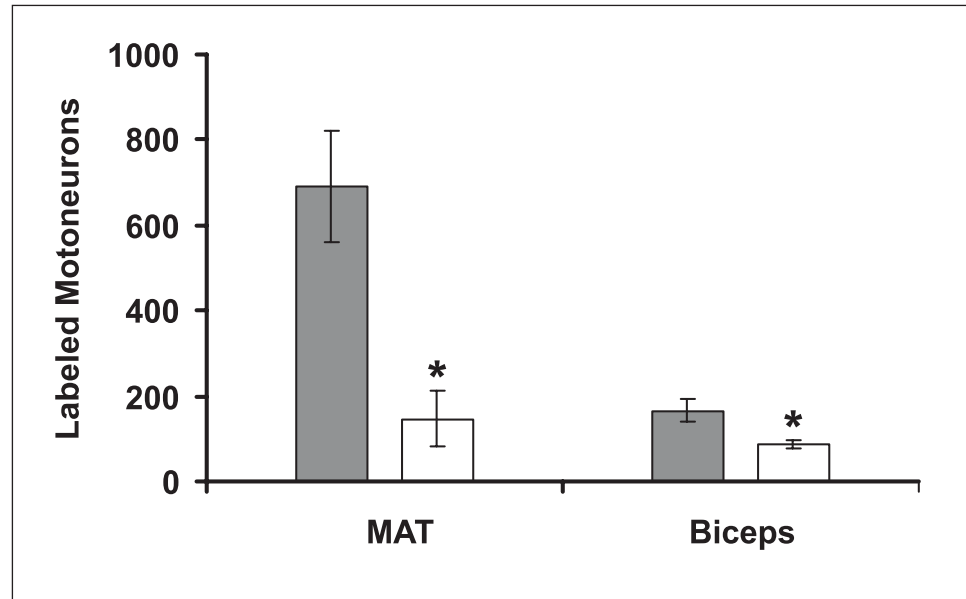
Figure 16. Numbers of retrogradely labeled MAT and biceps motoneurons are reduced in PEA3 mutants. Bars represent the average ± SEM from three normal (gray bars) and three mutant (white) animals. MAT and biceps motoneurons were labeled via retrograde transport of fluorescent-conjugated dextran in P6-P8 mice. Graph represents total numbers of labeled cells found in spinal segments C4-T1. (*) indicates significant change ($p < 0.05$).
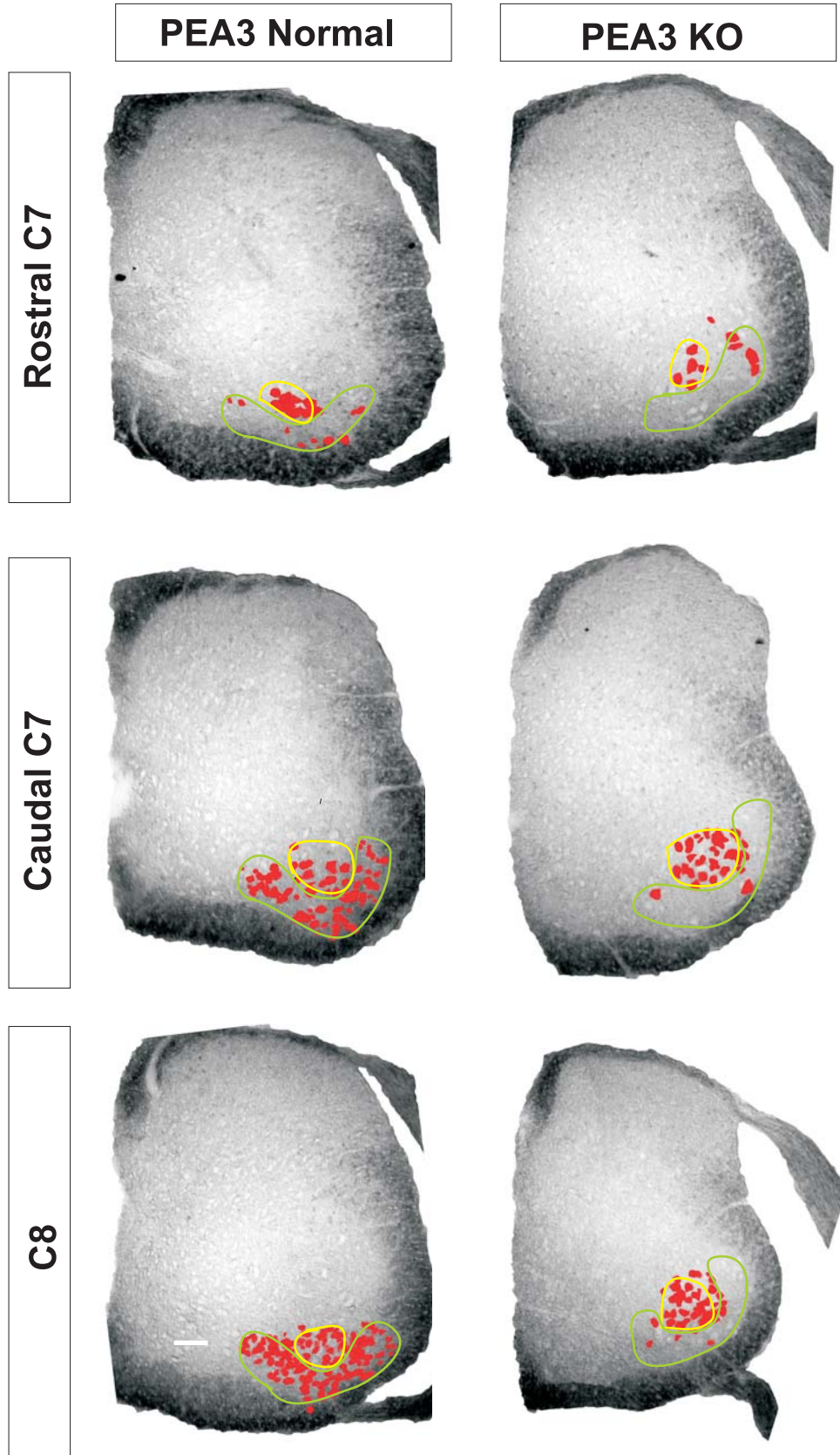
Figure 17. Motoneurons projecting in MAT nerve are reduced in PEA3 mutants.

MAT motoneurons were labeled via retrograde transport of fluorescent-conjugated

dextran in PEA3 normal (P7) and PEA3 mutant (P6) mice. The location of labeled

motoneuronal pools was determined by aligning corresponding bright-field images.

Because rostral and caudal halves of the C7 segments had ventral horns of different

shapes, the halves are shown separately. Clusters of motoneurons are most evident in

rostral segments. Outlines corresponding to published reports (Baulac and Meininger,

1981) of pectoralis minor (yellow) and cutaneous maximus (green) motor pools are

shown for normal and mutant mice. Scale bar equals 50 μm.
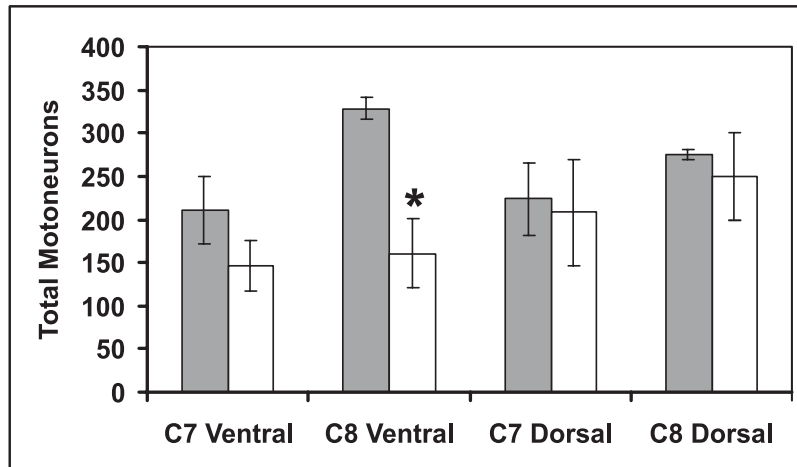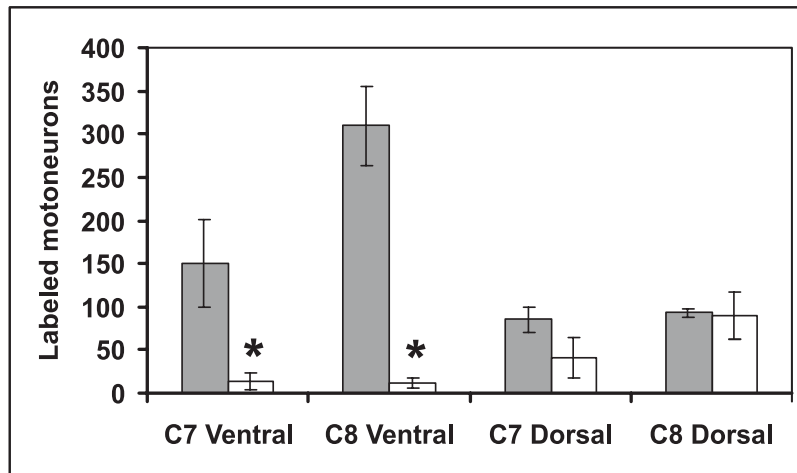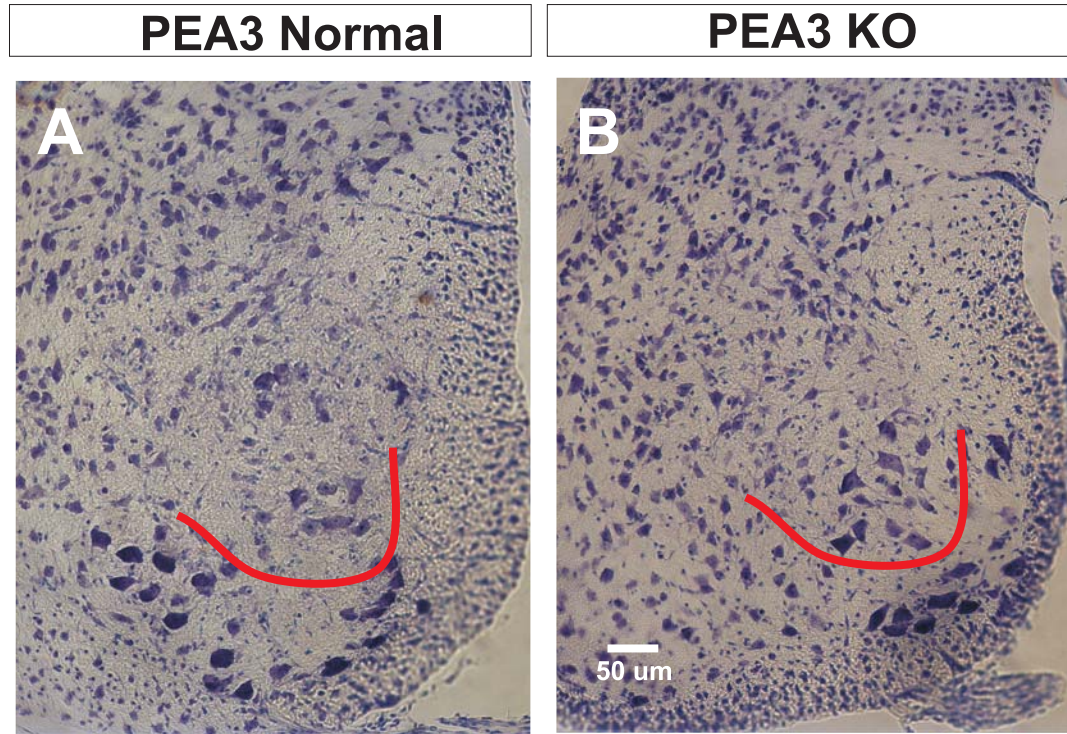
Figure 18. Ventral population of motoneurons is reduced in PEA3 mutant mice.

(A, B) Representative sections from C8 segment in normal and PEA3 mutant mice counterstained with thionin. Line illustrates division between ventral (region of c. maximus pool) and dorsal (motor pools other than c. maximus) regions of LMC. *Middle panel:* Counts of MAT motoneurons located in dorsal and ventral compartments of C7 and C8 visualized by retrograde labeling of MAT nerve. *Bottom panel:* Counts of total motoneuronal populations in dorsal and ventral compartments from C7 and C8. Counts of thionin stained cells were done according to standards of Clarke and Oppenheim, 1995. Bars show the average number of motoneurons $\pm$ SEM of three normal (gray bars) and three mutant (white bars) animals. (*) indicates significant changes ($p<0.05$).
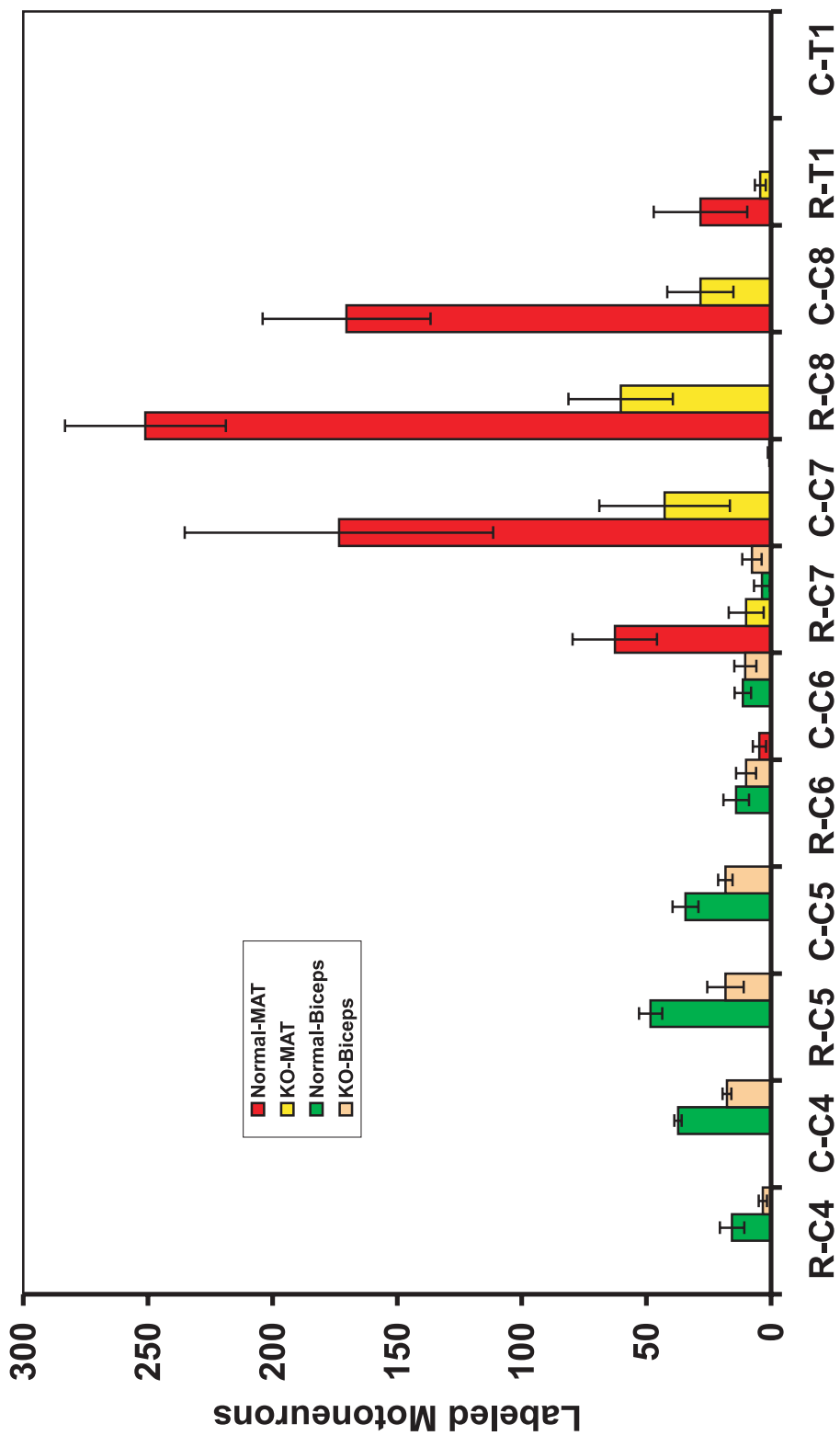
Figure 19. Distribution of MAT and biceps motoneurons along the A-P axis is normal in PEA3 mutant mice. Numbers of retrogradely labeled cells projecting to MAT and biceps muscles were quantified in the rostral (R) and caudal (C) halves of spinal segments C4-T1. Although the number of labeled MAT motoneurons is significantly reduced in all spinal segments, the segmental distribution of these cells is normal. Biceps motoneurons are reduced in some segments, but the distribution of biceps motoneurons is normal. Bars represent average ± SEM of 3 normal and 3 mutant animals.

Because these "PEA3+" cells are found in inappropriate locations in the lateral motor column (LMC) in mutant animals, we analyzed the distribution of all motoneurons in the LMC in various regions of interest. In PEA3 mutants, fewer motoneurons are found in segment C8 and this difference approaches significance (normal: 523 ± 28; mutant: 345 ± 63; p=0.06; n=3). Large numbers of c. maximus motoneurons are found in this segment in normal animals (Baulac and Meininger, 1981), suggesting that a significant number of cells fated to become c. maximus motoneurons fail to develop or survive postnatally in PEA3 mutants. Indeed, the total number of motoneurons located in the ventral region (region of c. maximus pool) is reduced; suggesting that some cells in this region, in the absence of PEA3, do not instead project to other muscles (see Figure 18).

The total number of motoneurons located in the dorsal region (outside of c. maximus pool) of C8 LMC is unchanged in PEA3 mutants. This leaves open the possibility that at least a fraction of the dorsally located "PEA3+" cells observed in PEA3 mutants do survive, presumably by innervating other muscle targets, possibly even pectoralis major and minor (see Figure 17). In this way the PEA3 mutation could affect motoneurons that normally do not express this protein. Therefore we next investigated the development of other PEA3- motoneurons in adjacent cervical segments to determine if there were any indirect effects of the PEA3 mutation on general motoneuron development.

Because biceps motoneurons are located in segments C5 and C6, segments where PEA3 is not expressed, we analyzed the number and position of biceps motoneurons via retrograde labeling. Curiously, the number of labeled biceps motoneurons in PEA3

mutants was reduced two-fold (see Figure 16). The segmental distribution of labeled

biceps motoneurons in mutant animals remained normal (see Figure 19). To determine if

the reduction of biceps motoneurons reflected a general decrease in motoneurons at this

level, we counted all LMC motoneurons in these segments. Counts of total motoneurons

in C5 and C6 segments show no reduction in motoneuron number in PEA3 mutants

(normal: 556 ± 30; mutant: 462 ± 60; n=3). Thus, the reduction in labeled biceps

motoneurons does not reflect a general perturbation in motoneuron development in PEA3

mutants.

2.   Normal numbers of sensory neurons are found in PEA3 mutants.

PEA3 is expressed by E12.0 in mice and >90% of trkC+ sensory neurons co-

express PEA3. Er81 is also co-expressed eventually in most of these sensory neurons,

but is not detected until E13.5 (Arber et al., 2000). By E16.5 PEA3 expression is

downregulated in sensory neurons so that only ~10 % of trkC+ neurons are PEA3+. In

contrast, by E16.5, the time at which sensory neurons have reached their targets in the

periphery, Er81 is expressed by virtually all trkC+ sensory neurons. Our studies of Er81

mutant mice revealed that this gene was required for the development of central axon

projections to motoneurons, a distinct feature of Ia afferents that appears during the time

when most proprioceptive sensory neurons express Er81 and not PEA3 (E15.5-16.5).

Because PEA3 is expressed by most proprioceptive sensory neurons early in

development, even before Er81 expression is detected, we examined whether the

development and/or maturation of proprioceptive sensory neurons was defective in PEA3

mutant mice.

Normal numbers of large diameter sensory neurons project in the MAT and biceps muscle nerves in P6-P8 mutant mice (see Figure 20). Thus, in the absence of PEA3, sensory neurons are generated and survive into the postnatal period, well after the end of normally occurring cell death. Even in the face of a four-fold reduction in motoneuron number, as for the combined pectoralis minor plus c. maximus muscle pool, the number of sensory neurons projecting to these muscles is normal. This suggests that normal numbers motoneuronal targets are not required for the maintenance of muscle sensory afferents. This is consistent with other studies that suggest that trophic factors in the periphery rather than central connections are most critical for the maintenance of normal numbers of muscle sensory afferents (Oakley et al., 1997; Taylor et al., 2001; Wright et al., 1997). Alternatively, pectoralis minor and c. maximus muscles may receive different sensory inputs. As normal numbers of pectoralis minor motoneurons are observed in PEA3 mutants, perhaps the majority of sensory neurons that project in the MAT nerve supply this muscle and are therefore maintained by peripheral support. This possibility is discussed below.

3.   Ib afferents respond normally in PEA3 mutants.

ETS genes appear to play an important role in the development of specialized muscle sensory structures. Muscle spindles, for example, express both Er81 and PEA3 and require Er81 expression for maintenance of spindles postnatally. Golgi tendon organs (GTO), the other major muscle sensory structure, express PEA3 but not Er81 (Arber et al., 2000). The restriction of PEA3 expression to GTO suggested that this ETS
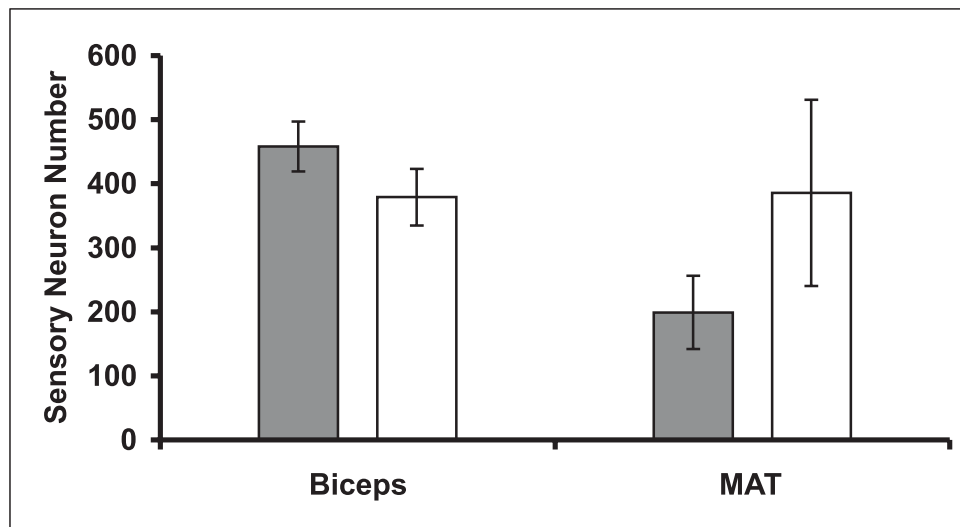
Figure 20. Number of large-diameter sensory neurons is normal in PEA3 mutant mice. Bars represent the average ± SEM from three normal (gray bars) and three mutant (white bars) animals. MAT and biceps sensory neurons were labeled via retrograde transport of fluorescent-conjugated dextran in P6-P8 mice. Counts were restricted to large-diameter (>15 um) cells within the DRG. Bars show the total numbers of labeled cells found in DRG C5-T1. MAT sensory neurons were located primarily in C7 and C8, while biceps neurons were found in C5 and C6. The increase in MAT sensory neurons was not significant.

gene might be critical in the development of these organs and/or their associated sensory innervation by Ib afferents.

No differences were noted in Ib responsiveness between normal and mutant mice (see Figure 21). The firing pattern of Ib afferents in response to selective activation of GTO was recorded in the dorsal root using extracellular recording techniques (see Materials and Methods). As shown in Figure 21, the latency of the first recorded responses in both normal and mutant animals was approximately 15 ms. Responses were most intense in the first 30-40 ms following the stimulus and then declined to occasional spikes afterwards. The initial delay results from the delayed rise of muscle tension after activation of extrafusil muscle fibers (see Materials and Methods).

Motoneuron responses to selective Ib stimulation, recorded in the ventral root in PEA3 mutants, were also normal in mutant animals (see Figure 21). In P8 mice, the latency of motoneuronal responses to Ib selective stimulation was approximately 20 ms in both cases. Also the rise-time and amplitude of the initial ventral root responses were qualitatively similar in normal and mutant mice. Longer latency components were also observed in both groups of mice. Therefore the development of functional GTO and Ib sensory neurons, as well as the central projections these neurons make within the spinal cord, are not critically dependent on the expression of PEA3.

4. Ia afferents project to and make connections with motoneurons in PEA3 mutants.

Ia afferents, which supply the major sensory innervation of muscle spindles, also develop normally in PEA3 mutant mice. A distinctive morphological feature of Ia fibers
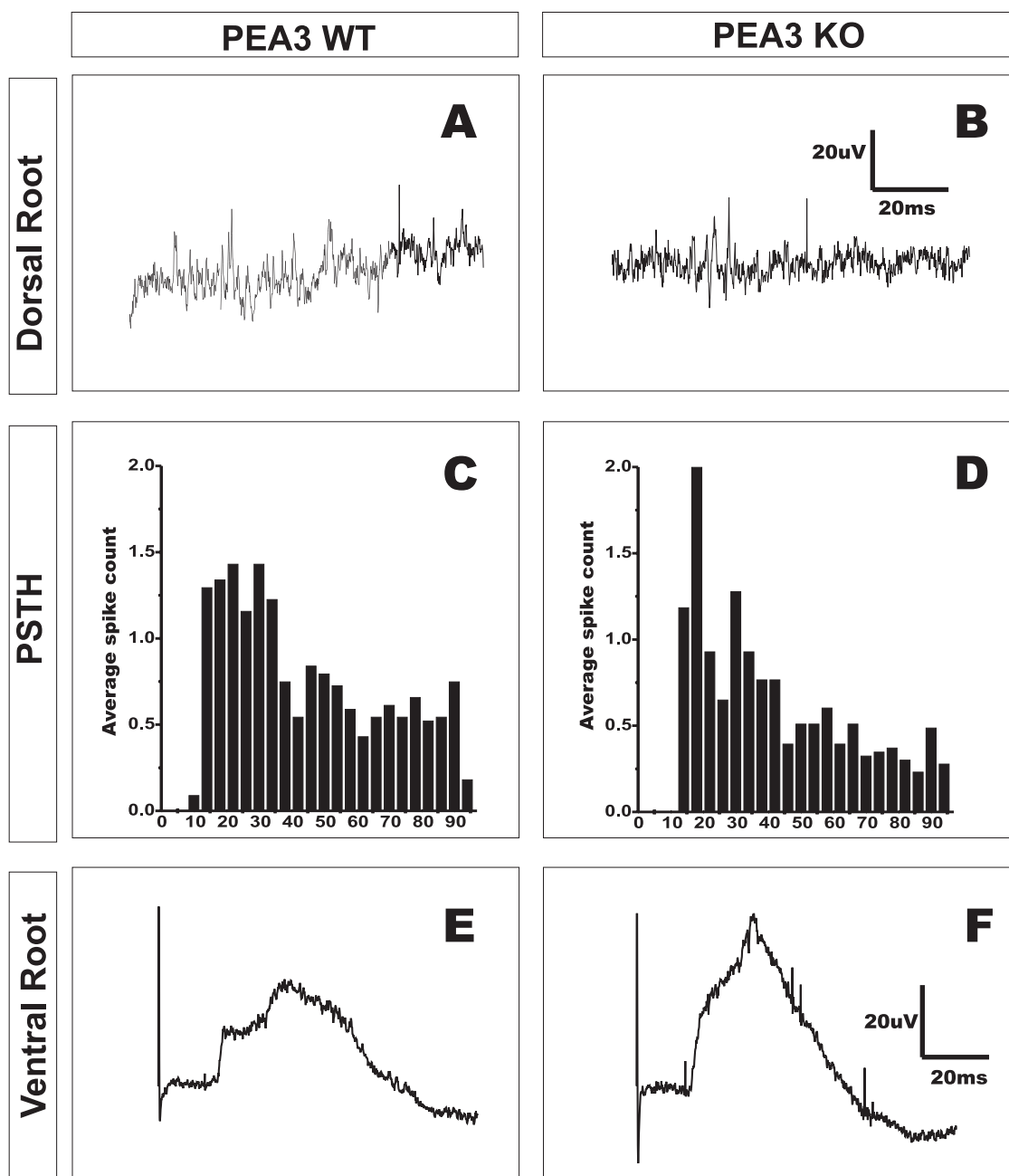
Figure 21. Ib afferent responses recorded at dorsal and ventral roots are normal in PEA3 mutants. (**A, B**) Representative traces from normal and PEA3 mutant animals recorded in the dorsal root following Ib afferent selective stimulation. (**C**, **D**) Post stimulus time histograms (~40 trials) of Ib afferent responses to selective stimulation of GTO recorded in the L3 dorsal root show that the latency and temporal distribution of action potentials are similar in normal and mutant mice. (**E, F**) Ib afferent stimulation evokes a similar delayed synaptic response in motoneurons, recorded in ventral root L3, in normal and mutant mice. The trace and histogram in **A** and **C**, and in **B** and **D**, were recorded from the same P8 animal. Scales in **B** and **F** apply to **A** and **E,** respectively.

is that they are the only primary sensory axons to project down into the LMC, where they make monosynaptic connections with motoneurons. Fluorescent-conjugated dextran labeling of sensory neurons at the dorsal root, revealed a normal pattern of sensory afferent projections in mutant mice (see Figure 22). Ia axon collaterals extended ventrally into the region of the motor pools and arborized there as in normal mice. These ventral projections contrast with the phenotype observed in Er81 mutant mice, where Ia collaterals extend ventrally only to the central canal (Arber et al., 2000).

The robust projection of Ia afferents into the LMC made it likely that there were functional connections as well. This was confirmed by recording motoneuronal responses to muscle nerve stimulation. The monosynaptic component of ventral root responses to stimulation of various muscle nerves in the hindlimb appeared normal in PEA3 mutants (see Figure 23). Normal responses were observed when stimulating muscle nerves projecting to muscles whose motoneurons were PEA3+ (gluteus, rectus femoris), Er81+ (vastus, obturator), or PEA3/Er81- (soleus). Stimulation of two muscle nerves supplying the forelimb, biceps and pectoralis major, also evoked normal responses in PEA3 mutant mice (see Figure 24).

5.   Input from two muscle nerves was altered in PEA3 mutants.

Motoneuron responses evoked by MAT nerve stimulation are reduced by 40% in PEA3 mutants (see Figure 24). This reduction is surprisingly modest considering the four-fold reduction in the number of motoneurons projecting in the MAT nerve in PEA3 mutants. If the projection of MAT afferents to each MAT motoneuron were normal, one would have expected a four-fold reduction in the amplitude of the ventral root response

| PEA3 +/+ | PEA3 -/- |
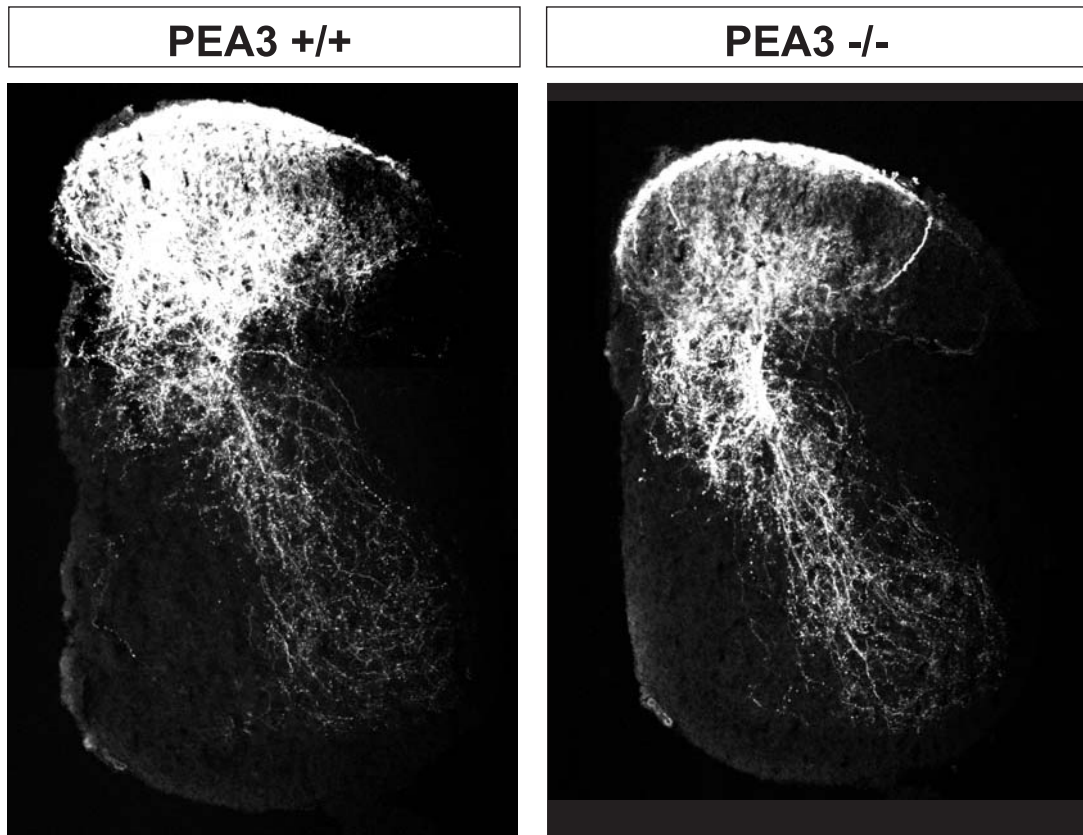
Figure 22. Ia afferent projections are normal in PEA3 mutant mice. Central projections of sensory afferents visualized by application of fluorescent-conjugated dextran dye to L3 dorsal root. Note strong projections of Ia afferents into the ventral horn of both PEA3 normal and mutant animals. The normal projection pattern in PEA3 mutants contrasts the profound Ia afferent projection deficit observed in Er81 mutants (see Figure 27).

PEA3 Normal / PEA3 KO

Vastus

A

100 μV

10ms

Rectus Femoris

B

Obturator

C

Sup Gluteus

D

Soleus

E
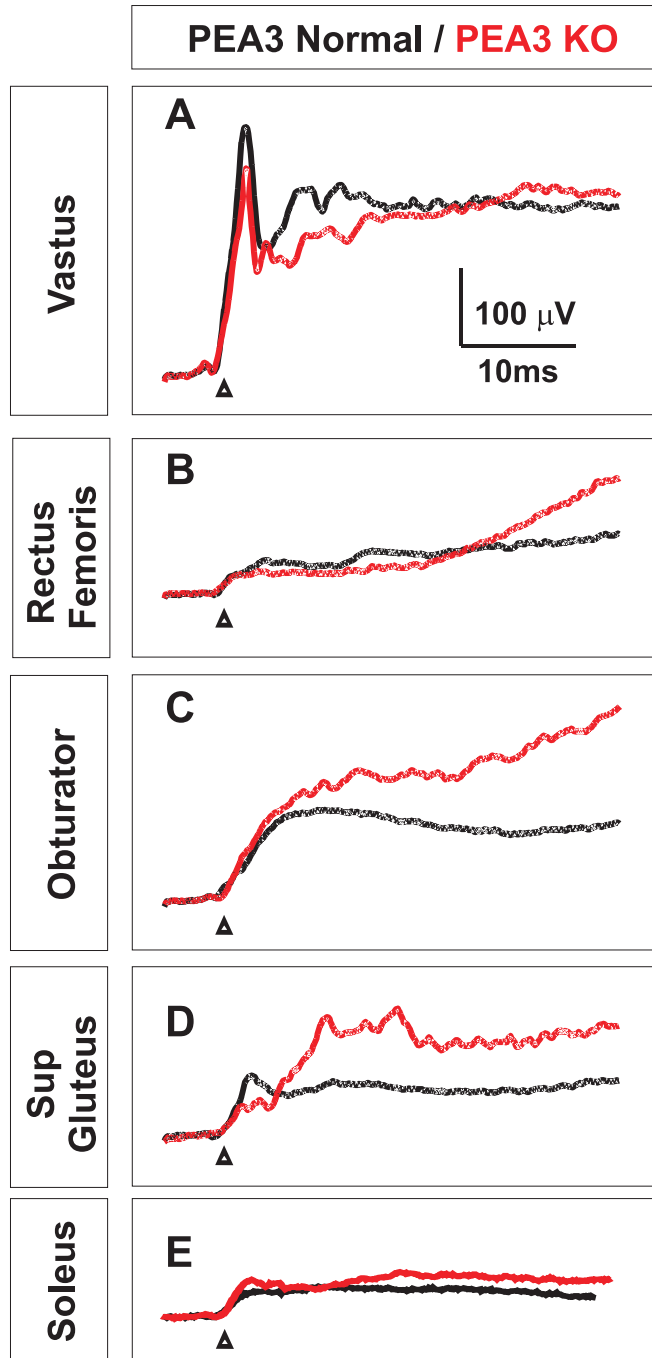
Figure 23. Motoneurons in the hindlimb of PEA3 mutant mice respond to Ia afferent stimulation. Representative traces from normal (black) and PEA3 mutant (red) animals during the first postnatal week show robust motoneuron responses to stimulation of various muscle nerves in the hindlimb. Monosynaptic inputs from Ia afferents (time of onset indicated by black arrowheads) were determined using scalable monosynaptic models (see Materials and Methods). Scale bar applies to all panels.
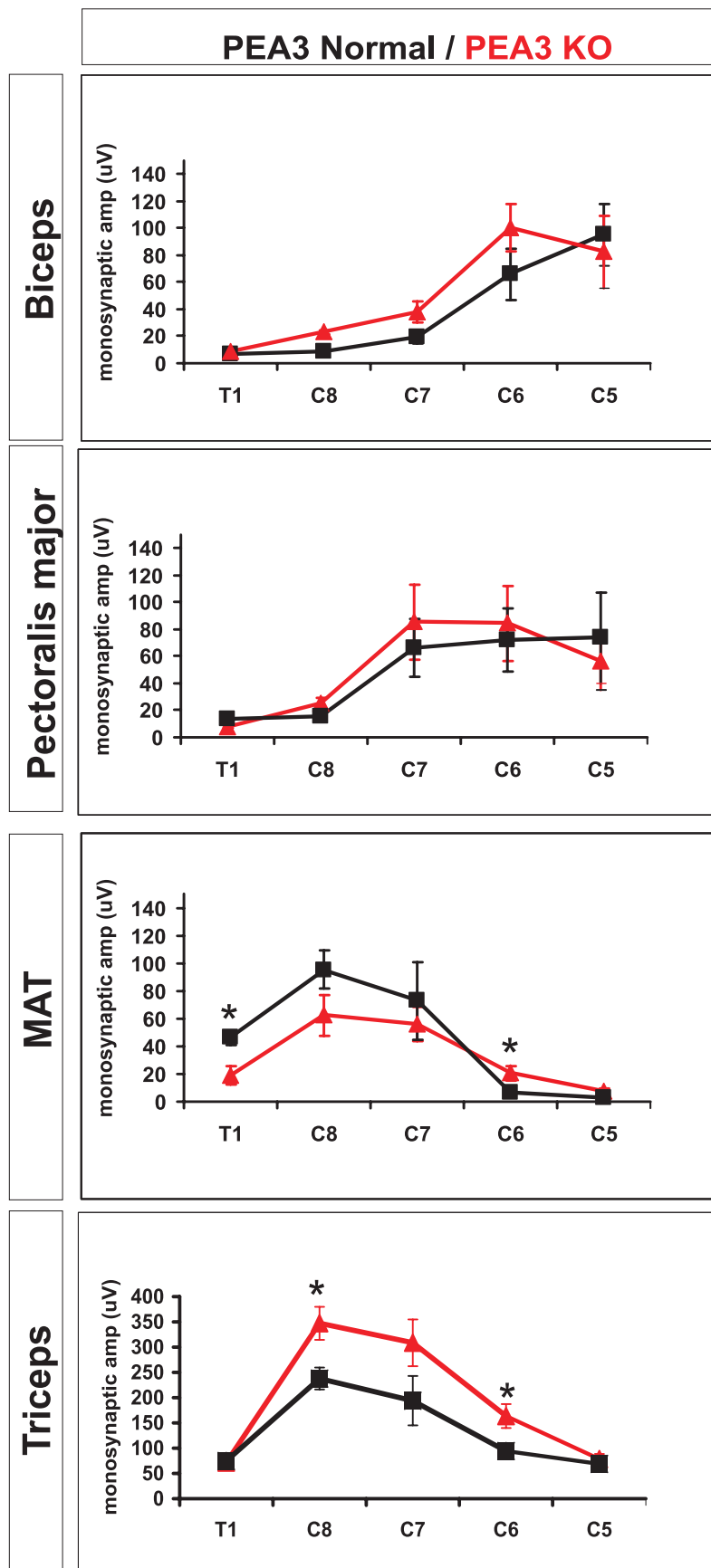
Figure 24. Segmental specificity of Ia inputs to brachial motoneurons is preserved in PEA3 mutant mice. Motoneuron responses were recorded from brachial ventral roots following stimulation of biceps, pectoralis major, MAT, and triceps muscle nerves. Average responses ± SEM from 6 (P6-P8) normal (black) and 6 mutant (red) mice are shown. No changes were observed in the segmental distribution of Ia inputs in mutant mice. Motoneuron responses to MAT muscle nerve stimulation were reduced ~40%. Triceps inputs were larger in mutant mice. (*) indicates significant changes (p<0.05).

as well. A plausible explanation for this moderate decrease in MAT nerve input is that the different motor pools contained in this muscle nerve are different with respect to the amount of input they receive. The pectoralis minor muscle is important for maintaining posture and for locomotion in rodents, functions requiring significant proprioceptive inputs. On the other hand, c. maximus, a subcutaneous muscle found in all fur-bearing mammals, functions to allow the skin to move in response to tactile stimuli (Haase and Hrycyshyn, 1985; Holstege et al., 1987). Although cutaneous muscles have numerous sensory receptors, they contain relatively few muscle spindles (Zelena, 1994). In fact, only 3-5 muscle spindles are found in c. maximus muscle, while pectoralis minor contains 9-12 muscles in normal animals (Silvia Arber, personal communication). Thus, it is likely that a significant fraction of Ia afferents in the MAT nerve innervate pectoralis minor motoneurons and not c. maximus motoneurons. Because pectoralis minor motoneurons appear to be present in normal numbers, it follows that the reduction in ventral root response may be less severe than the total loss of motoneurons.

In contrast to the reduction of inputs from the MAT nerve, inputs from triceps afferents were actually increased above normal in mutant mice, from ~200 µV to ~300 µV (see Figure 24). In the C8 segment, which has the largest triceps input, this increase was significant ($p<0.05$). One explanation for the increase is a possible increase in the number of triceps motoneurons in this area (see Figure 17). Some presumptive c. maximus motoneurons that fail to migrate into the ventral compartment may instead adopt the fate of dorsal motoneurons and project to novel muscles, including triceps. If these motoneurons received normal input from triceps Ia afferents, the triceps response in the ventral root would be larger than normal.

A second contributing factor might result from the loss of large numbers of c. maximus axons in the ventral roots of mutant mice. A reduction in numbers of non-triceps motor axons would cause each remaining axon (triceps or otherwise) to contribute a greater individual signal in the ventral root. As an extreme example of this effect, one can consider a case in which a recording suction electrode is small enough to allow only one axon to fit inside it. An evoked response recorded from this axon would be quite large due to the fact that there was no surrounding tissue acting to shunt the electrical response evoked in that axon. On the other hand, if this single activated axon were now surrounded by many quiescent axons, the response recorded from it would be smaller because the longitudinal currents in it would be reduced by the shunting effect of the other inactive axons. Thus in a ventral root with many axons, each axon will contribute a relatively small signal. Conversely, in a ventral root with fewer axons each axon will contribute a greater individual signal.

This effect would contribute to the increased triceps response observed at C7-T1. Interestingly, this phenomenon acts to increase the individual response of all axons exiting through these roots, even remaining MAT axons. Thus the recorded ventral root response to MAT stimulation in PEA3 mutants is likely to be an overestimate of the actual input strength of MAT Ia afferents and may explain, in part, why the observed change is less than would be expected from a four-fold reduction in motoneuron number.

These experiments demonstrate that Ia afferents make functional connections with motoneurons of all ETS phenotypes at limb levels in PEA3 mutant mice, and that changes in the amount of input can be plausibly explained simply by changes in the number of motoneurons, not requiring a change in the specificity of these connections.

6.   Segmental specificity of Ia inputs is preserved in PEA3 mutants.

The segmental distribution of inputs from forelimb muscle nerves was unchanged

in PEA3 mutants (see Figure 24). For example, the location of the biceps motor pool is

reflected in the distribution of ventral root responses to stimulation of biceps sensory

afferents.   Stimulation of biceps nerve in normal animals evokes the strongest responses

in C5 and C6 ventral roots while eliciting much smaller responses in C7, C8, and T1.

This pattern is also observed in PEA3 mutants. The pectoralis major nerve demonstrates

a broader distribution of inputs from Ia afferents than biceps and suggests a broader

distribution of target motoneurons. Equally strong responses (~70 µV) were recorded

from C5, C6, and C7 in normal animals. A similar pattern was observed in PEA3

mutants. Despite the changes in amplitude of ventral root responses observed for MAT

and triceps nerve stimulation, the overall segmental pattern of inputs from these nerves

also remained normal. Therefore Ia afferents from various forelimb muscles continue to

restrict their innervation to motoneurons located in their normal projection zones. The

nature of ventral root recordings, however, makes it impossible to determine if the fine

pattern of synaptic specificity within a segment is altered in PEA3 mutant mice (see

Materials and Methods). This question was addressed by making intracellular recordings

from identified motoneurons.

7.   PEA3 is not required for formation of appropriate sensory-motor

**   connections in the hindlimb.**

The pool-specific expression pattern of PEA3 and Er81 in motoneurons led to the

idea that ETS genes may determine aspects of pool identity (Arber et al., 2000; Lin et al.,

1998). One manifestation of this identity is the specificity of inputs they receive from muscle sensory afferents. We therefore tested if the disruption of PEA3 expression perturbed the pattern of muscle sensory inputs to identified motoneurons. Motoneurons in the lumbar region of the spinal cord provided an excellent system in which to study this question because the normal pattern of connections in this region has been studied in detail, and adjacent pools of synergistic and antagonistic motoneurons are known to have different patterns of ETS gene expression.

Our experiments focused on the synaptic connections between Ia afferents and motoneurons innervating the quadriceps and adductor muscle groups. Motoneurons projecting to 3 of the 4 heads of the quadriceps muscle (vastus medius, vastus lateralis, and vastus intermedius muscles) express Er81, while motoneurons projecting to the remaining head (rectus femoris) express PEA3 (Arber et al., 2000). The common function of this muscle group in extending the knee joint suggests that Ia afferents projecting to each of these four muscles make significant inputs to all 4 types of quadriceps motoneurons, both to motoneurons projecting to the same muscle (homonymous connections) and to the other quadriceps heads (synergistic connections).

Obturator motoneurons project to the adductor muscle group, whose functions are antagonistic or unrelated to quadriceps muscles. These motoneurons, like vastus, express Er81, but not PEA3. Significantly, quadriceps and obturator motoneurons are located in the same lumbar spinal segments (L2-3) and have overlapping dendritic arbors, indicating that in normal animals a high degree of discrimination is required by Ia afferents in the formation of appropriate synaptic connections (McHanwell and Biscoe, 1981).

The strength of monosynaptic inputs from quadriceps and obturator afferents was

measured by making intracellular recordings from functionally identified motoneurons (see Materials and Methods and Figure 25). In normal mice, the strongest connections exist between Ia sensory afferents and motoneurons projecting to the same muscle target (homonymous connections). The average amplitude of homonymous projections was not different for any of the motoneuron types studied, suggesting that all populations of motoneurons received significant input from their own Ia afferents (see Figure 26).

Significant synergistic inputs (~50 % of homonymous input strength) were also observed within the different quadriceps pools. In contrast, inputs to quadriceps motoneurons from Ia afferents in the obturator nerve were small, rarely above 0.5 mV. A similar pattern was observed for obturator motoneurons; there is strong monosynaptic homonymous input, but vastus or rectus femoris afferents only rarely evoke measurable inputs. These results confirm those of previous experiments (Mears and Frank, 1997).

In PEA3 mutant mice, significant homonymous monosynaptic inputs were recorded from all 3 motoneuron types (see Figure 26). Homonymous inputs from both the obturator and the vastus muscles were, on average, the same size as in normal mice. A slight (15%) but significant increase in input from rectus femoris afferents to both rectus femoris and vastus motoneurons was observed. There were no changes in the inputs from afferents supplying antagonistic muscles. Significantly, the absence of PEA3 expression in rectus femoris motoneurons did not change the inputs these motoneurons received from synergistic vastus afferents.

If rectus femoris afferents required PEA3 for appropriate modulation of synaptic inputs, this could explain the modest increase in synergistic and homonymous inputs from these afferents in PEA3 mutant mice. The identitiy of PEA3 sensory neurons
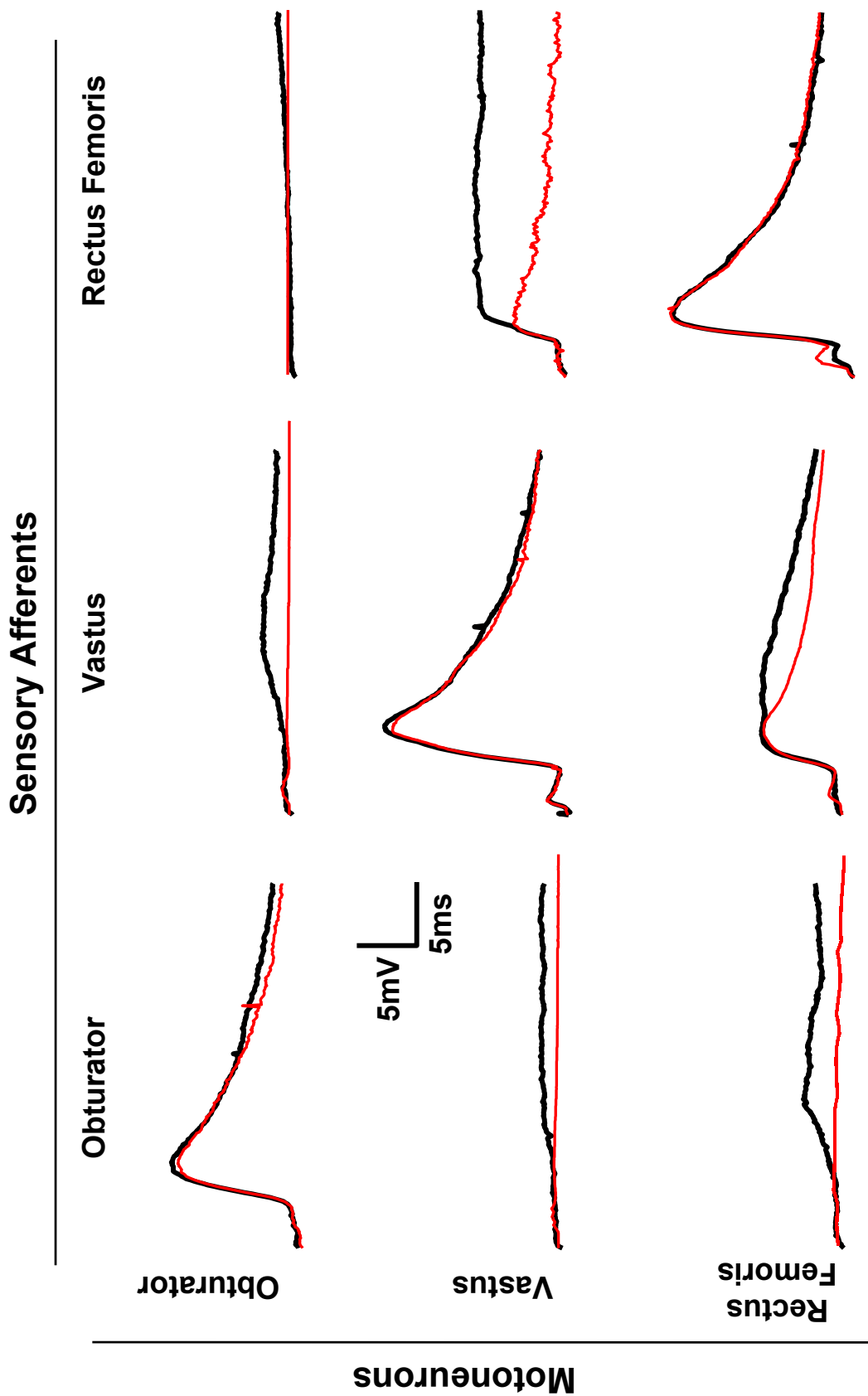
Figure 25. Ia afferents form monosynaptic connections with motoneurons supplying related muscles. Representative recordings from identified motoneurons in PEA3 normal animals. Responses are from obturator, vastus and rectus femoris motoneurons (arranged in rows) following stimulation of obturator, vastus and rectus femoris muscle nerves (arranged in columns). Maximal responses following full-strength stimulation recordings are shown in black. Matching model traces obtained from low-strength stimulation are shown in red to illustrate the method of determining monosynaptic amplitudes (see Materials and Methods).
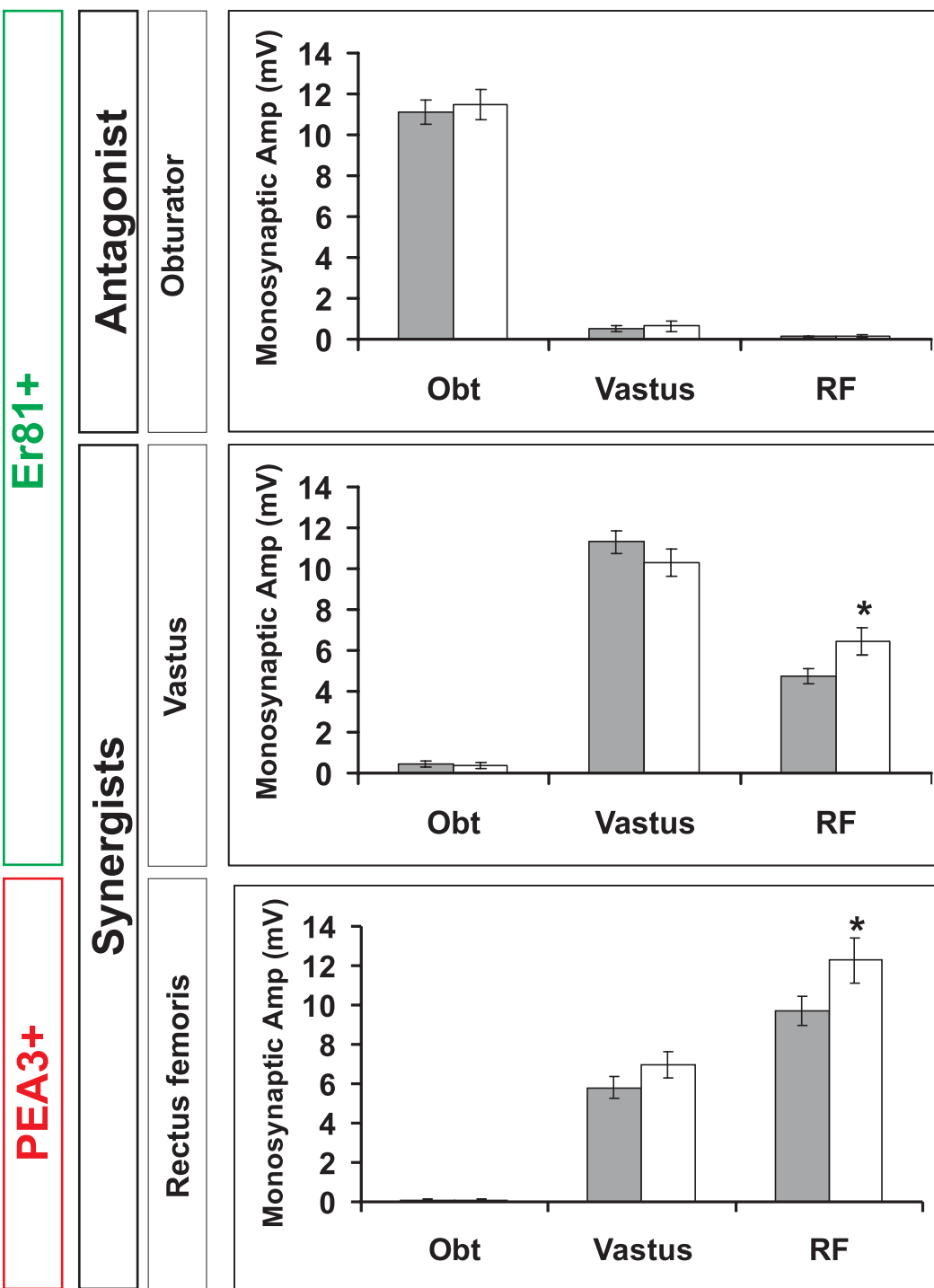
Figure 26. Specific pattern of Ia inputs to motoneurons is normal in PEA3 mutant mice. Intracellular recordings from obturator, vastus, and rectus femoris motoneurons (shown in three vertical panels) were made in P4-P6 mice in response to stimulation of obturator, vastus, and rectus femoris muscle nerves (listed at bottom of each panel). Both obturator and vastus motor pools express ER81 (green) while rectus femoris motoneurons express PEA3 (red). Obturator motoneurons supply muscles with antagonistic functions to those of both vastus and rectus femoris. Average monosynaptic responses ± SEM for >30 cells from each of these three pools in both normal (gray bars) and mutant (white bars) mice are shown. (*) indicates significant changes (p< 0.05).

remains unknown, however, because PEA3 expression in sensory neurons is below the limits of detection postnatally (Silvia Arber, personal communication).

These results demonstrate that in the absence of PEA3 in rectus femoris motoneurons, vastus and rectus femoris afferents still distinguish between rectus femoris and vastus motoneurons, establishing stronger connections with their homonymous partners in each case. Moreover, Ia afferents from antagonistic muscles (obturator afferents) still recognize rectus femoris motoneurons as inappropriate targets and avoid making contact with them.

8.   Conclusions

Experiments with mice deficient in the ETS gene Er81 showed profound deficits in muscle sensory neuron development, in particular the development of Ia afferents (Arber et al., 2000). In contrast, our studies of PEA3 mutant mice suggest that PEA3 is not required for the normal development of sensory neurons. The major classes of muscle sensory neurons (Ia and Ib afferents) appear to develop normally and make functional connections with spinal neurons in PEA3 mutants.

These experiments demonstrate that PEA3 does play a role in the formation of elements of motor pool identity; in the brachial spinal cord many fewer motoneurons project to c. maximus and those that remain are clustered in an inappropriate location. In the absence of PEA3, normally PEA3+ motoneurons may fail to survive the period of normally occurring cell death or may not extend axons into the periphery and die from the resulting lack of trophic support. If normally PEA3+ motoneurons do survive they may be unable to migrate to the correct location and instead adopt the fate of other

motoneuron neighbors that surround them. These possibilities are explored in the Discussion.

Other aspects of motor pool identity apparently do not require PEA3. The specificity of sensory connections to motoneurons in PEA3-expressing motor pools is not altered in PEA3 mutants. Motoneurons that normally express PEA3 receive appropriate patterns of homonymous, synergistic, and antagonistic synaptic inputs from Ia afferents in the absence of PEA3 expression.

5.   Discussion

The goal of these experiments was to determine if the ETS genes Er81 and PEA3 played a role in the formation of selective synapses between Ia sensory afferents and motoneurons. The major results of these experiments are as follows: Er81 is required for the formation of synapses between Ia afferents and motoneurons by controlling the stereotypic projections of Ia afferents into the ventral horn. In contrast, PEA3 is not required for the general formation of sensory-motor connections. In fact, intracellular recordings demonstrate that PEA3 is not required either in motoneurons or sensory neurons for the formation of specific synaptic connections between Ia afferents and motoneurons. PEA3 expression in some brachial motoneurons, however, is required for development of appropriate motoneuronal identity. The results of individual experiments with ETS knock-out mice will be discussed separately, followed by a discussion of the relevance of these findings in a broader context.

1.   Ia afferent sensory neurons are affected in Er81 mutant mice.

We have demonstrated that in Er81 mutant mice monosynaptic connections with motoneurons are dramatically reduced. Preliminary experiments also showed that Ia afferents do not project ventrally to the area of motoneurons in postnatal animals. It was unclear, however, if Ia sensory afferents made transient projections that were later retracted, or if these projections never developed at all. Further experiments by Silvia Arber described the time course of Ia afferent central projections during embryonic development (Arber et al., 2000).

In normal animals, beginning at E12, sensory afferents invade the dorsal portion

of the spinal cord and subsequently grow axon branches within the dorsal columns both rostral and caudal to the point of entry. Later (~E13), muscle sensory afferents begin to send collaterals into the gray matter of the spinal cord and by E15.5, Ia, but not Ib, afferents have grown ventrally into the motoneuron pools located in the ventral horn, where they develop monosynaptic connections with motoneurons.

In Er81 mutant animals, central projections of sensory neurons and axon collateral growth proceed normally until E15.5 (see Figure 27). Beginning at E16.5, however, Ia afferent growth toward the ventral horn is significantly reduced in mutant animals. Labeling of all sensory neurons by application of HRP to dorsal roots demonstrates that throughout development only ~1% of axons that normally project to the ventral horn do so in mutant animals (Arber et al., 2000). This deficit is observed not only in lumbar and brachial regions of the cord, but also in thoracic segments where motoneurons do not express Er81 or PEA3.

Because HRP applied to dorsal roots labels all sensory axons, it was important to determine if Ia afferents project into the spinal cord at all. Indeed, cutaneous afferents make dense projections in the dorsal laminae of the cord and these projections could obscure Ia projections in the dorsal horn. The projections of both Ia and Ib afferents can be visualized with antibodies to parvalbumin, a calcium binding protein (see Introduction). In normal animals, dense projections of Group I afferents can be seen in the area of Clarke's column and Ia afferent projections are seen throughout the ventral portion of the cord where motoneuron cell bodies are located. Clarke's column is a nucleus of interneurons that project to the brain via the spinocerebellar tract and receive sensory input from both Ia and Ib afferents (Brown, 1981). In Er81 mutant animals,

HRP

Er81^{+/+}

A — E15.5

C — E16.5

E — E18.5

G — P5 — CC — MN

Er81^{-/-}

B — E15.5

D — E16.5

F — E18.5

H — P5 — CC — MN

PV

Er81^{+/+}

I — E16.5

K — E18.5

M — P5

Er81^{-/-}

J — E16.5

L — E18.5

N — P5
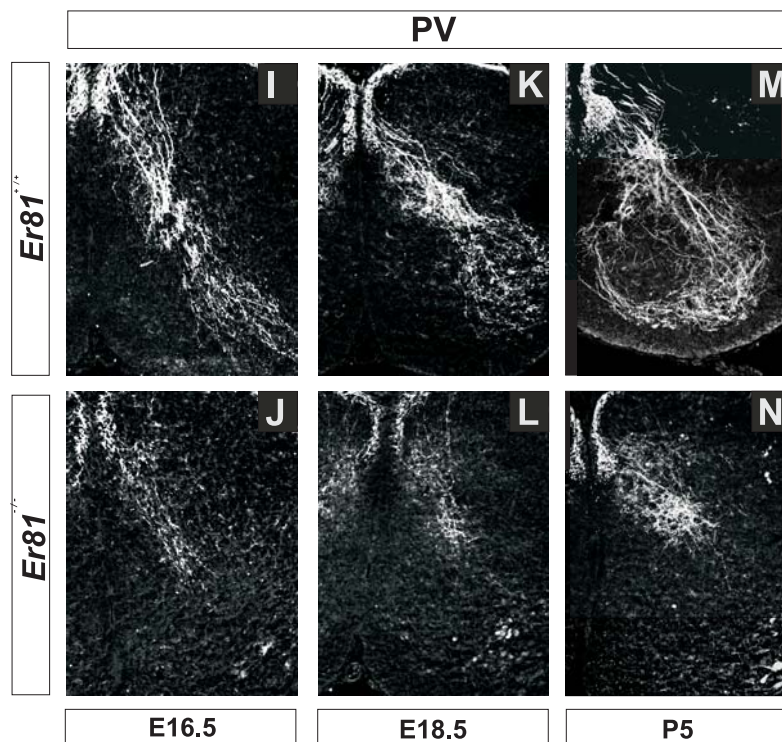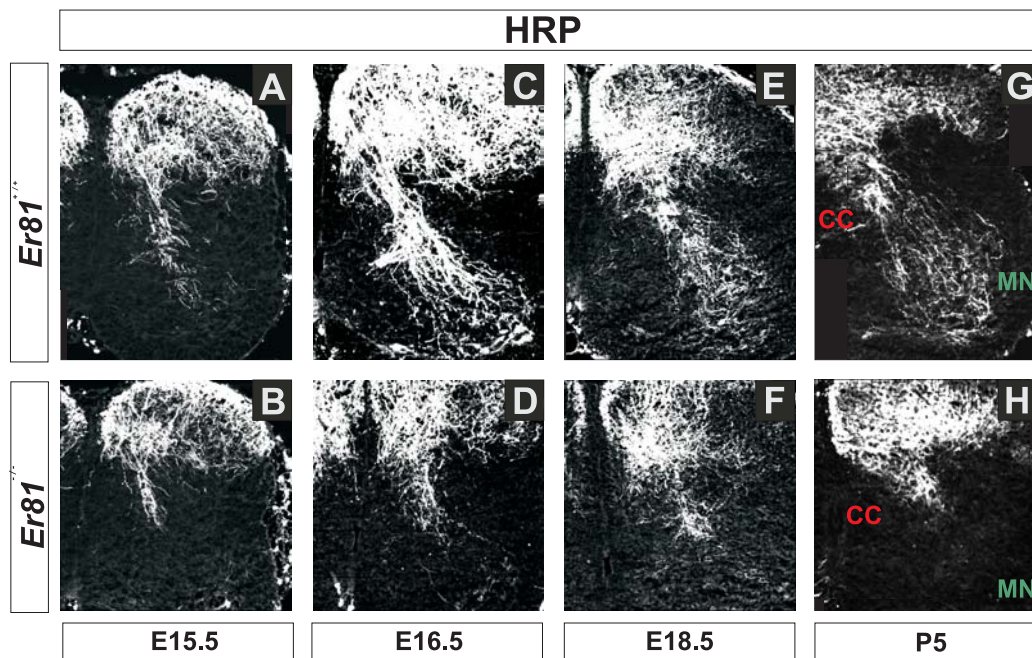
Figure 27. Ia afferents fail to make axonal projections to motoneurons in the ventral cord. (**A-H**) HRP was injected into L4/5 DRGs (E15.5 and E16.5) or L4/5 dorsal roots (E18.5 and P5) to visualize the general development of sensory afferent projections into the spinal cords of Er81 normal (**A, C, E, G**) and mutant (**B, D, F, H**) mice. Sensory afferent projections in the dorsal region of the spinal cord develop normally in Er81 mutants up to E15.5. After this time, however, Er81 mutants do not grow axon collaterals ventrally toward motoneurons (**MN**). In normal mice, muscle afferents terminate on dorso-spinocerebellar neurons located in Clarke's column (**CC**), and in the ventral spinal cord near motoneuron cell bodies (**MN**). (**I-N**) Staining of muscle sensory afferents in spinal cord confirms result of HRP labeling of all sensory afferents—Ia afferents fail to make stereotypic projections to motoneurons in Er81 mutant mice. Sections from L4/5 spinal cord level were reacted with antibody against parvalbumin (**PV**), a specific marker of muscle sensory afferents. Level of PV expression in Er81 mutant spinal cords was reduced 5-10 fold. Figure adapted from Arber et al, 2000.

Group I afferents project ventrally only as far as Clarke's column. No significant

staining is observed near motoneuron somata. Because PV labels both Ia and Ib afferents

it is not possible to determine visually if Ia afferents in Er81 mutants project into the

spinal cord at all. Residual monosynaptic inputs were observed with ventral root

recordings, however (see Table 1). The presence of these potentials, which in some cases

were as large as 25% of normal, strongly suggest that Ia afferents do project into the

spinal cord and make some synaptic connections on distal dendrites.

Retrograde fills of motoneurons in Er81 mutant animals indicate that

motoneuronal dendrites extend up into the spinal gray matter much as in normal animals

(see Figure 14). The loss of Ia afferent-motoneuron synaptic function is therefore not

likely to be the result of a failure of dendrites to project into the appropriate area. In fact,

dendrites in this figure appear to project more robustly in mutant animals. Perhaps radial

growth of motoneuron dendrites continues until dendrites contact axonal arbors from Ia

sensory afferents. In normal animals the dense projections of Ia afferents in the ventral

horn might inhibit exuberant growth of motoneuron dendrites. If axonal arbors fail to

develop in the region of motoneuron cell bodies, as in Er81 mutants, motoneuron

dendrites might continue to grow until they reach the location of the Ia afferent arbors.

2.   Does Er81 instruct Ia afferents to project to motoneurons?

Er81 is required for the growth of Ia afferent axons into the ventral regions of the

spinal cord, but it is unclear whether it acts via an instructive or permissive mechanism.

ETS proteins are powerful transcriptional activators and, in some cases, are repressors as

well, depending on the cellular context (Mavrothalassitis and Ghysdael, 2000). Thus it is

likely that Er81 is required for the activation and/or repression of certain genes unique to Ia afferents that permit growth toward motoneuron targets. At present, however, no candidate molecules have been identified. Current investigations in the lab of Silvia Arber are examining expression differences in trkC+ sensory neurons between Er81 normal and mutant mice.

Is Er81 required for the formation of the Ia afferent phenotype? Ia and Ib afferents, both trkC+, differ in both central and peripheral projections. In the periphery Ia afferents innervate muscle spindles while Ib afferents supply Golgi tendon organs (Jami, 1992). Centrally, Ia afferents project ventrally to motoneuron cell bodies, but Ib afferents project ventrally only as far as Clarke's column. Thus, despite a common molecular marker, Ia and Ib afferents have remarkably different phenotypes. Although Er81 is expressed in all trkC+ and PV+ sensory neurons, Er81 plays a critical role in the development of Ia afferents, while Ib afferents develop normally in the absence of Er81. Both PV staining and ventral root recordings following selective stimulation indicate that Ib afferent development is unaffected by the Er81 mutation. Perhaps in Er81 mutants Ia afferents adopt phenotypic characteristics of Ib afferents. The similar central projection pattern of Ia and Ib afferents in Er81 mutants suggests this possibility. In the periphery, however, stereotypic projections of Ia and Ib afferents develop in Er81 mutants. Muscle spindles as well as Golgi tendon organs are generated and Ia afferents remain sensitive to stretch, albeit at a reduced level. Thus, although Er81 is critical for the development of the unique central projections of Ia afferents, it is not required for the emergence of the Ia afferent phenotype.

Alternatively, Er81 might contribute to the ventral growth of axon collaterals in an indirect manner. Er81 may not be required for the activation or repression of specific genes that regulate axon growth, but rather it may control other genes required by Ia afferents for general health. Therefore, in Er81 mutants, less healthy Ia afferents may extend axons into the dorsal region of the cord, but fail to support ventral axon projections. Our results suggest that health of Ia afferents is compromised during both prenatal and postnatal development.

The calcium binding protein, parvalbumin (PV), has been shown to specifically label the soma and axons of both Ia and Ib afferents (Arber et al., 2000; Tourtellotte and Milbrandt, 1998). In normal animals, antibodies against PV robustly label these structures and allow visualization of both central and peripheral axon terminals. In Er81 mutants, however, the intensity of the PV signal is reduced 5-10 fold (Arber et al., 2000). Although PV continues to label these neurons, the reduction in signal intensity suggests that normal levels of this protein in both Ia and Ib afferents are dependant on Er81 expression. Levels of calcium binding proteins are often diagnostic for general health of cells (Shaw and Eggett, 2000). Significantly, reduced PV staining in Er81 mutants is evident embryonically, even before Ia axon collaterals enter the ventral cord in normal animals.

Reduced PV staining may suggest a cellular mechanism for the projection deficit observed in Er81 mutant mice. Active growth cones are sensitive to changes in intracellular calcium concentrations. Both increases and decreases from the optimum concentration cause growth cone collapse (Kater and Mills, 1991). Action potentials can result in increases in the intracellular calcium concentration. Ia afferents begin to fire

action potentials in response to muscle stretch soon after they arrive at their muscle

targets at E15 (Kozeka and Ontell, 1981; Kudo and Yamada, 1985). Thus, reduced

calcium-buffering capacity in Er81 mutant muscle sensory afferents might cause

premature collapse of Ia afferent growth cones beginning at the time at which these

sensory afferents become functionally active.

Our recordings during the first postnatal week also suggest that the health of Ia

afferents is compromised in at least two ways in Er81 mutants. First, recordings made

from the dorsal root following electrical stimulation of all sensory afferents demonstrate

that at least some Group I afferents conduct more slowly in Er81 mutants (see Figure 9).

Selective activation of Ia afferents by passive stretches of the muscle showed that the

conduction velocities of Ia afferents were lower in Er81 mutant animals (see Figure 11).

Second, Ia afferents do not respond well to muscle stretch. Ia afferents were not

responsive to high frequency muscle spindle stimulation in Er81 mutants. Also, the

amplitude of dorsal root responses to selective Ia stimulation was decreased in Er81

mutants. This could be explained by a decrease in the caliber of Ia axons, resulting in

reduced amplitude of action potentials from each afferent recorded in the dorsal root.

Alternatively, the number of axons projecting to muscle spindles may be reduced.

Selective activation of Ib afferents, however, suggested no deficits in activation in Er81

mutants.

Both Er81 and PEA3 are expressed by intrafusal muscle fibers that constitute the

muscle spindle (Arber et al., 2000). Thus, postnatal deficits in spindle activation may be

related to defects in spindle development. This possibility led our collaborator, Silvia

Arber, to investigate the generation of muscle spindles in Er81 mutant mice. During

embryogenesis, Egr3, a transcription factor expressed only in intrafusal muscle fibers, is first expressed at E15, the time at which Ia afferents first contact myotubes and induce the differentiation of intrafusal fibers (Tourtellotte and Milbrandt, 1998). Egr3 continues to be expressed at high levels throughout embryogenesis and into the first two weeks of postnatal life (Tourtellotte and Milbrandt, 1998). In Er81 mutants, Egr3 is expressed normally up to E18.0, the time at which Er81 expression begins in normal muscle spindles (Arber et al., 2000). By P5, however, Egr3 expression in intrafusal fibers is reduced (see Figure 28). Diffuse labeling of α-bungratoxin, which binds to the nicotinic ACh receptor and is another molecular feature of intrafusal fibers, is also reduced in postnatal animals (Silvia Arber, personal communication). Morphological identification of spindles in Er81 mutants shows that many spindles are lost entirely. Interestingly, the loss of muscle spindles is not uniform in different muscles. The number of spindles in some muscles is unchanged in mutants, and muscles seem to be affected without regard to which ETS gene is expressed in the corresponding motoneurons. For example, consistently no spindles are found in mutant gluteus muscles (innervated by PEA3+ motoneurons), while many spindles remain in mutant adductor muscles (innervated by Er81+ motoneurons).

Postnatal degeneration of muscle spindles is a likely cause of decreased sensitivity to stretch observed in Er81 mutants. Degeneration of muscle spindles will likely impair physical contact between the Ia afferent and muscle spindle. In mice lacking Egr3, muscle spindles degenerate in a pattern similar to that observed in Er81 mutants. Analysis of sensory contacts with intrafusal fibers demonstrates that
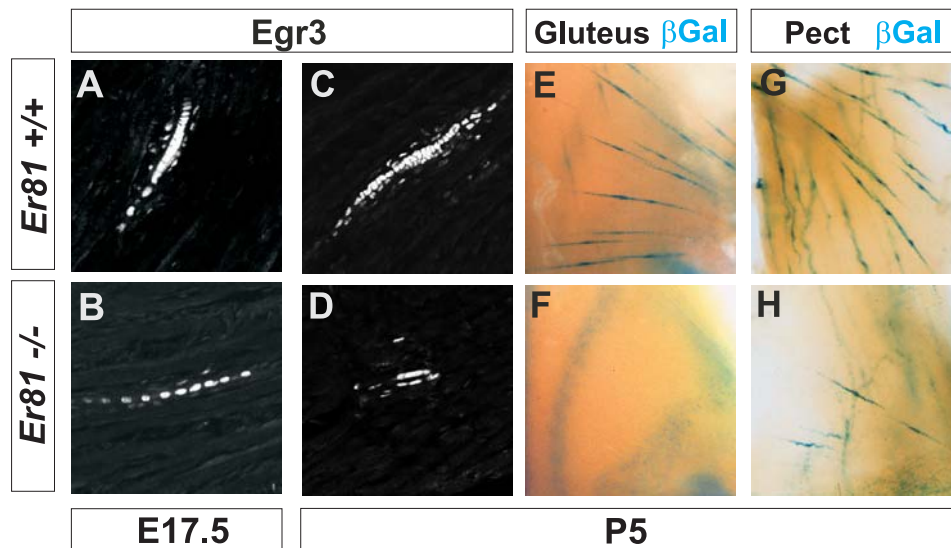
Figure 28. **Muscle spindles degenerate during the first postnatal week in Er81 mutant mice.** (**A, B**) Muscle spindles are present at E17.5 in hindlimb muscles of both Er81 normal and mutant mice. Muscle spindles are visualized using antibodies against Egr-3. At this stage, muscle spindles in Er81 mutants appear normal. (**C-H**) In Er81 mutants, muscle spindles in many muscles degenerate over the first postnatal week. Quadriceps muscle spindles stained for Egr-3 suggest degeneration of intrafusal fibers in Er81 mutant mice (compare **C** and **D**). Whole-mount gluteus (**E, F**) and pectoralis muscles (**G, H**) processed for β-galactosidase activity show that not all muscles are affected equally. Note the continued presence of some spindles in the pectoralis muscle (**H**) of Er81 mutant mice. Figure adapted from Arber et al, 2000.

concomitant with spindle degeneration, Ia afferents withdraw from the intrafusal fibers (Tourtellotte et al., 2001). Because action potentials in Ia afferents are generated via mechanically sensitive sodium channels, destabilization of Ia contact with intrafusal fibers will reduce the Ia afferent's ability to respond to stretch (Hunt, 1990).

Degeneration of muscle spindles may affect the conduction velocity of Ia afferents indirectly. The extent of sensory neuron myelination is positively correlated with axon diameter; larger axons are more heavily myelinated (Voyvodic, 1989). Among sensory neurons, muscle sensory afferents have the largest diameter axons and, as a result, the fastest conduction velocities. Sensory axon diameter is directly related to the extent of contact made with peripheral targets; larger targets are served by larger diameter axons (Voyvodic, 1989). Presumably this reflects the increased need for cytoplasmic flow to maintain extensive peripheral projections. If Ia afferents withdraw from degenerating intrafusal fibers in Er81 mutants as they do in Egr3 mutants, then Ia axons might shrink. These withdrawing axons would not require large amounts of cytoplasmic flow to maintain reduced connections. Significantly, axon withdrawal in Egr3 mutants occurs during the time of extensive myelination of peripheral axons— during the first postnatal week (Hildebrand et al., 1994). Thus, withdrawal of axons and shrinking of axon diameter might result in a corresponding reduction in myelination and conduction velocity.

Spindle degeneration is also likely to reduce the levels of peripheral neurotrophins available to sustain Ia afferents. Separate experiments involving Egr3 mutant mice show that mutant spindles do not produce NT3 (Chen et al., 2002). Interestingly, monosynaptic inputs to motoneurons are also reduced during the first postnatal week as

muscle spindles degenerate, despite normal anatomical Ia afferent projections to the ventral horn. Injection with NT3 rescues the monosynaptic inputs to motoneurons, suggesting that Ia afferents require NT3 to maintain functional monosynaptic connections (Chen et al., 2002). Thus, spindle degeneration in Er81 mutants likely reduces NT3 expression and may account for some of the loss of monosynaptic input observed in these animals.

3.   Is Er81 involved in specifying stretch reflex circuit connections?

The failure of Ia afferents to project to the ventral spinal cord makes it difficult to test if Er81 is required to form specific connections in the stretch reflex circuit. Although the monosynaptic input to motoneurons in Er81 mutants is dramatically reduced, there is significant variability in the recorded responses. Ventral root responses from rostral lumbar roots (L1-L3) are consistently about 10% of normal. In these segments, there are many ETS+ motor pools, both Er81+ (obturator and vastus pools) and PEA3+ (rectus femoris pool). The responses recorded from more caudal ventral roots (L4 and L5) evoked by stimulation of branches of the sciatic nerve (tibial and peroneal) were sometimes as much as 25% of normal. In these segments, there are relatively few Er81+ motor pools; ETS+ pools in this region are mainly PEA3+. Because the residual monosynaptic input to motoneurons from tibial and peroneal Ia afferents is measurable, it should be possible to measure these inputs with intracellular recordings as well. Thus, one could test if stretch reflex connections between Ia afferents and motoneurons supplying the muscles of the lower leg and foot are appropriate in Er81 mutants. A shortcoming of this experiment, however, is that it would only test the role of Er81 in Ia afferents, as motoneurons projecting in these nerves do not normally express Er81.

Manipulation of the Er81 locus such that Er81 is expressed in sensory neurons but not in motoneurons would allow for a more direct determination of the role of Er81 in the generation of specific synaptic connections. Presumably, Er81 expression in sensory neurons would rescue the Ia afferent projection phenotype observed in Er81 mutant mice. One could then test the specificity of these connections with intracellular recordings. Analysis of the connections between obturator and quadriceps afferents and motoneurons, described in this thesis for PEA3 mutants, would be a strong test of the role of Er81 in controlling specific synaptic connections. Silvia Arber is currently generating such mice (Silvia Arber, personal communication).

In conclusion, the deficits observed in Er81 mutant mice are primarily due to a requirement for Er81 in the normal development of Ia afferents. In the absence of Er81 Ia afferents fail to make axon projections to motoneurons and this results in a dramatic decrease in monosynaptic inputs to motoneurons. During the first postnatal week, some muscle spindles degenerate in Er81 mutants. This degeneration may influence the general health of Ia afferents postnatally.

4. PEA3 contributes to the formation of motoneuron identity.

In contrast to studies of Er81 mutants, sensory neuron development in PEA3 mutants appears unaffected. Our results show, however, that PEA3 is required for formation of the c. maximus motor pool in the brachial cord. PEA3 may be required in c. maximus motoneurons for survival during the period of naturally occurring cell death, for extension of axons into the periphery, or for migration to correct locations in the ventral

horn. The contributions of each of these mechanisms to the phenotype observed in PEA3 mutant mice will be discussed in turn.

Embryonic analysis of c. maximus motoneurons by Silvia Arber demonstrates that these cells represent a unique neural population. During early development of most motor pools, approximately two times the final number of motoneurons are generated. Beginning about E12 in the mouse, half of these motoneurons die, leaving motor pools populated by functionally appropriate numbers of motoneurons (Oppenheim, 1991; Yamamoto and Henderson, 1999). The c. maximus motor pool is unique in that very few motoneurons in this pool die (Silvia Arber, personal communication). Thus this large muscle, covering the entire dorsal surface of the animal, is supplied by an appropriately large motor pool.

Presumptive c. maximus motoneurons are generated in normal numbers in PEA3 mutant mice. The DNA construct inserted into the PEA3 locus contains the lacZ gene; therefore cells that would have normally expressed PEA3 can be visualized by staining for β-galactosidase activity in PEA3 mutants. The onset of lacZ expression in PEA3 mutants is similar to that observed in wild type animals and normal numbers of cells are found migrating laterally away from the neuroepithelium. Thus PEA3 is not required for the generation of presumptive c. maximus motoneurons.

Retrograde labeling of c. maximus and pectoralis minor muscle nerves in postnatal animals demonstrates that very few motoneurons project to c. maximus in PEA3 mutants. One possibility is that normally PEA3+ motoneurons fail to survive in the absence of PEA3. In fact, the total number of motoneurons in C8, the segment where a significant portion of c. maximus motoneurons are located, appears reduced in PEA3

mutants although the difference is not significant (see Figure 18). PEA3 may be required for activation or suppression of target genes that promote survival during the period of programmed cell death. Indeed, ETS genes have been most intensively studied with regard to their roles in the development of cancer. PEA3 is upregulated in certain breast cancers (Shepherd et al., 2001). Perhaps PEA3 in c. maximus motoneurons functions in a way similar to that observed in cancer to promote cell survival. Alternatively, PEA3, like Er81, may regulate genes that control axonal growth. Thus, in PEA3 mutants, presumptive c. maximus motoneurons that fail to extend axons into the periphery may, as an indirect consequence, die from lack of trophic support provided by the periphery.

Another identifying characteristic of the c. maximus motor pool is that these motoneurons follow a two-stage migration to their final location. Motoneurons of most motor pools migrate only laterally away from the neuroepithelium to their final pool locations. In contrast, once c. maximus motoneurons have migrated laterally away from the neuroepithelium they begin to descend ventrally, displacing other ventrally located motoneurons. Eventually, they settle along the ventral border of the gray matter. During this secondary ventral migration they displace other ventrally located motoneurons that will ultimately project into the limb. Thus, motoneurons that originally migrate laterally along the ventral border of the gray matter (for example, pectoralis major, minor, and triceps) are displaced by the ventral migration of c. maximus motoneurons and eventually settle in the dorsal portion of the LMC (Silvia Arber, personal communication). In the absence of PEA3, however, normally PEA3+ motoneurons (visualized by virtue of lacZ expression) fail to follow this second migratory program and remain in the dorsal portion of the LMC. As a consequence, other LMC motoneurons remain ventral to the c.

maximus pool. Thus, PEA3 is required for the proper migration of c. maximus

motoneurons and, indirectly, for establishment of the appropriate topographical

distribution of other motor pools as well.

The primary defect observed in PEA3 mutant mice is the failure of brachial

PEA3+ motoneurons to follow the appropriate migratory sequence. By what mechanism

does PEA3 influence this migration? One possibility is that without expression of PEA3,

these cells are insensitive to guidance cues. Netrin-1, a diffusible factor secreted by cells

in the floor plate, is present in a graded distribution in the ventral spinal cord (Kennedy et

al., 1994; Serafini et al., 1994). This factor was first identified as an attractive factor for

axon guidance, but can also influence cell migration (Kennedy, 2000). In the absence of

PEA3, motoneurons fated to become c. maximus motoneurons may fail to respond to

these or other guidance cues and remain in an aberrant dorsal location.

Another possibility is that the migratory capacity of presumptive c. maximus

motoneurons may be reduced in PEA3 mutants. Migration of developing neurons is

facilitated by glia that guide neurons along predetermined tracks in the nervous system

(Rakic, 1971). This migration involves complex interactions between the migrating

neuron and its glial scaffold, as well the surrounding extracellular matrix (ECM). As

mentioned above, ETS genes are known to regulate expression of proteins found on the

cell surface that mediate cell-cell adhesion. Significantly, ECM degrading proteases are

upregulated by ETS factors during tumor invasion and metastasis (de Launoit et al.,

2000; Trojanowska, 2000). Thus, c. maximus motoneurons may be unable to interact

with the appropriate glial scaffold during their ventral migration or may be unable to

remodel the ECM to allow migration in PEA3 mutants.

5.   Is there a role for PEA3 in sensory neurons?

Although the onset and order of ETS expression in mice is similar to that observed in chick, the final distribution of ETS genes in sensory neurons in mouse is significantly different (see Introduction). Many late-stage sensory neurons in chick express PEA3, but at similar stages in the mouse very few sensory neurons express PEA3, while nearly all ETS+ sensory neurons express Er81. What then is the role of PEA3 in mouse sensory neurons? PEA3 loss of function does not appear to impair early development of sensory neurons, despite the fact that PEA3 is expressed in developing sensory neurons before Er81. Perhaps the subsequent expression of Er81 is sufficient to compensate for the loss of PEA3 in sensory neuron development.

6.   Appropriate monosynaptic connections form between Ia afferents and motoneurons in the absence of PEA3.

Intracellular recordings from PEA3 mutant mice demonstrate that the pattern of Ia afferent inputs to quadriceps and obturator motoneurons is unchanged. These motoneurons were chosen for study because motoneurons projecting to different heads of quadriceps express both PEA3 (rectus femoris) and Er81 (vastus). Also, obturator motoneurons, supplying muscles antagonistic to quadriceps, are located nearby and express Er81. Thus it appears that in the absence of PEA3, motoneurons are able to synthesize the appropriate extracellular proteins to guide selective synaptogenesis with Ia afferents. Our results do not preclude the possibility that inappropriate connections are formed early on, but are refined before experiments are performed at P4-P6. Previous recordings in this system, however, demonstrate that the pattern of Ia afferent inputs in

normal mice is correct from the outset and does not change significantly during development (Mears and Frank, 1997).

This finding is of particular interest in light of the highly restricted expression of ETS genes in motoneurons. These are the only factors identified to date that are expressed by individual motor pools (Lin et al., 1998; Arber et al., 2000). The combinatorial expression of ETS genes with other LIM transcription factors uniquely identifies many motor pools. Moreover, the onset of ETS expression in motoneurons coincides with the arrival of motor axons at muscle targets (Lin et al., 1998; Tosney and Landmesser, 1985). Because ETS genes are strong transcriptional activators, it seemed likely that these factors controlled significant elements of motoneuron identity. Perhaps these factors were responsible for the expression of specific cell-surface molecules that would mediate selective synapse formation with Ia sensory afferents. Our experiments, however, suggest that PEA3 alone does not regulate the expression of the specific cell-surface molecules required for appropriate synaptic connections in the stretch reflex circuit.

Is there any evidence of specificity changes in PEA3 mutant mice? On average, the synaptic input from pectoralis afferents was decreased in PEA3 mutants. This is likely to be due to the dramatic decrease in motoneuron number in mutant mice. The response evoked in the same ventral roots by triceps stimulation, however, was larger in mutants than in normal mice. At first glance, this may be interpreted as a breakdown in specificity; triceps Ia afferents may be projecting to additional inappropriate motoneurons. An alternative explanation, however, is that this observation is most easily explained by alterations in motor pool size in PEA3 mutants. Some presumptive c.

maximus motoneurons remaining in more dorsal locations may adopt fates of the normally more dorsally located motoneurons and project axons toward muscles in the limb. Indeed, at later embryonic stages these motoneurons (visualized by lacZ expression) reduce expression of lacZ in PEA3 mutants (Silvia Arber, personal communication). This suggests that PEA3 expression in motoneurons may be dependant on environmental signals localized to the ventral portion of the LMC. Perhaps some motoneurons destined to innervate c. maximus instead innervate novel target muscles, including triceps. Thus, triceps muscle may be innervated by more motoneurons than normal. If each Ia afferent makes the same strength connection with each appropriate motoneuron it synapses with, then an increase in the number of triceps motoneurons would result in an increased ventral root response. Determining the number of triceps motoneurons in PEA3 mutants by retrograde labeling could test this idea.

An additional factor that argues against a change in specificity of sensory-motor connections in the brachial region of PEA3 mutants is the paucity of PEA3+ sensory neurons in the DRG that contain afferents that project to c. maximus (Silvia Arber, personal communication). Even at early developmental stages when most muscle sensory neurons co-express Er81 and PEA3, very few sensory afferents in the C7 and C8 DRG express PEA3 (Silvia Arber, personal communication). It is not known if these sensory neurons express Er81. Thus, loss of PEA3 expression would be unlikely to perturb the normal development of muscle sensory afferents projecting to motoneurons in these segments. If synaptic specificity is altered in the brachial region, it is likely due to a requirement of PEA3 in motoneurons. A specific role for PEA3 in determining specificity would be difficult to separate from PEA3's earlier role in the migration of

presumptive c. maximus motoneurons. The few motoneurons that project to c. maximus in PEA3 mutants may be incapable of formation of specific synaptic connections.

Direct analysis of possible specificity changes in PEA3 mutants would require intracellular recordings from identified motoneurons. While recordings from triceps, biceps, and pectoralis motoneurons in PEA3 mutants would be relatively easy to obtain, recordings from c. maximus motoneurons would be considerably more difficult because of the drastic reduction in cell number. An additional complication is the unknown amount of normal sensory input to c. maximus motoneurons. Preliminary studies suggest that only 3-5 muscle spindles are contained in c. maximus. By contrast, 9-12 spindles are found in pectoralis minor muscle, which is supplied by a small muscle pool in comparison to c. maximus (Silvia Arber, personal communication). Although Ia afferents from these spindles may make connections with c. maximus motoneurons, the strength of these connections could be weak. Analysis of c. maximus dendritic arbors suggests that these motoneurons may not receive significant Ia sensory input. Limb motoneuron dendrites project into the central gray matter of the cord where they can receive Ia input. In contrast, c. maximus motoneurons extend their dendrites medially and laterally in fasciculated bundles and avoid the central gray matter.

7.   Other candidate molecules that may direct formation of specific stretch

       reflex circuit connections.

If pool-specific expression of ETS-family transcription factors does not regulate the genes that generate synaptic specificity, what factors do? The most likely answer is that pool-specific gene expression is regulated by combinatorial interactions of identified

factors and other factors still to be determined. Although the restricted expression of ETS genes provides the most detailed identification of motor pools to date, ETS expression alone does not uniquely identify motor pools. Distinguishing various Er81+ motor pools, for example, requires that different pools be located in different compartments of the LMC or separated along the rostral-caudal axis. The combinatorial nature of this control makes it difficult to analyze.   Indeed, the identity of a motor pool is controlled by many different transcription factors, regulated both in time and space and continually influenced by signals from the organism as a whole (Briscoe et al., 2000; Lee and Pfaff, 2001; Tanabe and Jessell, 1996).

Molecular specification of synaptic connections in the stretch reflex circuit remains an appealing and reasonable hypothesis. Current evidence suggests that stretch reflex connections are appropriate from the outset and that, unlike other neural systems, coordinated pre- and post-synaptic activity is not required for the generation of these specific connections (Mears and Frank, 1997). A straightforward explanation of this phenomenon is that Ia afferent axons identify dendrites of appropriate motoneurons through a common chemical signal. Sperry first advanced this idea as the mechanism by which retinal afferents make appropriate topographical projections to postsynaptic neurons in the optic tectum (Sperry, 1963).

Molecular determination of an organism's stretch reflex circuits would require relatively few factors when compared to the complexity involved in creating the numerous and complex circuits in the brain. Even so, the molecular diversity required for specification of inputs to more than 100 distinct motor pools is significant. This problem becomes even more complex when sensory inputs to synergistic muscles are considered.

Our results demonstrate that Ia inputs to functionally related motoneurons are significant, as much as 60% the strength of homonymous connections (see Figure 26). If these synaptic connections are also molecularly determined how are they controlled? Synergistic sensory and motoneurons may express similar cell-surface molecules and the relative strength of these connections may be influenced by coordinated synaptic activity. Alternatively, synergistic input strength may be controlled by reduced expression in motoneurons of additional cell-surface molecules that match similar molecules expressed by sensory neurons.

What then are likely candidates to mediate this process? A class of molecules that has attracted significant interest is the cadherins. These molecules are characterized by strong homophilic binding. Early studies identified these molecules as important regulators of tissue differentiation in the developing nervous system (Takeichi et al., 1997). The classic cadherin family contains 8 members, including N-cadherin and L-cadherin. Significantly, cadherins are found at synaptic junctions and studies of N-cadherin demonstrate that cadherins strengthen the physical connections between pre- and post-synaptic cells following synaptic activity (Tanaka et al., 2000). Recent studies have identified three additional groups of cadherin-like genes (Kohmura et al., 1998; Wu and Maniatis, 1999). The tight clustering of these genes in DNA bears remarkable resemblance to the structure of the V-D-J domains of immunoglobulin genes. Each of the three gene clusters is composed of ~20 "variable" genes which code different extracellular domains, and one gene which codes for a "constant" intracellular domain (Wu and Maniatis, 1999). The method of recombination of these genes is not yet known, but the number of predicted cadherin genes generated from these clusters is in excess of

100 (Albright et al., 2000). Members of these families are expressed by interconnecting brain regions during development (Takeichi et al., 1997) suggesting that they may, indeed, be elements of the molecular lock-and-key mechanism hypothesized by Sperry (Sperry, 1963).

Another family of cell-surface proteins, the neurexins, also displays an enormous potential for variability. The neurexins are a relatively small family of genes, but are predicted to have a very large number of splice variants—approximately 1000 (Missler and Sudhof, 1998; Rudenko et al., 1999). These cell-surface molecules interact with cell-surface receptors, termed neuroligins, localized at post-synaptic membranes (Song et al., 1999). Although these interactions are just beginning to be studied, they provide evidence that cell-cell interactions may be specified to a high degree by molecular interactions.

Variations in expression levels of specific proteins can further differentiate neuronal populations. In developing muscle sensory neurons, Er81 is abundantly expressed in some but expressed just above the limits of detection in others. Perhaps sensory neurons destined to become Ia afferents require Er81 expression above a certain threshold for differentiation. Presumptive Ib afferents, on the other hand, may require only minimal expression of the gene. In the absence of Er81, Ia differentiation may be severely impacted, as evidenced by the observed projection deficit, while Ib afferents may develop normally or have deficits too subtle to detect in our analysis. Additionally, the phosphorylation state of proteins and other post-translation modifications can have a profound impact on function. These modifications are dependant on the intracellular state of a cell that is, in turn, influenced by neighboring cells. Neuronal populations with

the same molecular signature (and even the same expression levels) may respond differently to the same stimuli depending on their locations. For example, both obturator and vastus motor pools express only Er81. Obturator motoneurons, however, reside in the LMC_M, while vastus motoneurons reside in the LMC_L. These two columns are distinguished by Lim-1 expression in the LMC_L. Consequently, the differing molecular environments that surround obturator and vastus motoneurons may result in differential activity of Er81.

8.   Knockout mice are valuable tools to study developmental processes.

An overall goal of biology is to understand the interactions of cellular elements in the function of the entire organism. Reductionist experiments conducted *in vitro* benefit from the significant advantage that the physical parameters of a system can be relatively well controlled. In this way, precise biological interactions between molecules can be determined, but a significant caveat remains. Because the elements of these experiments are extremely limited and controlled, it is difficult to predict that a particular interaction observed *in vitro* will be observed *in vivo*. A more satisfying, but challenging, approach is to devise methods that will allow observation of biological processes in the context of the whole organism. In developmental biology, an effective approach is to reduce or eliminate a particular molecule from the outset and to observe changes in the developmental pattern of the embryo. Knockout technology available in mice has proven to be a valuable resource in the study of developmental biology (Joyner, 1993).

Analysis of knockout mice is not without limitations, however (Picciotto and Wickman, 1998). Often the effects are more severe than anticipated. Many knockouts of transcription factors die as early embryos, precluding analysis of their role in later

development. Conversely, many knockouts are viable, but display only a subtle

phenotype. A classic example is that of the cell adhesion molecule N-CAM. Given its

wide distribution in the brain and localization at synapses, the observed phenotype is

surprisingly subtle (Cremer et al., 1994).

Subtle phenotypes are often explained by compensation from related factors.

There is some evidence for compensation in Er81 and PEA3 mutant mice. The absence

of PEA3 expression in recently post-mitotic sensory neurons does not appear to affect the

final differentiation and function of these neurons. Since many ETS+ sensory neurons

express both PEA3 and Er81 during development, Er81 may function in place of PEA3

such that Er81 expression is sufficient for the generation of the appropriate cellular

identities of ETS+ sensory neurons. Conversely, Ib afferents appear normal in Er81

mutants, suggesting that Er81 is not required for the formation of the Ib afferent

phenotype. Perhaps in these sensory neurons PEA3 expression is sufficient to generate

the appropriate phenotype.

An advantage of current knock-out technology is that it permits temporal control

of gene expression; a particular gene can be turned off or on at a particular time. This is

accomplished with an inducible CRE/lox expression system by which the target gene is

eliminated following administration of a drug. Eliminating Er81 gene expression in late

gestation (after E17.5) would, presumably, rescue Ia axon collateral growth in the ventral

region of the spinal cord. The presence of robust monosynaptic connections would then

allow an analysis of later effects of Er81 on synaptic connectivity. If specific input

patterns remain unchanged in these mice, then one could conclude that late expression of

Er81 or PEA3 was not required for the formation of appropriate sensory-motor connections.

Our experiments have attempted to infer the roles of Er81 and PEA3 through analysis of mice lacking either Er81 or PEA3 expression. Of equal value would be experiments analyzing mice that over-express Er81 or PEA3. Unlike developing sensory neurons, motoneurons never co-express Er81 and PEA3. Mice in which PEA3, for example, was expressed under the control of the HB9 promoter would result in all motoneurons being PEA3+. In addition, PEA3 expression would be independent of induction from peripheral tissues. In these mice, motor pools that normally do not express either ETS gene would become ETS+ by virtue of PEA3 expression and normally Er81+ motor pools would co-express PEA3. Aberrant expression of PEA3 in motoneurons with different column locations and molecular identities might attract inputs from sensory neurons that normally would not make inputs to these motoneurons. Finally, HB9-driven PEA3 expression in normally PEA3+ motor pools would result in over-expression of the gene in these motor pools. One could then assess the effects of ETS protein levels on the formation of synaptic connections. These mice are currently being generated in the laboratory of Silvia Arber (personal communication).

9.   Summary

The experiments presented here were designed to determine if the ETS genes Er81 and PEA3 influenced the formation of specific monosynaptic sensory-motor connections by virtue of their expression patterns in functionally connected sensory and motoneurons. Our results demonstrate that these ETS genes are important for the

formation of the stretch reflex, but in unanticipated ways. Er81 is required for the formation of strong monosynaptic connections because it controls the growth of Ia axon collaterals that project to the region of motoneurons. PEA3 is required by c. maximus motoneurons to form an appropriate motor pool—an essential element of the stretch reflex circuit. Finally, PEA3 expression is not required for the formation of specific monosynaptic connections.

BIBLIOGRAPHY

Bibliography

Albright, T. D., Jessell, T. M., Kandel, E. R., and Posner, M. I. (2000). Neural science: a century of progress and the mysteries that remain. Cell *100 Suppl*, S1-55.

Anderson, D. J. (1999). Lineages and transcription factors in the specification of vertebrate primary sensory neurons. Current Opinion in Neurobiology *9*, 517-524.

Arber, S., Han, B., Mendelsohn, M., Smith, M., Jessell, T. M., and Sockanathan, S. (1999). Requirement for the homeobox gene Hb9 in the consolidation of motor neuron identity. [see comments]. Neuron *23*, 659-674.

Arber, S., Ladle, D. R., Lin, J. H., Frank, E., and Jessell, T. M. (2000). ETS gene Er81 controls the formation of functional connections between group Ia sensory afferents and motor neurons. Cell *101*, 485-498.

Baulac, M., and Meininger, V. (1981). Organisation des motoneurones des muscles pectoraux chez le rat. Contribution a l'etude de l'arc axillaire (Achselbogen). Acta Anatomica *109*, 209-217.

Bories, J. C., Willerford, D. M., Grevin, D., Davidson, L., Camus, A., Martin, P., Stehelin, D., and Alt, F. W. (1995). Increased T-cell apoptosis and terminal B-cell differentiation induced by inactivation of the Ets-1 proto-oncogene. Nature *377*, 635-638.

Briscoe, J., and Ericson, J. (2001). Specification of neuronal fates in the ventral neural tube. Current Opinion in Neurobiology *11*, 43-49.

Briscoe, J., Pierani, A., Jessell, T. M., and Ericson, J. (2000). A homeodomain protein code specifies progenitor cell identity and neuronal fate in the ventral neural tube. Cell *101*, 435-445.

Brown, A. G. (1981). Organization in the spinal cord: the anatomy and physiology of identified neurones (Berlin, Springer-Verlag).

Brown, K. T., and Flaming, D. G. (1986). Advanced micropipette techniques for cell physiology (New York, John Wiley & Sons).

Brown, M. C., and Booth, C. M. (1983). Postnatal development of the adult pattern of motor axon distribution in rat muscle. Nature *304*, 741-742.

Brown, T. A., and McKnight, S. L. (1992). Specificities of protein-protein and protein-DNA interaction of GABP alpha and two newly defined ets-related proteins. Genes & Development *6*, 2502-2512.

Catalano, S. M., and Shatz, C. J. (1998). Activity-dependent cortical target selection by thalamic axons. Science *281*, 559-562.

Celio, M. R. (1990). Calbindin D-28k and parvalbumin in the rat nervous system. Neuroscience *35*, 375-475.

Chen, H. H., and Frank, E. (1999). Development and specification of muscle sensory neurons. Curr Opin Neurobiol *9*, 405-409.

Chen, H. H., Tourtellotte, W. G., and Frank, E. (2002). Muscle spindle-derived neurotrophin 3 (NT3) regulates synaptic connectivity between muscle sensory and motor neurons. J Neurosci, In Press.

Cheng, H. J., Nakamoto, M., Bergemann, A. D., and Flanagan, J. G. (1995). Complementary gradients in expression and binding of ELF-1 and Mek4 in development of the topographic retinotectal projection map. Cell *82*, 371-381.

Clarke, P. G. H., and Oppenheim, R. W. (1995). Neuron death in vertebrate development: in vivo methods. Methods in Cell Biology *46*, 277-321.

Copray, J. C., Mantingh-Otter, I. J., and Brouwer, N. (1994). Expression of calcium-binding proteins in the neurotrophin-3-dependent subpopulation of rat embryonic dorsal root ganglion cells in culture. Brain Research Developmental Brain Research *81*, 57-65.

Cremer, H., Lange, R., Christoph, A., Plomann, M., Vopper, G., Roes, J., Brown, R., Baldwin, S., Kraemer, P., and Scheff, S. (1994). Inactivation of the N-CAM gene in mice results in size reduction of the olfactory bulb and deficits in spatial learning. Nature *367*, 455-459.

Crossley, P. H., Minowada, G., MacArthur, C. A., and Martin, G. R. (1996). Roles for FGF8 in the induction, initiation, and maintenance of chick limb development. Cell *84*, 127-136.

de Launoit, Y., Chotteau-Lelievre, A., Beaudoin, C., Coutte, L., Netzer, S., Brenner, C., Huvent, I., and Baert, J. L. (2000). The PEA3 group of ETS-related transcription factors. Role in breast cancer metastasis. Advances in Experimental Medicine & Biology *480*, 107-116.

Dou, C., Ye, X., Stewart, C., Lai, E., and Li, S. C. (1997). TWH regulates the development of subsets of spinal cord neurons. Neuron *18*, 539-551.

Ernfors, P., Merlio, J.-P., and Persson, H. (1992). Cells expressing mRNA for

neurotrophins and their receptors during embryonic rat development. Eur J Neurosci *4*, 1140-1158.

Farinas, I., Jones, K. R., Backus, C., Wang, X. Y., and Reichardt, L. F. (1994). Severe sensory and sympathetic deficits in mice lacking neurotrophin-3. Nature *369*, 658-661.

Farinas, I., Yoshida, C. K., Backus, C., and Reichardt, L. F. (1996). Lack of neurotrophin-3 results in death of spinal sensory neurons and premature differentiation of their precursors. Neuron *17*, 1065-1078.

Feng, G., Laskowski, M. B., Feldheim, D. A., Wang, H., Lewis, R., Frisen, J., Flanagan, J. G., and Sanes, J. R. (2000). Roles for ephrins in positionally selective synaptogenesis between motor neurons and muscle fibers. Neuron *25*, 295-306.

Frank, E. (1987). The influence of neuronal activity on patterns of synaptic connections. TINS *10*, 188-190.

Frank, E., and Mendelson, B. (1990). Specification of synaptic connections between sensory and motor neurons in the developing spinal cord. Journal of Neurobiology *21*, 33-50.

Frisen, J., Yates, P. A., McLaughlin, T., Friedman, G. C., O'Leary, D. D. M., and Barbacid, M. (1998). Ephrin-A5 (AL-1/RAGS) is essential for proper retinal axon guidance and topographic mapping in the mammalian visual system. Neuron *20*, 235-243.

Gille, H., Kortenjann, M., Thomae, O., Moomaw, C., Slaughter, C., Cobb, M. H., and Shaw, P. E. (1995). ERK phosphorylation potentiates Elk-1-mediated ternary complex formation and transactivation. EMBO Journal *14*, 951-962.

Gille, H., Sharrocks, A. D., and Shaw, P. E. (1992). Phosphorylation of transcription factor p62TCF by MAP kinase stimulates ternary complex formation at c-fos promoter. Nature *358*, 414-417.

Gory, S., Dalmon, J., Prandini, M. H., Kortulewski, T., de Launoit, Y., and Huber, P. (1998). Requirement of a GT box (Sp1 site) and two Ets binding sites for vascular endothelial cadherin gene transcription. Journal of Biological Chemistry *273*, 6750-6755.

Gradwohl, G., Fode, C., and Guillemot, F. (1996). Restricted expression of a novel murine atonal-related bHLH protein in undifferentiated neural precursors. Developmental Biology *180*, 227-241.

Greene, E. C. (1935). The anatomy of the rat (Philadelphia, The American Philosophical Society).

Haase, P., and Hrycyshyn, A. W. (1985). Labeling of motoneurons supplying the

cutaneous maximus muscle in the rat, following injection of the triceps brachii muscle with horseradish peroxidase. Neuroscience Letters *60*, 313-318.

Helmbacher, F., Schneider-Maunoury, S., Topilko, P., Tiret, L., and Charnay, P. (2000). Targeting of the EphA4 tyrosine kinase receptor affects dorsal/ventral pathfinding of limb motor axons. Development - Supplement *127*, 3313-3324.

Hendricks, T., Francis, N., Fyodorov, D., and Deneris, E. S. (1999). The ETS domain factor Pet-1 is an early and precise marker of central serotonin neurons and interacts with a conserved element in serotonergic genes. Journal of Neuroscience *19*, 10348-10356.

Hildebrand, C., Bowe, C. M., and Remahl, I. N. (1994). Myelination and myelin sheath remodelling in normal and pathological PNS nerve fibres. Progress in Neurobiology *43*, 85-141.

Holstege, G., van Neerven, J., and Evertse, F. (1987). Spinal cord location of the motoneurons innervating the abdominal, cutaneous maximus, latissimus dorsi and longissimus dorsi muscles in the cat. Experimental Brain Research *67*, 179-194.

Honig, M. G., Frase, P. A., and Camilli, S. J. (1998). The spatial relationships among cutaneous, muscle sensory and motoneuron axons during development of the chick hindlimb. Development *125*, 995-1004.

Hunt, C. C. (1990). Mammalian muscle spindle: peripheral mechanisms. Physiological Reviews *70*, 643-663.

Jacob, J., Hacker, A., and Guthrie, S. (2001). Mechanisms and molecules in motor neuron specification and axon pathfinding. Bioessays *23*, 582-595.

Jami, L. (1992). Golgi tendon organs in mammalian skeletal muscle: functional properties and central actions. Physiological Reviews *72*, 623-666.

Joyner, A. L., ed. (1993). Gene Targeting: A Practical Approach (Oxford, Oxford University Press).

Kania, A., Johnson, R. L., and Jessell, T. M. (2000). Coordinate roles for LIM homeobox genes in directing the dorsoventral trajectory of motor axons in the vertebrate limb. Cell *102*, 161-173.

Karim, F. D., Urness, L. D., Thummel, C. S., Klemsz, M. J., McKercher, S. R., Celada, A., Van Beveren, C., Maki, R. A., Gunther, C. V., and Nye, J. A. (1990). The ETS-domain: a new DNA-binding motif that recognizes a purine-rich core DNA sequence. Genes & Development *4*, 1451-1453.

Kater, S. B., and Mills, L. R. (1991). Regulation of growth cone behavior by calcium. J Neurosci *11*, 891-899.

Kennedy, T. E. (2000). Cellular mechanisms of netrin function: long-range and short-range actions. Biochemistry & Cell Biology *78*, 569-575.

Kennedy, T. E., Serafini, T., de la Torre, J. R., and Tessier-Lavigne, M. (1994). Netrins are diffusible chemotropic factors for commissural axons in the embryonic spinal cord. Cell *78*, 425-435.

Kilpatrick, T. J., Brown, A., Lai, C., Gassmann, M., Goulding, M., and Lemke, G. (1996). Expression of the Tyro4/Mek4/Cek4 gene specifically marks a subset of embryonic motor neurons and their muscle targets. Molecular & Cellular Neurosciences *7*, 62-74.

Koblar, S. A., Krull, C. E., Pasquale, E. B., McLennan, R., Peale, F. D., Cerretti, D. P., and Bothwell, M. (2000). Spinal motor axons and neural crest cells use different molecular guides for segmental migration through the rostral half-somite. Journal of Neurobiology *42*, 437-447.

Kohmura, N., Senzaki, K., Hamada, S., Kai, N., Yasuda, R., Watanabe, M., Ishii, H., Yasuda, M., Mishina, M., and Yagi, T. (1998). Diversity revealed by a novel family of cadherins expressed in neurons at a synaptic complex. Neuron *20*, 1137-1151.

Kozeka, K., and Ontell, M. (1981). The three-dimensional cytoarchitecture of developing murine muscle spindles. Dev Biol *87*, 133-147.

Krogh, J. E., and Towns, L. C. (1984). Location of the cutaneous trunci motor nucleus in the dog. Brain Research *295*, 217-225.

Kucera, J., Walro, J. M., and Reichler, J. (1993). Differential effects of neonatal denervation on intrafusal muscle fibers in the rat. Anat Embryol (Berl) *187*, 397-408.

Kudo, N., and Yamada, T. (1985). Development of the monosynaptic stretch reflex in the rat: an in vitro study. J Physiol (Lond) *369*, 127-144.

Kuno, M., and Llinas, R. (1970). Alterations of synaptic action in chromatolysed motoneurones of the cat. Journal of Physiology *210*, 823-838.

Lagercrantz, H., and Ringstedt, T. (2001). Organization of the neuronal circuits in the central nervous system during development. Acta Paediatrica *90*, 707-715.

Landmesser, L. (1978). The development of motor projection patterns in the chick hind limb. Journal of Physiology *284*, 391-414.

Landmesser, L., and Honig, M. G. (1986). Altered sensory projections in the chick hind limb following the early removal of motoneurons. Developmental Biology *118*, 511-531.

Lee, S.-K., and Pfaff, S. L. (2001). Transcriptional networks regulating neuronal identity in the developing spinal cord. Nature Neuroscience *4*, 1183-1191.

Lentz, S. I., Knudson, C. M., Korsmeyer, S. J., and Snider, W. D. (1999). Neurotrophins support the development of diverse sensory axon morphologies. J Neurosci *19*, 1038-1048.

Leprince, D., Gegonne, A., Coll, J., de Taisne, C., Schneeberger, A., Lagrou, C., and Stehelin, D. (1983). A putative second cell-derived oncogene of the avian leukaemia retrovirus E26. Nature *306*, 395-397.

Lewandoski, M., Sun, X., and Martin, G. R. (2000). Fgf8 signalling from the AER is essential for normal limb development. Nature Genetics *26*, 460-463.

Li, R., Pei, H., and Watson, D. K. (2000). Regulation of Ets function by protein - protein interactions. Oncogene *19*, 6514-6523.

Liang, H., Mao, X., Olejniczak, E. T., Nettesheim, D. G., Yu, L., Meadows, R. P., Thompson, C. B., and Fesik, S. W. (1994). Solution structure of the ets domain of Fli-1 when bound to DNA. Nature Structural Biology *1*, 871-875.

Lin, J. H., Saito, T., Anderson, D. J., Lance-Jones, C., Jessell, T. M., and Arber, S. (1998). Functionally related motor neuron pool and muscle sensory afferent subtypes defined by coordinate ETS gene expression [see comments]. Cell *95*, 393-407.

Llinas, R., and Yarom, Y. (1981). Electrophysiology of mammalian inferior olivary neurones in vitro. Different types of voltage-dependent ionic conductances. Journal of Physiology *315*, 549-567.

Ma, Q., Fode, C., Guillemot, F., and Anderson, D. J. (1999). Neurogenin1 and neurogenin2 control two distinct waves of neurogenesis in developing dorsal root ganglia. Genes & Development *13*, 1717-1728.

Ma, Q., Kintner, C., and Anderson, D. J. (1996). Identification of neurogenin, a vertebrate neuronal determination gene. Cell *87*, 43-52.

Martin, G. R. (1998). The roles of FGFs in the early development of vertebrate limbs. Genes & Development *12*, 1571-1586.

Mavrothalassitis, G., and Ghysdael, J. (2000). Proteins of the ETS family with transcriptional repressor activity. Oncogene *19*, 6524-6532.

McHanwell, S., and Biscoe, T. J. (1981). The localization of motoneurons supplying the hindlimb muscles of the mouse. Philos Trans R Soc Lond B Biol Sci *293*, 477-508.

McKercher, S. R., Torbett, B. E., Anderson, K. L., Henkel, G. W., Vestal, D. J.,

Baribault, H., Klemsz, M., Feeney, A. J., Wu, G. E., Paige, C. J., and Maki, R. A. (1996). Targeted disruption of the PU.1 gene results in multiple hematopoietic abnormalities. EMBO Journal *15*, 5647-5658.

Mears, S. C., and Frank, E. (1997). Formation of specific monosynaptic connections between muscle spindle afferents and motoneurons in the mouse. J Neurosci *17*, 3128-3135.

Mendelson, B., and Frank, E. (1991). Specific monosynaptic sensory-motor connections form in the absence of patterned neural activity and motoneuronal cell death. J Neurosci *11*, 1390-1403.

Milner, L. D., and Landmesser, L. T. (1999). Cholinergic and GABAergic inputs drive patterned spontaneous motoneuron activity before target contact. Journal of Neuroscience *19*, 3007-3022.

Missler, M., and Sudhof, T. C. (1998). Neurexins: three genes and 1001 products. Trends in Genetics *14*, 20-26.

Monschau, B., Kremoser, C., Ohta, K., Tanaka, H., Kaneko, T., Yamada, T., Handwerker, C., Hornberger, M. R., Loschinger, J., Pasquale, E. B*., et al.* (1997). Shared and distinct functions of RAGS and ELF-1 in guiding retinal axons. EMBO Journal *16*, 1258-1267.

Monte, D., Baert, J. L., Defossez, P. A., de Launoit, Y., and Stehelin, D. (1994). Molecular cloning and characterization of human ERM, a new member of the Ets family closely related to mouse PEA3 and ER81 transcription factors. Oncogene *9*, 1397-1406.

Munson, J. B., and Sypert, G. W. (1979a). Properties of single central Ia afferent fibres projecting to motoneurones. Journal of Physiology *296*, 315-327.

Munson, J. B., and Sypert, G. W. (1979b). Properties of single fibre excitatory post-synaptic potentials in triceps surae motoneurones. Journal of Physiology *296*, 329-342.

Muthusamy, N., Barton, K., and Leiden, J. M. (1995). Defective activation and survival of T cells lacking the Ets-1 transcription factor. Nature *377*, 639-642.

Nunn, M. F., Seeburg, P. H., Moscovici, C., and Duesberg, P. H. (1983). Tripartite structure of the avian erythroblastosis virus E26 transforming gene. Nature *306*, 391-395.

Oakley, R. A., Garner, A. S., Large, T. H., and Frank, E. (1995). Muscle sensory neurons require neurotrophin-3 from peripheral tissue during the period of normal cell death. Development *121*, 1341-1350.

Oakley, R. A., Lefcort, F. B., Clary, D. O., Reichardt, L. F., Prevette, D., Oppenheim, R. W., and Frank, E. (1997). Neurotrophin-3 promotes the differentiation of muscle spindle

afferents in the absence of peripheral targets. J Neurosci *17*, 4262-4274.

O'Leary, D. D. M., and Wilkinson, D. G. (1999). Eph receptors and ephrins in neural development. Current Opinion in Neurobiology *9*, 65-73.

Oppenheim, R. W. (1991). Cell death during development of the nervous system. Annual Review of Neuroscience *14*, 453-501.

Patak, A., Proske, U., Turner, H., and Gregory, J. E. (1992). Development of the sensory innervation of muscle spindles in the kitten. Int J Dev Neurosci *10*, 91-92.

Patapoutian, A., Backus, C., Kispert, A., and Reichardt, L. F. (1999). Regulation of neurotrophin-3 expression by epithelial-mesenchymal interactions: the role of Wnt factors. Science *283*, 1180-1183.

Patapoutian, A., and Reichardt, L. F. (2001). Trk receptors: mediators of neurotrophin action. Current Opinion in Neurobiology *11*, 272-280.

Pfaff, S. L., Mendelsohn, M., Stewart, C. L., Edlund, T., and Jessell, T. M. (1996). Requirement for LIM homeobox gene Isl1 in motor neuron generation reveals a motor neuron-dependent step in interneuron differentiation. Cell *84*, 309-320.

Picciotto, M. R., and Wickman, K. (1998). Using knockout and transgenic mice to study neurophysiology and behavior. Physiological Reviews *78*, 1131-1163.

Raible, F., and Brand, M. (2001). Tight transcriptional control of the ETS domain factors Erm and Pea3 by Fgf signaling during early zebrafish development. Mechanisms of Development *107*, 105-117.

Rakic, P. (1971). Neuron-glia relationship during granule cell migration in developing cerebellar cortex. A Golgi and electronmicroscopic study in Macacus Rhesus. Journal of Comparative Neurology *141*, 283-312.

Reiner, A., Veenman, C. L., Medina, L., Jiao, Y., Del Mar, N., and Honig, M. G. (2000). Pathway tracing using biotinylated dextran amines. Journal of Neuroscience Methods *103*, 23-37.

Ringstedt, T., Kucera, J., Lendahl, U., Ernfors, P., and Ibanez, C. F. (1997). Limb proprioceptive deficits without neuronal loss in transgenic mice overexpressing neurotrophin-3 in the developing nervous system. Development *124*, 2603-2613.

Roehl, H., and Nusslein-Volhard, C. (2001). Zebrafish pea3 and erm are general targets of FGF8 signaling. Current Biology *11*, 503-507.

Rudenko, G., Nguyen, T., Chelliah, Y., Sudhof, T. C., and Deisenhofer, J. (1999). The structure of the ligand-binding domain of neurexin Ibeta: regulation of LNS domain

function by alternative splicing. Cell *99*, 93-101.

Sander, M., Paydar, S., Ericson, J., Briscoe, J., Berber, E., German, M., Jessell, T. M., and Rubenstein, J. L. (2000). Ventral neural patterning by Nkx homeobox genes: Nkx6.1 controls somatic motor neuron and ventral interneuron fates. Genes & Development *14*, 2134-2139.

Scott, E. W., Simon, M. C., Anastasi, J., and Singh, H. (1994). Requirement of transcription factor PU.1 in the development of multiple hematopoietic lineages. Science *265*, 1573-1577.

Sementchenko, V. I., and Watson, D. K. (2000). Ets target genes: past, present and future. Oncogene *19*, 6533-6548.

Serafini, T., Kennedy, T. E., Galko, M. J., Mirzayan, C., Jessell, T. M., and Tessier-Lavigne, M. (1994). The netrins define a family of axon outgrowth-promoting proteins homologous to C. elegans UNC-6. Cell *78*, 409-424.

Shapiro, L., and Colman, D. R. (1999). The diversity of cadherins and implications for a synaptic adhesive code in the CNS. Neuron *23*, 427-430.

Sharma, K., and Frank, E. (1998). Sensory axons are guided by local cues in the developing dorsal spinal cord. Development *125*, 635-643.

Sharma, K., Sheng, H. Z., Lettieri, K., Li, H., Karavanov, A., Potter, S., Westphal, H., and Pfaff, S. L. (1998). LIM homeodomain factors Lhx3 and Lhx4 assign subtype identities for motor neurons. Cell *95*, 817-828.

Sharrocks, A. D. (2001). The ETS-domain transcription factor family. Nature Reviews Molecular Cell Biology *2*, 827-837.

Shaw, P. J., and Eggett, C. J. (2000). Molecular factors underlying selective vulnerability of motor neurons to neurodegeneration in amyotrophic lateral sclerosis. Journal of Neurology *247 Suppl 1*, I17-27.

Shepherd, T. G., Kockeritz, L., Szrajber, M. R., Muller, W. J., and Hassell, J. A. (2001). The pea3 subfamily of ets genes are required for HER2/Neu-mediated mammary oncogenesis. Current Biology *11*, 1739-1748.

Song, J.-Y., Ichtchenko, K., Sudhof, T. C., and Brose, N. (1999). Neuroligin 1 is a postsynaptic cell-adhesion molecule of excitatory synapses. Proceedings of the National Academy of Sciences of the United States of America *96*, 1100-1105.

Sperry, R. W. (1963). Chemoaffinity in the orderly growth of nerve fiber patterns and connections. Proceedings of the National Academy of Sciences of the United States of America *50*, 703-710.

Takeichi, M., Uemura, T., Iwai, Y., Uchida, N., Inoue, T., Tanaka, T., and Suzuki, S. C. (1997). Cadherins in brain patterning and neural network formation. Cold Spring Harbor Symposia on Quantitative Biology *62*, 505-510.

Tanabe, Y., and Jessell, T. (1996). Diversity and Pattern in the Developing Spinal Cord. Science *274*, 1115-1123.

Tanaka, H., Shan, W., Phillips, G. R., Arndt, K., Bozdagi, O., Shapiro, L., Huntley, G. W., Benson, D. L., and Colman, D. R. (2000). Molecular modification of N-cadherin in response to synaptic activity. Neuron *25*, 93-107.

Taylor, M. D., Vancura, R., Patterson, C. L., Williams, J. M., Riekhof, J. T., and Wright, D. E. (2001). Postnatal regulation of limb proprioception by muscle-derived neurotrophin-3. Journal of Comparative Neurology *432*, 244-258.

Tosney, K. W., and Landmesser, L. T. (1985). Development of the major pathways for neurite outgrowth in the chick hindlimb. Developmental Biology *109*, 193-214.

Tourtellotte, W. G., Keller-Peck, C., Milbrandt, J., and Kucera, J. (2001). The transcription factor Egr3 modulates sensory axon-myotube interactions during muscle spindle morphogenesis. Developmental Biology *232*, 388-399.

Tourtellotte, W. G., and Milbrandt, J. (1998). Sensory ataxia and muscle spindle agenesis in mice lacking the transcription factor Egr3. Nat Genet *20*, 87-91.

Trojanowska, M. (2000). Ets factors and regulation of the extracellular matrix. Oncogene *19*, 6464-6471.

Tsuchida, T., Ensini, M., Morton, S. B., Baldassare, M., Edlund, T., Jessell, T. M., and Pfaff, S. L. (1994). Topographic organization of embryonic motor neurons defined by expression of LIM homeobox genes. [see comments]. Cell *79*, 957-970.

Verhage, M., Maia, A. S., Plomp, J. J., Brussaard, A. B., Heeroma, J. H., Vermeer, H., Toonen, R. F., Hammer, R. E., van den Berg, T. K., Missler, M*., et al.* (2000). Synaptic assembly of the brain in the absence of neurotransmitter secretion. Science *287*, 864-869.

Voyvodic, J. T. (1989). Target size regulates calibre and myelination of sympathetic axons. [see comments]. Nature *342*, 430-433.

Wang, H., Chadaram, S. R., Norton, A. S., Lewis, R., Boyum, J., Trumble, W., Sanes, J. R., and Laskowski, M. B. (1999). Positionally selective growth of embryonic spinal cord neurites on muscle membranes. Journal of Neuroscience *19*, 4984-4993.

Wang, H. U., and Anderson, D. J. (1997). Eph family transmembrane ligands can mediate repulsive guidance of trunk neural crest migration and motor axon outgrowth. Neuron *18*, 383-396.

Watt, D. G. D., Stauffer, E. K., Taylor, A., Reinking, R. M., and Stuart, D. G. (1976). Analysis of muscle receptor connections by spike-triggered averaging. 1. Spindle primary and tendon organ afferents. Journal of Neurophysiology *39*, 1375-1392.

Wenner, P., and Frank, E. (1995). Peripheral target specification of synaptic connectivity of muscle spindle sensory neurons with spinal motoneurons. J Neurosci *15*, 8191-8198.

Whitmarsh, A. J., Shore, P., Sharrocks, A. D., and Davis, R. J. (1995). Integration of MAP kinase signal transduction pathways at the serum response element. Science *269*, 403-407.

Wright, D. E., Zhou, L., Kucera, J., and Snider, W. D. (1997). Introduction of a neurotrophin-3 transgene into muscle selectively rescues proprioceptive neurons in mice lacking endogenous neurotrophin-3. Neuron *19*, 503-517.

Wu, Q., and Maniatis, T. (1999). A striking organization of a large family of human neural cadherin-like cell adhesion genes. Cell *97*, 779-790.

Xin, J. H., Cowie, A., Lachance, P., and Hassell, J. A. (1992). Molecular cloning and characterization of PEA3, a new member of the Ets oncogene family that is differentially expressed in mouse embryonic cells. Genes & Development *6*, 481-496.

Yamamoto, Y., and Henderson, C. E. (1999). Patterns of programmed cell death in populations of developing spinal motoneurons in chicken, mouse, and rat. Developmental Biology *214*, 60-71.

Zelena, J. (1994). Nerves and Mechanoreceptors: the role of innervation in the development and maintenance of mammalian mechanoreceptors (London, Chapman & Hall).